DESIGN AND SYNTHESIS OF INHIBITORS FOR SERINE AND CYSTEINE PROTEASES

A Dissertation
Presented to
The Academic Faculty

By

Karrie Eileen Adlington Rukamp

In Partial Fulfillment
Of the Requirements for the Degree
Doctor of Philosophy in Chemistry

Georgia Institute of Technology
December, 2003

DESIGN AND SYNTHESIS OF INHIBITORS FOR SERINE AND CYSTEINE PROTEASES

Approved by:

Dr. James C. Powers, Advisor

Dr. David M. Collard

Dr. Sheldon W. May

Dr. Alfred H. Merrill

Dr. Suzanne B. Shuker

Date Approved 11/20/03

To my husband Brian J. Rukamp, my parents Dr. Merywn G. Adlington and Linda M. Adlington, my sister Deanna L. Adlington, and my brother Ryan T. Adlington. I have been truly blessed to have such a wonderful and supportive family! Thanks for always being there for me! Also, in memory of those no longer with us, but here in spirit: my uncle Kevin R. Reitzel and my grandparents Carl R. Reitzel, Eileen V. Reitzel, Christopher G. Adlington, and Margaret A. Adlington.

ACKNOWLEDGEMENT

I would like to thank all the faculty, staff, and students in the School of Chemistry and Biochemistry for helping to create a welcoming, collaborative environment where ideas could be freely shared. It has been a pleasure working with so many of you over the years! Special thanks to the members of my committee, for graciously agreeing to serve in that capacity!

It has been my privilege to have Dr. James C. Powers as my research advisor. Thank you, Dr. Powers, for all your guidance during my time here. I would also like to thank Dr. Chih-Min Kam for all her research advice, wisdom and patience during my first three years. Special thanks to Dr. Robert Braga, who taught me almost everything I know about teaching and keeping a lab running! To my friends and colleagues in Dr. Powers' group, Brian Rukamp, Özlem Dogan Ekici, Sylvia Shadinger, Marion Götz, Amy Campbell, Temam Juhar, Zhao-Zhao Li, Joel Krauser, Karen Ellis James, and Juliana Gheura Asgian, I was blessed to have worked with you during my time here- I could not have asked for better lab-mates!

I would like to thank Dr. Guy Salvesen and Jowita Mikolajczyk for giving us the Caspase 3, 6, and 8, and for their invaluable assistance with caspase kinetics. I would also like to thank Dr. Dieter Jenne and Edward Fellows for testing the phosphonates against Granzyme H.

I would like to thank several people for their assistance, both research and otherwise, over the years. First, a special thank you to the staff in the main office, for all their help with everything and for patiently dealing with all of us students! I would like

to thank Dave Bostwick and Sarah Shealy for their invaluable assistance on mass spectrometry, and Dr. Les Gelbaum for all his help and training on NMR. Finally, I would like to thank all of our lab's undergraduates, both past and present, for their energy and creativity, which made our lab a much more interesting place to work!

TABLE OF CONTENTS

LIST OF TABLES

LIST OF FIGURES

LIST OF SCHEMES

LIST OF ABBREVIATIONS

[A]	concentration of compound A
$[A]_0$	initial concentration of compound A
AA	amino acid
AAsp	aza-aspartic acid
Ac	acetyl
Aca	aminocaproic acid
Ala	alanine
AMC	7-amino-4-methylcoumarin
AmPhGly	4-amidino-phenylglycine
APPA	4-amidinophenylpyruvate
Arg	arginine
Asn	asparagine
Asp	aspartic acid
Bi	biotinyl
°C	degrees Celsius
Cat B	cathepsin B
Cat G	cathepsin G
Cbz	benzyloxycarbonyl
CCP	cytotoxic cell protease
$CDCl_3$	deuterated chloroform
Chaps	3-[(3-Cholamidopropyl)dimethylammonio]-1-propanesulfonate

$CHCl_3$	chloroform
CH_2Cl_2	dichloromethane, or methylene chloride
ChT	chymotrypsin
^{13}C NMR	carbon 13 nuclear magnetic resonance
CSP	cytotoxic serine protease
CTL	cytotoxic T-lymphocyte
Cys	cysteine
DCC	dicyclohexyl carbodiimide
DCI	3,4-dichloroisocoumarin
DCU	dicyclohexyl urea
-dε/dt	rate of decrease of active enzyme species
DMF	dimethyl formamide
DMSO	dimethyl sulfoxide
DMSO-d_6	deuterated dimethyl sulfoxide
DNA	deoxyribonucleic acid
DTT	DL-1,4-dithiothreitol
DTNB	5,5'-Dithiobis(2-nitrobenzoic acid)
ε	concentration of active enzyme species in an assay
E	enzyme
[E]	concentration of enzyme
EDTA	ethylenediaminetetraacetic acid
EI	enzyme-inhibitor complex
E•I	reversible enzyme-inhibitor complex

E-I	covalent (irreversible) enzyme-inhibitor complex
em	emission
Enz	enzyme
EP	epoxide
eq	equivalence
ES	enzyme-substrate complex
ESI	electrospray ionization
E_T	total enzyme concentration in an assay
Et_3N	triethylamine
EtOAc	ethyl acetate
EtOH	ethanol
ex	excitation
FAB	fast atom bombardment
Ftc	5-fluoresceinyl-(thiocarbamoyl)
Glu	glutamic acid
Gln	glutamine
Gly	glycine
GrA	granzyme A
GrB	granzyme B
GrH	granzyme H
GrK	granzyme K
GrM	granzyme M
H_2	hydrogen gas

HCl	hydrochloric acid
HCN	cyanohydrin
Hepes	4-(2-hydroxyethyl)-1-piperazineethanesulfonic acid
His	histidine
HLE	human leukocyte elastase
^{1}H NMR	proton nuclear magnetic resonance
Hphe	homophenylalanine
H_2O	water
HOBt	hydroxybenzotriazole
hr	hour
HRMS	high-resolution mass spectrometry
I	inhibitor
[I]	inhibitor concentration
IBCF	*iso*-butyl chloroformate
Ile	isoleucine
k_1	rate constant for formation of E•I complex in irreversible inhibition
k_{-1}	rate constant for breakdown of E•I complex
k_2	rate constant for formation of E-I complex in irreversible inhibition
kDa	kilo-Dalton
k_{cat}	catalytic constant
$K_{i,app}$	apparent dissociation constant for EI complex
K_i	dissociation constant for EI complex in reversible inhibition
K_I	dissociation constant for E•I complex in irreversible inhibition

K_m	Michaelis constant
k_{obs}	observed pseudo first-order inactivation rate constant
$k_{obs}/[I]$	apparent second order rate constant; reflects inhibitor potency
λ	wavelength
L	liters
Leu	leucine
ln	natural log
Lys	lysine
M	molarity
mL	milliliters
mmol	millimole
MeOH	methanol
MES	2-(N-Morpholino)ethanesulfonic acid
Met	methionine
$MgSO_4$	magnesium sulfate
Mp	melting point
MS	mass spectrometry
NaCl	sodium chloride
$NaHCO_3$	sodium bicarbonate
NaOH	sodium hydroxide
NCBI	National Center for Biotechnological Information
NK	natural killer cell
Nle	norleucine

NMM	N-methylmorpholine
Nva	norvaline
O_2	oxygen gas
OMe	methoxy
OPh	phenoxy
P	product of substrate hydrolysis
PDB	Protein Data Bank
Pd/C	palladium on carbon
Ph	phenyl
Phe	phenylalanine
PhGly	phenylglycine
Pipes	piperazine-1,4-bis(2-ethanesulfonic acid)
pNA	*p*-nitroanilide
PPE	porcine pancreatic elastase
ppt	precipitate
Pro	proline
R_f	retention factor
RNKP	rat natural killer cell protease
rt	room temperature
s	second
S	substrate
[S]	concentration of substrate
SBzl	thiobenzyl ester

Ser	serine
Suc	succinyl
t	time
$t_{1/2}$	half-life
tBu	*t*-butyl
TFA	trifluoroacetic acid
THF	tetrahydrofuran
Thr	threonine
TLC	thin layer chromatography
TMS	tetramethylsilane
Trp	tryptophan
Tyr	tyrosine
Val	valine
v_t	rate at a given time t
v_o	initial rate
Xaa	generic amino acid
Z	benzyloxycarbonyl

SUMMARY

In the first project, a series of peptide phosphonate inhibitors was designed for Granzyme H (GrH), both for predicted greater potency and to help elucidate the specificity of the various rat and mouse chymases, most of which have been incompletely studied. Phosphonates are highly efficient irreversible inhibitors that are effective against serine proteases while showing no activity towards cysteine proteases. They are stable under physiological conditions and are unreactive to most nucleophiles. The phosphonates in this project were designed using the known preference of GrH for Phe or Phe analogs at P1, combined with various N-terminal blocking groups to determine what structures were preferred for potency. A series of 14 inhibitors was designed using the sequences Suc-Phe-Leu-$AA_1{}^P(OPh)_2$ and 3-phenoxybenzoyl-$AA_1{}^P(OPh)_2$ as starting points, where AA_1 was Phe, Hphe, or PhGly.

Based on the reported optimal tetrapeptide sequences, a series of α-keto amide inhibitors was designed in the second project. α-Keto amides are competitive reversible transition state inhibitors that often exhibit slow binding inhibition. They have the advantage of being fairly stable and having decent cell permeability, as well as demonstrated biological activity *in vivo*. The biggest advantage, however, is that α-keto amides can be extended in the P' direction, allowing for additional enzyme-inhibitor interactions and generating increased potency and specificity. With that in mind, the 7 inhibitors synthesized utilized an optimal sequence for either Caspase 6 (Z-Val-Glu-(Ile/Val)-Asp-CO-NH-**R**) or Caspase 8 (Z-Leu-Glu-Thr-Asp-CO-NH-**R**), as well as a

variety of P' residues such as those where **R**= CH_2Ph, $(CH_2)_2Ph$, $(CH_2)_3Ph$, and $(CH_2)_3OCH_3$.

CHAPTER 1

PEPTIDE PHOSPHONATES AS INHIBITORS OF GRANZYME H (CHYMASE)

INTRODUCTION

Cytotoxic T-lymphocytes (CTL) and natural killer (NK) cells are involved in a variety of immune reactions in the body, including defense against viral infections and tumor cells by apoptosis. However, they are also involved in autoimmune diseases and other disorders such as rheumatoid arthritis. There are two pathways through which the cytotoxic lymphocytes can operate: exocytosis of cytotoxic granules containing perforin and other proteases, and Fas-mediated cell death, which is granule-independent and will not be discussed here.[1] Although NK cells in circulation are active, with mature granzymes and perforin stored in granules, CTLs in circulation lack granzymes, perforin, and cytotoxicity. When antigens re-stimulate the CTLs, perforin and granzymes are synthesized and stored in granules. These granules are then ready for exocytosis after CTL interaction with the target cell.[2-4] Following exocytosis of the granule, perforin is inserted into the target cell's membrane, where it polymerizes and forms pores (Figure 1.1a).[2,5,6] These pores can be lethal alone, since they disrupt the membrane barrier of the cell, but they are also gateways for other lymphocyte proteases stored in the granules to enter the cell.[3] These enzymes, which are responsible for the activity of NKs and CTLs, are a family of serine proteases called granzymes. They are involved both in the initiation of perforin-dependent pore formation in the target cells, and in the initiation of nuclear changes associated with cell death (Figure 1.1b), such as membrane blebbing,

a)

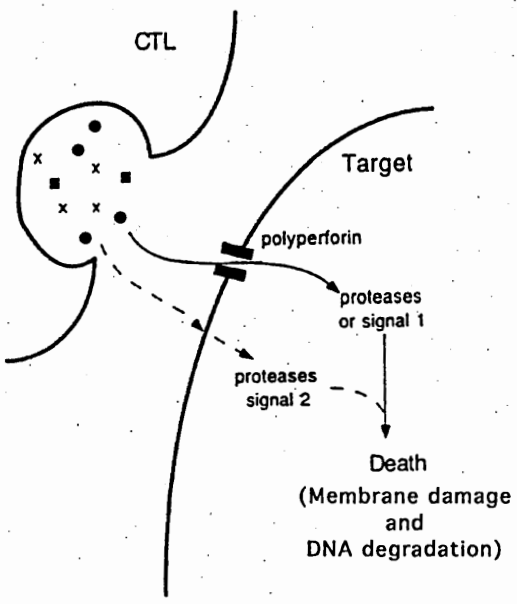

b)

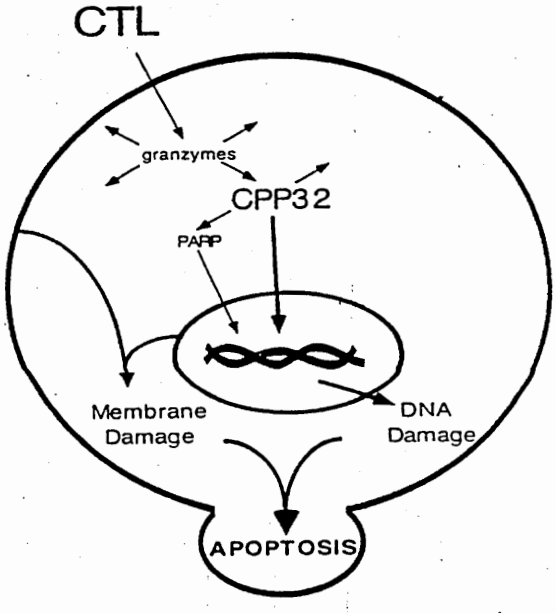

Figure 1.1 Lymphocyte-Mediated Cell Death. **a)** Granule exocytosis leads to target cell lysis, either by perforin pore formation and uptake of granzymes (solid line alone), or by perforin and granzyme signals in concert (solid and dashed lines). **b)** Involvement of granzymes in CTL-mediated cell death.[5]

condensation of chromatin, and DNA degradation, which ultimately lead to apoptosis of the infected cells.[2,3,5] Although perforin alone does not cause DNA fragmentation, and purified granzymes alone have no lytic activity, the inhibition of granzymes by serine protease inhibitors has been shown to prevent CTL- and NK-mediated lysis of cells.[2,7,8] For example, the general serine protease inhibitor 3,4-dichloroisocoumarin (DCI) inactivated isolated granule proteases and blocked lytic activity in rat natural killer cells.[7,9,10] In addition, if the isocoumarin inhibitor was chemically removed by hydroxylamine, lytic activity was restored to the granules, thus implying that granzymes play a regulatory role in lymphocyte mediated and granule mediated cytolysis.[7,9,10]

Granzymes (*gran*ule-associated en*zymes*) are a family of highly homologous (38-71% amino acid homology)[2,11] chymotrypsin-like serine proteases. They are expressed by NKs and CTLs and are stored as active enzymes in the cytoplasmic granules secreted by these cells.[3] Granzymes have also been called cytotoxic cell proteases (CCPs), cytotoxic serine proteases (CSPs), fragmentins, and rat natural killer proteases (RNKPs).[2] Humans express five different granzymes (A, B, H, K, and M), while at least nine granzymes are known to be expressed in mice and rats.[2,4] The granzymes can be classified on the basis of their substrate specificity. Granzyme B (GrB) cleaves after Asp residues (Asp-ase activity), while granzyme A (GrA) and granzyme K (GrK) have trypsin-like activity (tryptase), preferring to cleave after basic residues such as Arg or Lys. Granzyme M (GrM) prefers to cleave after Met or other long unbranched hydrophobic residues, and granzyme H (GrH) has chymotrypsin-like (chymase) activity, cleaving after Phe residues.[2,4,7,12] Granzymes C-G and I-J are rat and murine granzymes

of unknown enzyme activity, although D-G are predicted, from computer models, to cleave after Phe/Leu residues, thus suggesting chymase activity.[1,2,4,13,14]

Each granzyme is believed to play a specific role in granule-mediated cytolysis. GrB is believed to be involved in DNA degradation, since studies have shown that target cells treated with purified perforin and GrB display rapid DNA fragmentation, and CTL from GrB knockout mice cannot induce rapid DNA degradation.[2,15-17] GrB is also involved in activating the pro-apoptotic caspases, thereby beginning the apoptotic cascade and leading to cell death.[4] GrA and GrK are also involved in stimulating DNA degradation, although less efficiently than GrB.[2] GrH is thought to be involved in the activation of perforin, since the lytic activity of perforin preparations is blocked when the chymase activity is inhibited.[18] GrH is therefore believed to play a role in pore formation, since perforin preparations generally contain chymase activity. When this activity is inhibited, pore formation is blocked.[1,2] Woodard *et al.*[1,10] have shown that a phosphonate inhibitor (Bi-Aca-Aca-Phe-Leu-Phe^{P}(OPh)$_2$) specific for chymases blocked NK-mediated cell death and diminished the granule mediated lysis of cells.[1,10,18] Therefore the chymases, and GrH in particular, are ideal targets for drug design, as the ability to block apoptosis would be of great therapeutic benefit.

Granzymes are highly homologous in mature form, exhibiting 71% amino acid homology between GrB (the best-characterized granzyme) and GrH.[4,11] GrH also has a high degree of sequence similarity (55%) with human neutrophil cathepsin G (Cat G), another chymotrypsin-like serine protease.[11] This degree of amino acid similarity leads to highly conserved structural features in the granzyme family and Cat G, such as the conserved catalytic triad of His^{57}, Asp^{102}, and Ser^{195} (chymotrypsin numbering), and six

conserved Cys residues, which form three internal disulfide bridges.[2,11] GrH also has a seventh free Cys residue at position 166, which may be surface exposed and could participate in intermolecular disulfide bridges.[11] GrH, like the other granzymes and Cat G, is synthesized as a pre-pro-peptide. An 18-residue "pre", or leader, sequence is cleaved at the endoplasmic reticulum by signal peptidase to give the inactive progranzyme (zymogen). Activation of the zymogen by cleavage of an N-terminal dipeptide (Glu-Glu for GrH, Gly-Glu for Cat G) gives the fully mature active granzyme.[2,11]

The nomenclature proposed by Schecter and Berger[19] is used throughout this work to define the position of the amino acids (P4-P2') in the peptides and the corresponding positions in the active site of the enzyme (S4-S2') with respect to the scissile bond (Figure 1.2). GrH, along with the rat and murine chymases,

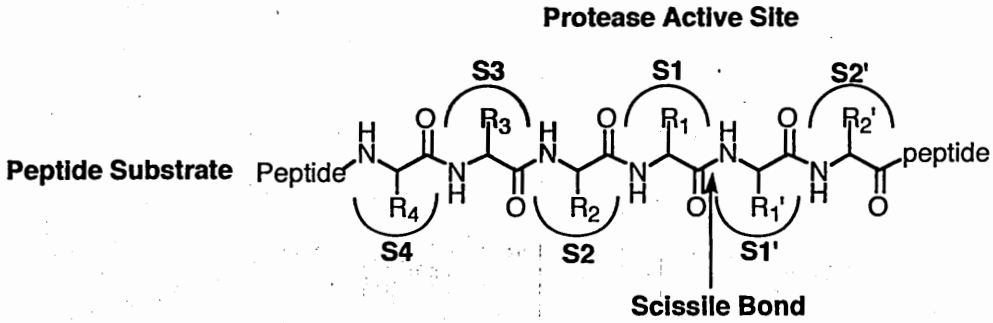

Figure 1.2 Schecter and Berger Nomenclature.[19]

prefers aromatic residues such as Phe or Tyr at P1, as demonstrated by the rapid hydrolysis of thiobenzyl ester substrates such as Suc-Phe-Leu-Phe-SBzl.[4] GrH also has

limited activity towards substrates containing Tyr, Met, Nle, or Nva at P1, but demonstrates no tryptase or Asp-ase activity.[4] GrH has been successfully inhibited by several different classes of inhibitors: chloromethyl ketones such as Suc-Phe-Leu-Phe-CH_2Cl; isocoumarins such as 3,4-dichloroisocoumarin (DCI), a general serine protease inhibitor; and peptide phosphonates such as Ftc-Aca-Phe-Leu-Phe$^P(OPh)_2$[4,20]. Surprisingly, a second peptide phosphonate, 3-phenoxybenzoyl-4-AmPhGly$^P(OPh)_2$, which was originally designed for GrA and GrK,[21] was active toward GrH as well and was a very potent cytolysis inhibitor (Dorothy Hudig, unpublished results).

Peptide derivatives of (α-aminoalkyl)phosphonate diphenyl esters are highly efficient irreversible inhibitors that work against a variety of serine proteases, while showing no inhibitory activity towards cysteine proteases.[22-24] These peptide phosphonates are substrate analogs in which the scissile bond has been replaced with a diphenyl phosphonate functional group (Figure 1.3).[2,20,24]

Peptide Substrate **Peptide Phosphonate**

Figure 1.3 Structural Comparison of Substrates to Peptide Phosphonate Inhibitors.

Since enzyme specificity is largely a function of the peptide sequence of the inhibitor, this class of inhibitors can easily discriminate between various serine proteases. For

example, Suc-Val-Pro-Phe^{P}(OPh)$_2$ strongly inhibits chymotrypsin (ChT, $k_{obs}/[I] = 44{,}000$ M^{-1} s^{-1}), while showing no inhibition of porcine pancreatic elastase (PPE) or human leukocyte elastase (HLE).[24] Phosphonates have many advantages over other types of inhibitors: they are easily synthesized and purified, unreactive to most nucleophiles, and stable under most common peptide synthesis reaction conditions. Phosphonates are also very stable under physiological conditions, with most being stable in buffer for 3 to 7 days, and in plasma for 8 to 24 hours.[23,25] Unlike chloromethyl ketones, phosphonates do not react with other enzymes such as acetyl cholinesterase, thus decreasing their toxicity.[2,23] Phosphonates also show good cell permeability and form stable enzyme-inhibitor complexes, making them ideal for enzyme localization studies in cells.[20,23]

Phosphonates that incorporate a peptide sequence similar to the natural substrate for an enzyme are generally specific inhibitors for that enzyme. In order to achieve greater potency against GrH, and to help elucidate the specificity of the various rat and mouse chymases, most of which have been incompletely studied, a series of phosphonate inhibitors was designed. The phosphonates synthesized were designed using GrH's known preference for Phe or its analogs at P1. Several different N-terminal blocking groups were also utilized in order to determine what structures were required for potency and specificity against GrH. The series of fifteen inhibitors designed in this project used the sequences Suc-Phe-Leu-$AA_1{}^{P}(OPh)_2$ and 3-phenoxybenzoyl-$AA_1{}^{P}(OPh)_2$, where AA_1 was Phe, Hphe, or PhGly (Figure 1.4).

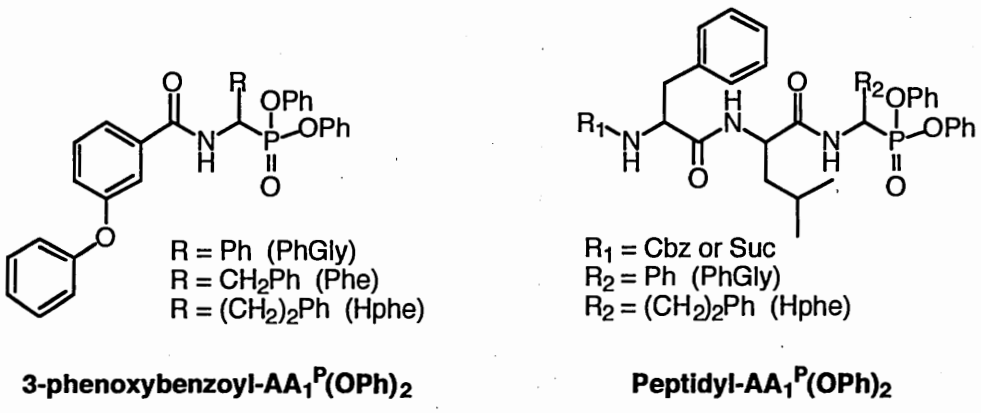

Figure 1.4 Phosphonate Inhibitors Synthesized for Granzyme H.

RESULTS AND DISCUSSION

Based on previously studied substrates and inhibitors of the chymase granzymes, a series of peptide phosphonate inhibitors was designed for GrH. The phosphonates synthesized were built using the known preference of GrH for Phe or Phe analogs at P1, combined with various N-terminal blocking groups to determine what structures were required for potency. The first class of phosphonates synthesized was composed of peptide phosphonates with a general structure of R-Phe-Leu-$AA_1{}^P(OPh)_2$, where AA_1 represents the hydrophobic P1 residues (Hphe or PhGly) used, and R represents the two possible N-terminal groups, Cbz (Z) or succinyl (Suc). This design was based on the peptide substrate Suc-Phe-Leu-Phe-SBzl, which is efficiently hydrolyzed by GrH,[4] and the inhibitor analogs of that substrate, Suc-Phe-Leu-Phe-CH_2Cl and Ftc-Aca-Phe-Leu-$Phe^P(OPh)_2$. The second class of phosphonates was composed of 3-phenoxybenzoyl phosphonate derivatives, with the general structure 3-phenoxybenzoyl-$AA_1{}^P(OPh)_2$, where AA_1 again denotes the various hydrophobic P1 residues used (Phe, Hphe, or PhGly). This class was based on 3-phenoxybenzoyl-4-$AmPhGly^P(OPh)_2$[21], which, although designed for GrA and GrK, was also active against GrH and was a potent cytolysis inhibitor (Dorothy Hudig, unpublished results).

Synthesis. The parent compounds, N-benzyloxycarbonyl-protected (α-aminoalkyl)phosphonate diphenyl esters (**1a-1c**), were synthesized by the Oleksyszyn reaction (Scheme 1.1), which involves amidoalkylation of triphenyl phosphite by an aldehyde and benzyl carbamate.[26] The Cbz group was then removed by hydrogenolysis to give the (α-aminoalkyl)phosphonate diphenyl esters (**2a-2c**). The deblocked

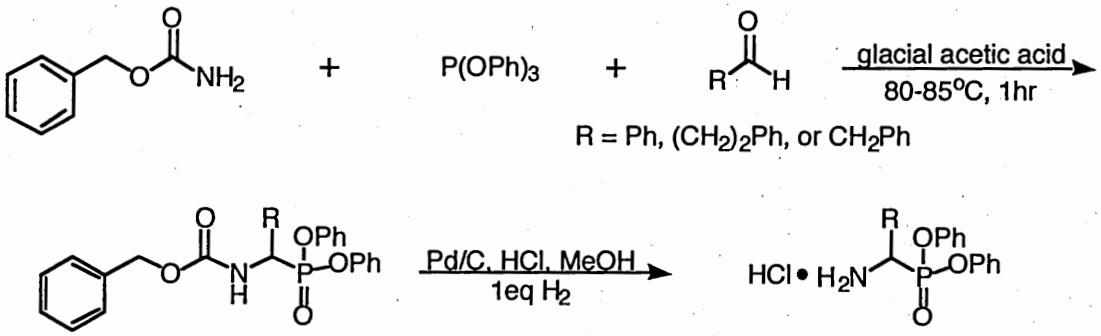

1a, R = Ph (PhGly)

1b, R = $(CH_2)_2Ph$ (Hphe)

1c, R = CH_2Ph (Phe)

2a, R = Ph (PhGly)

2b, R = $(CH_2)_2Ph$ (Hphe)

2c, R = CH_2Ph (Phe)

Scheme 1.1 Synthesis of (α-Aminoalkyl)phosphonate Diphenyl Esters by the Oleksyszyn Reaction.[26]

phosphonates were then coupled (Scheme 1.2) to either 3-phenoxybenzoic acid or Z-Phe-Leu-OH by the DCC activated ester coupling method to give the phosphonate derivatives (**3a-3c** and **4a-4b**). Peptide derivatives Z-Phe-Leu-PhGly$^P(OPh)_2$ (**4a**) and Z-Phe-Leu-Hphe$^P(OPh)_2$ (**4b**) were deprotected by hydrogenolysis to their HCl salts (**5a** and **5b**), which were then coupled with succinic anhydride to give the peptide phosphonates Suc-Phe-Leu-PhGly$^P(OPh)_2$ (**6a**) and Suc-Phe-Leu-Hphe$^P(OPh)_2$ (**6b**). All new compounds were characterized by ^1H NMR, HRMS, elemental analysis (Table 1.1), and melting point (Mp).

Serine Proteases. Granzyme H and cathepsin G are serine endopeptidases of the chymotrypsin family. As such, they share many common structural and mechanistic

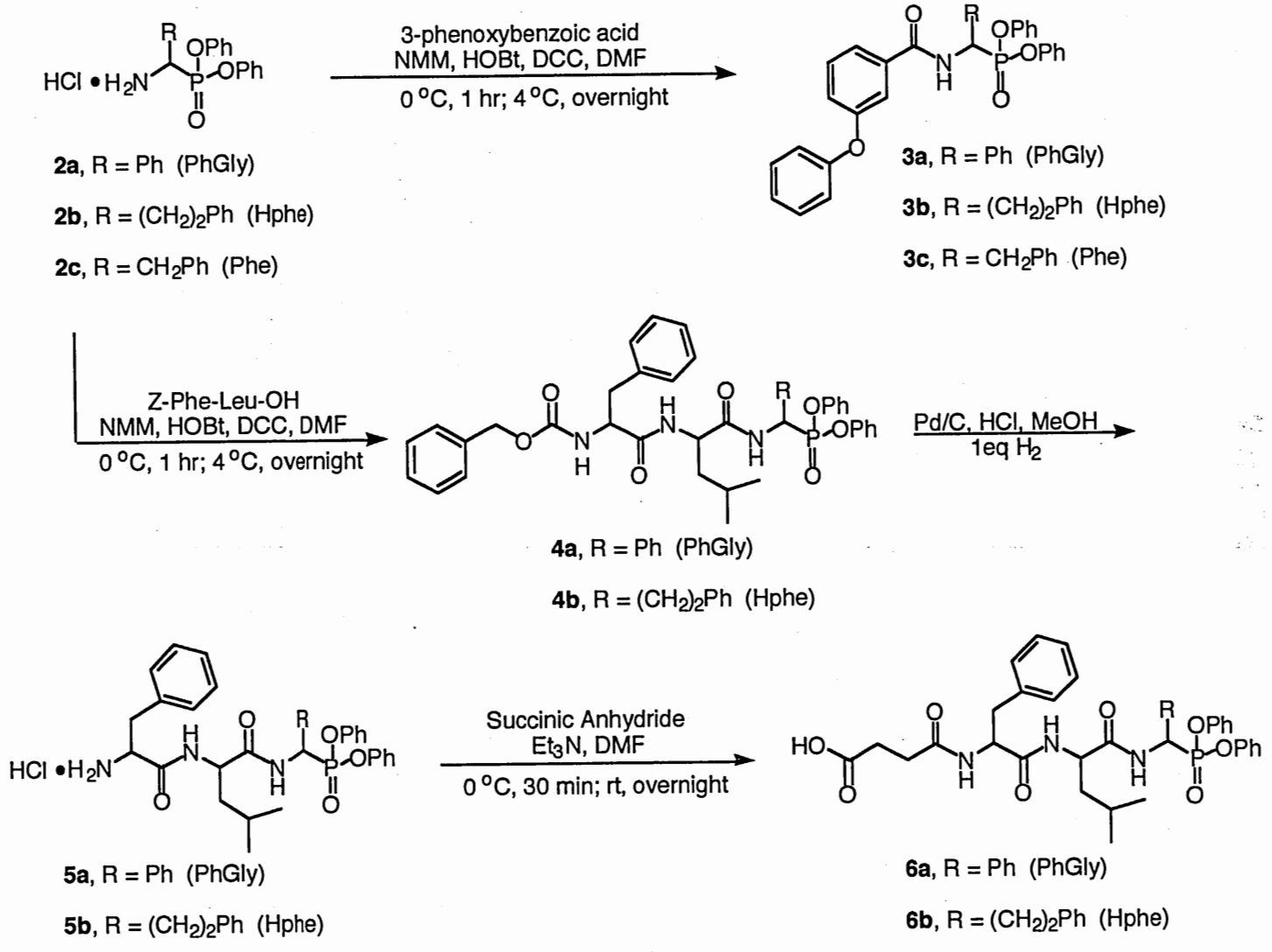

Scheme 1.2 Synthesis of Peptide Derivatives of (α-Aminoalkyl)phosphonate Diphenyl Esters.

Table 1.1 Elemental Analysis of (α-Aminoalkyl)phosphonate Diphenyl Ester Inhibitors

Compound	Formula	Calculated			Found		
		C	H	N	C	H	N
Z-PhGly^P(OPh)$_2$	$C_{27}H_{24}NO_5P$	68.49	5.11	2.96	68.70	5.21	3.03
Z-Hphe^P(OPh)$_2$	$C_{29}H_{28}NO_5P \cdot 0.25\ H_2O$	68.84	5.64	2.77	68.69	5.60	2.76
HCl•PhGly^P(OPh)$_2$	$C_{19}H_{19}NO_3PCl \cdot 0.5\ H_2O$	59.29	5.20	3.64	59.12	4.99	3.66
HCl•Hphe^P(OPh)$_2$	$C_{21}H_{23}NO_3PCl \cdot 0.5\ H_2O$	61.09	5.82	3.39	61.06	5.67	3.48
3-phenoxybenzoyl-PhGly^P(OPh)$_2$	$C_{32}H_{26}NO_5P$	71.77	4.89	2.62	71.60	4.96	2.59
3-phenoxybenzoyl-Hphe^P(OPh)$_2$	$C_{34}H_{30}NO_5P$	72.46	5.37	2.49	72.21	5.39	2.51
3-phenoxybenzoyl-Phe^P(OPh)$_2$	$C_{33}H_{28}NO_5P$	72.12	5.14	2.55	72.14	5.16	2.60
Z-Phe-Leu-PhGly^P(OPh)$_2$	$C_{42}H_{44}N_3O_7P$	68.75	6.04	5.73	68.58	6.01	5.74
Z-Phe-Leu-Hphe^P(OPh)$_2$	$C_{44}H_{48}N_3O_7P$	69.37	6.35	5.52	69.28	6.50	5.73
HCl•Phe-Leu-PhGly^P(OPh)$_2$	$C_{34}H_{39}N_3O_5PCl \cdot 1.0\ H_2O$	62.43	6.27	6.47	62.20	6.13	6.47
HCl•Phe-Leu-Hphe^P(OPh)$_2$	$C_{36}H_{43}N_3O_5PCl \cdot 1.0\ H_2O$	63.39	6.60	6.16	63.40	6.57	6.22
Suc-Phe-Leu-PhGly^P(OPh)$_2$	$C_{38}H_{42}N_3O_8P \cdot 0.5\ H_2O$	64.41	6.07	5.93	64.36	6.17	6.19

Table 1.1 (cont'd.)

Compound	Formula	Calculated			Found		
		C	H	N	C	H	N
Suc-Phe-Leu-Hphe^{P}(OPh)$_2$	$C_{40}H_{46}N_3O_8P \bullet 0.5\ H_2O$	65.22	6.39	5.71	65.28	6.39	5.90

features with chymotrypsin, such as the catalytic triad of Ser^{195}, His^{57}, and Asp^{102} (chymotrypsin numbering). All three enzymes share a preference for aromatics such as Phe, Tyr, or Trp at P1, and can often tolerate bulky hydrophobics such as Met or Lys as well.

The mechanism of substrate hydrolysis by serine proteases (Figure 1.5) begins with the formation of the initial enzyme-substrate (ES) complex at the active site.[27] Ser^{195} nucleophilically attacks the carbonyl of the scissile bond in the substrate to form a tetrahedral adduct, with the negatively charged oxygen of the adduct stabilized by hydrogen-bonding interactions in the oxyanion hole. His^{57} takes up the proton from the hydroxyl of Ser^{195}, generating an imidazolium ion with the positive charged stabilized by electrostatic interactions with the negatively charged Asp^{102}. The adduct decomposes to form the acyl-enzyme intermediate, releasing the peptide from the C-terminal side of the scissile bond. Deacylation of the enzyme then occurs through attack by water on the acyl-enzyme intermediate, generating a tetrahedral intermediate. This intermediate decomposes, regenerating the active enzyme and releasing the peptide from the N-terminal side of the scissile bond. Ser^{195} and His^{57} are the residues most often targeted in design of inhibitors, due to their crucial roles in the catalytic mechanism.[28]

Enzyme Inhibitors. Five major classes of synthetic protease inhibitors are known, encompassing both reversible and irreversible inhibition.[2,29] The two classes of reversible inhibitors are transition state analogs, such as peptide aldehydes, and simple substrate analogs. The three classes of irreversible inhibitors are mechanism based or suicide inhibitors (e.g. isocoumarins), alkylating agents (e.g. chloromethyl ketones), which react with the His of the enzyme active site, and acylating agents, such as

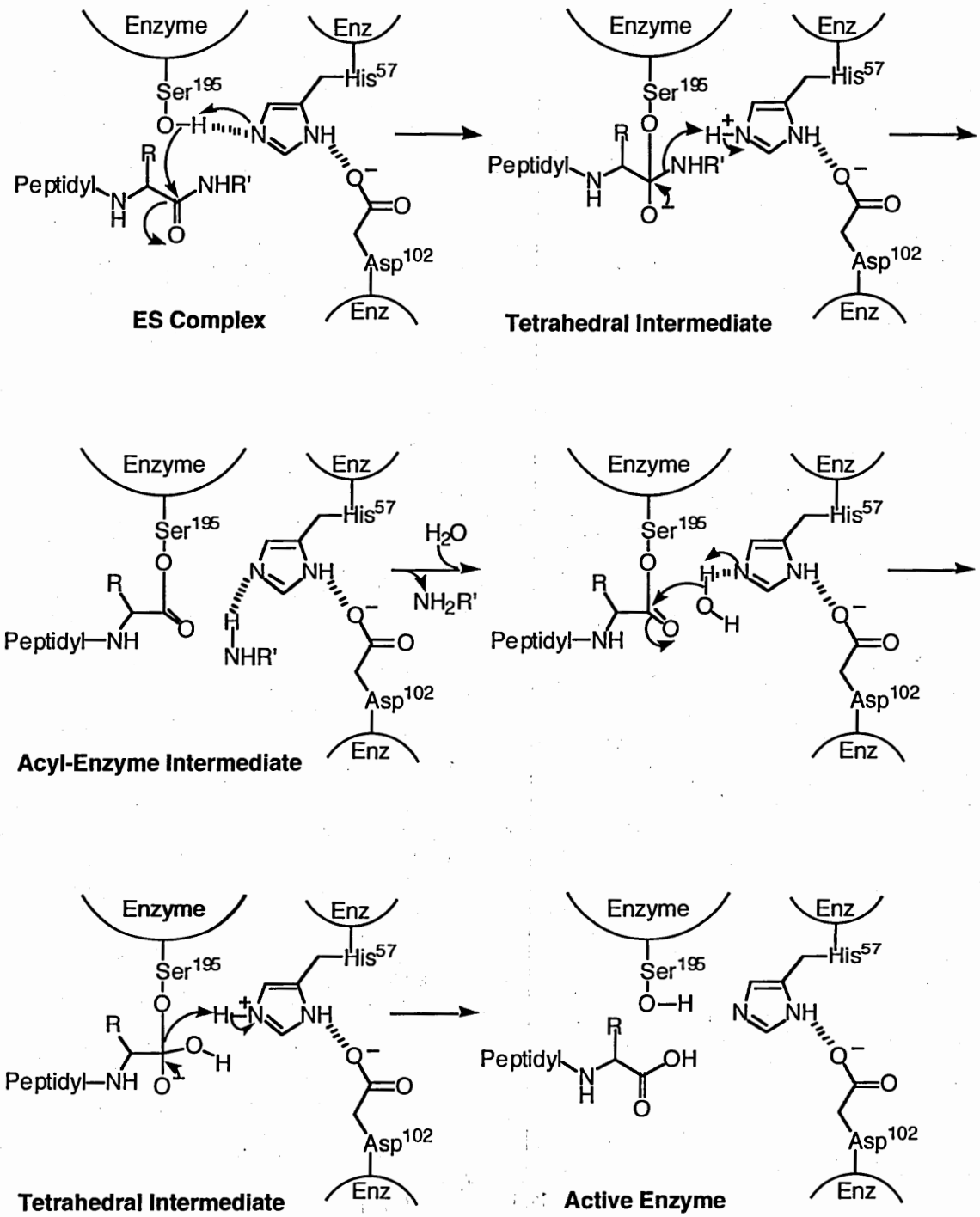

Figure 1.5 Mechanism of Hydrolysis by Serine Proteases.[27]

phosphonylating or sulfonylating agents, which react with the Ser of the enzyme active site to from stable intermediates. Reversible inhibitors depend on binding interactions with the active site for potency, since the enzyme-inhibitor complex dissociates easily. Enzymatic activity can therefore be restored by simply removing the inhibitor from the system, either by degradation of the compound, or through physical means such as dialysis.[30] The equilibrium between inhibitor and enzyme is the defining characteristic of reversible inhibition. This equilibrium is usually represented by an constant, K_i, which is the dissociation constant for the enzyme-inhibitor complex and is a measure of the effectiveness of the inhibitor.[2] Reversible inhibition exhibits a specific degree of inactivation of the enzyme, usually attained quickly, that is determined by the concentration of the inhibitor in the system. Once this degree of inactivation is reached, the reaction is independent of time as long as the inhibitor is not degraded.[30]

Irreversible inhibition, on the other hand, is time-dependent, with the degree of inactivation progressively increasing over time until complete inhibition is reached, providing that the inhibitor is stable and is sufficiently in excess of the enzyme.[30] Activity cannot be restored to the enzyme through removal of inhibitor by simple physical means such as filtration or dialysis. The mechanism of irreversible inhibition involves covalent bond formation after the initial enzyme-inhibitor complex is formed. The potency of irreversible inhibitors is expressed by a rate constant, $k_{obs}/[I]$, where k_{obs} is the pseudo first-order inhibition constant, and [I] is the concentration of the inhibitor.[2,30]

Phosphonate Inhibitors. (α-Aminoalkyl)phosphonate diphenyl esters are irreversible inhibitors of serine proteases. These phosphonates are analogs of α-amino

carboxylic acid substrates, with a phosphonate group replacing the scissile bond of the substrate.[2,24] Peptide derivatives of (α-aminoalkyl)phosphonate diphenyl esters are very specific and reactive inhibitors for many serine proteases.[2] The two phenyl esters on the phosphonic acid moiety are good leaving groups, thereby helping to activate the phosphorous atom for attack by the active site Ser^{195} of the enzyme.[24]

The mechanism of inhibition of serine proteases by peptide phosphonates begins with the formation of the initial non-covalent enzyme-inhibitor (EI) complex (Figure 1.6).[2,23] Ser^{195} attacks the phosphorous atom, forming a pentacoordinate intermediate that quickly decomposes to a tetrahedral covalent complex, losing one phenoxy group in the process. Over time the second phenoxy group is lost due to an aging process, probably due to the imidazole of the active site His^{57}, which could assist in the hydrolysis of the second group.[31] The covalent complex between proteases and peptide phosphonates is remarkably stable, with the half life ($t_{1/2}$) for the dephosphonylation and regeneration of the active enzyme varying from 8 hours to over a week for different enzymes. For example, in stability studies with chymotrypsin and Z-Phe-Pro-$Phe^{P}(OPh)_2$, the $t_{1/2}$ for the dephosphonylation of chymotrypsin was 26 hours.[24] Elastase-phosphonate complexes generally exhibit $t_{1/2}$'s for dephosphonylation of greater than 48 hours, as do many trypsin-phosphonate complexes.[24,25] Complexes of chymotrypsin with phosphonates are even more stable at pH less than 4, which indicates a role for the active site His^{57} in the dephosphonylation reaction.[23]

Inhibition Kinetics. The rates of irreversible inhibition of chymotrypsin by phosphonate inhibitors were measured using an incubation method. In this technique, inhibitor and enzyme are incubated together in buffer, and aliquots of the mixture are

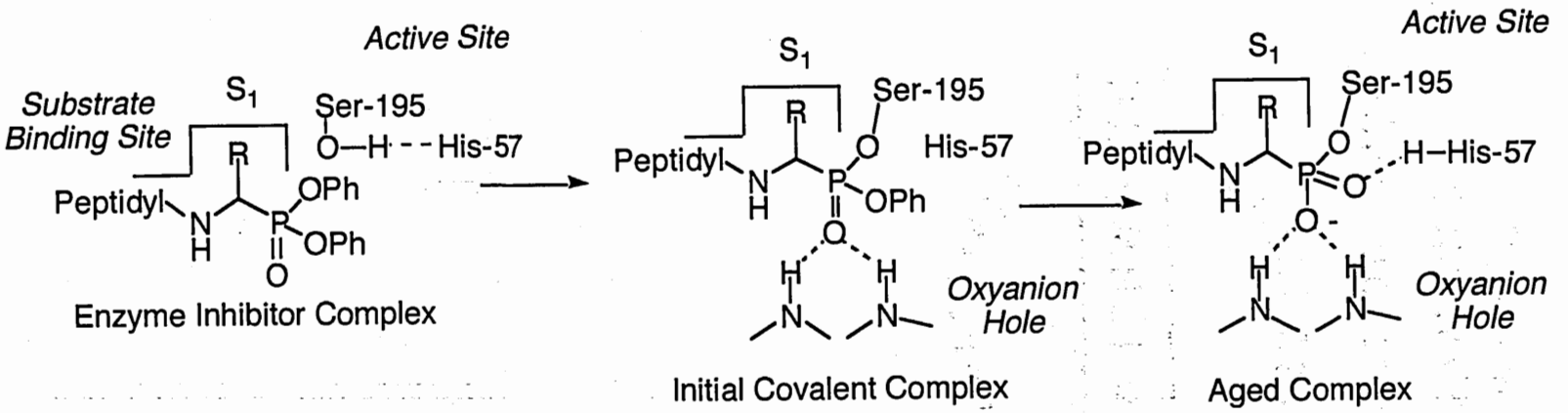

Figure 1.6 Mechanism of Inhibition of Serine Proteases by Peptide Phosphonates.[23]

removed at various times after initiation of inhibition. The aliquots are diluted into a mixture containing buffer and a chromogenic or fluorogenic substrate for the protease. This dilution in essence quenches the inhibition reaction, as the inhibitor and enzyme are at low enough concentrations that they are unlikely to interact at any significant rate. The residual enzyme activity is then measured by monitoring the change in absorbance or fluorescence due to substrate hydrolysis.

The general reaction model for enzyme inactivation by irreversible inhibitors is

$$E + I \underset{k_{-1}}{\overset{k_1}{\rightleftharpoons}} E{\bullet}I \xrightarrow{k_2} E\text{-}I$$

where E is the enzyme and I is the inhibitor. Irreversible inhibition generally proceeds by the rapid formation of a reversible E•I complex, followed by the slower formation of a covalently bound E-I complex, where k_1 and k_{-1} are the rates of formation and breakdown of the reversible E•I complex, respectively, and k_2 is the rate constant for the formation of the stable E-I complex. Inhibition assays are generally performed under pseudo-first order conditions, where the inhibitor concentration ([I]) is at least 10-fold greater than the total enzyme concentration (E_T), and the kinetics are described by the equations of Kitz and Wilson.[32] The total enzyme concentration in the assay is the sum of all enzyme species present, and can be represented by the equation

$$E_T = [E] + [E{\bullet}I] + [E\text{-}I]$$

Since the enzyme-inhibitor solution is diluted before assaying with substrate, the total of the active enzyme species (those without the inhibitor covalently bound to the enzyme) in the assay is given by the equation

$$\varepsilon = [E] + [E\bullet I]$$

The rate of decrease of active enzyme species ($-d\varepsilon/dt$) in the assay is then represented by

$$\frac{-d\varepsilon}{dt} = k_2 [E\bullet I]$$

Substituting the definition of [E•I] into the rate equation gives

$$\frac{-d\varepsilon}{dt} = k_2 (\varepsilon - [E])$$

which can be rearranged into the equation

$$\frac{d\varepsilon}{\varepsilon} = k_2 \left(\frac{[E]}{\varepsilon} - 1\right) dt$$

Integrating both sides of this equation from time 0 to time t (ε_o to ε_t on the left, and 0 to t on the right) gives the equation

$$\ln \left(\frac{\varepsilon_t}{\varepsilon_o}\right) = k_2 t \left(\frac{[E]}{\varepsilon} - 1\right)$$

where ε_o is the concentration of active enzyme species at time 0, and ε_t is the concentration of active enzyme species at time t. As stated previously, the total enzyme concentration (E_T) is equal to

$$E_T = [E] + [E\bullet I] + [E\text{-}I] = \varepsilon + [E\text{-}I]$$

At time 0, [E•I] = 0 and [E-I] = 0, so this equation reduces to $\varepsilon_o = [E]_o = E_T$, and the integrated equation therefore becomes

$$\ln\left(\frac{\varepsilon_t}{E_T}\right) = k_2 t \left(\frac{[E]}{\varepsilon} - 1\right)$$

Substituting for ε on the right side of the equation and rearranging gives

$$\ln\left(\frac{\varepsilon_t}{E_T}\right) = k_2 t \left(\frac{-[E\bullet I]}{[E] + [E\bullet I]}\right)$$

The formation and dissociation of the reversible enzyme-inhibitor complex (E•I) is represented by the dissociation constant K_I

$$K_I = \frac{[E][I]}{[E\bullet I]}$$

Substituting the definition of [E•I] from the K_I equation into the integrated equation and rearranging gives

$$\ln\left(\frac{\varepsilon_t}{E_T}\right) = -k_2 t \left(\frac{[I]}{K_I\,(1 + [I]/K_I)}\right)$$

or, alternatively,

$$\ln\left(\frac{\varepsilon_t}{E_T}\right) = -k_2 t \left(\frac{[I]}{K_I + [I]}\right)$$

Since $[I] >> E_T$, we can define an apparent rate constant, k_{obs}, as

$$k_{obs} = \frac{k_2[I]}{K_I + [I]}$$

where k_{obs} is the pseudo first-order rate constant. Substituting this into the equation gives

$$\ln\left(\frac{\varepsilon_t}{E_T}\right) = -k_{obs}t$$

Since the exact concentration of the active enzyme species at each assay time (ε_t) is unknown, the rate of substrate hydrolysis by residual active enzyme at time t must be used instead. The rate of substrate hydrolysis by residual active enzyme at time t (denoted as v_t) can be substituted for ε_t, and the rate of substrate hydrolysis by a control reaction (v_o), where no inhibitor is present, can be substituted for the total enzyme concentration (E_T). The equation then becomes

$$\ln (v_t/v_o) = -k_{obs} \bullet t$$

A plot of ln (v_t/v_o) versus time (Figure 1.7) gives a straight line whose slope is equal to the negative of the observed rate of inactivation ($-k_{obs}$). The apparent second order rate constant, $k_{obs}/[I]$, is a measure of the potency of an inhibitor and is used to compare the potency of different inhibitors with a given enzyme.

Inhibition of granzyme H by phosphonates was reported in terms of percent inhibition, due to the lack of sufficient enzyme for time-dependent kinetic studies. In this method, small quantities of inhibitor and enzyme are incubated for a set period of time (20 minutes, in this case). After this time period, the mixture is diluted by addition of buffer to quench the inhibition reaction, and the residual enzyme activity is assayed using a chromogenic or fluorogenic substrate. A plot of absorbance versus time was obtained for each inhibitor tested, as well as for a control reaction (no inhibitor present). The slope of the line obtained in such a graph is equivalent to the rate of hydrolysis of the substrate

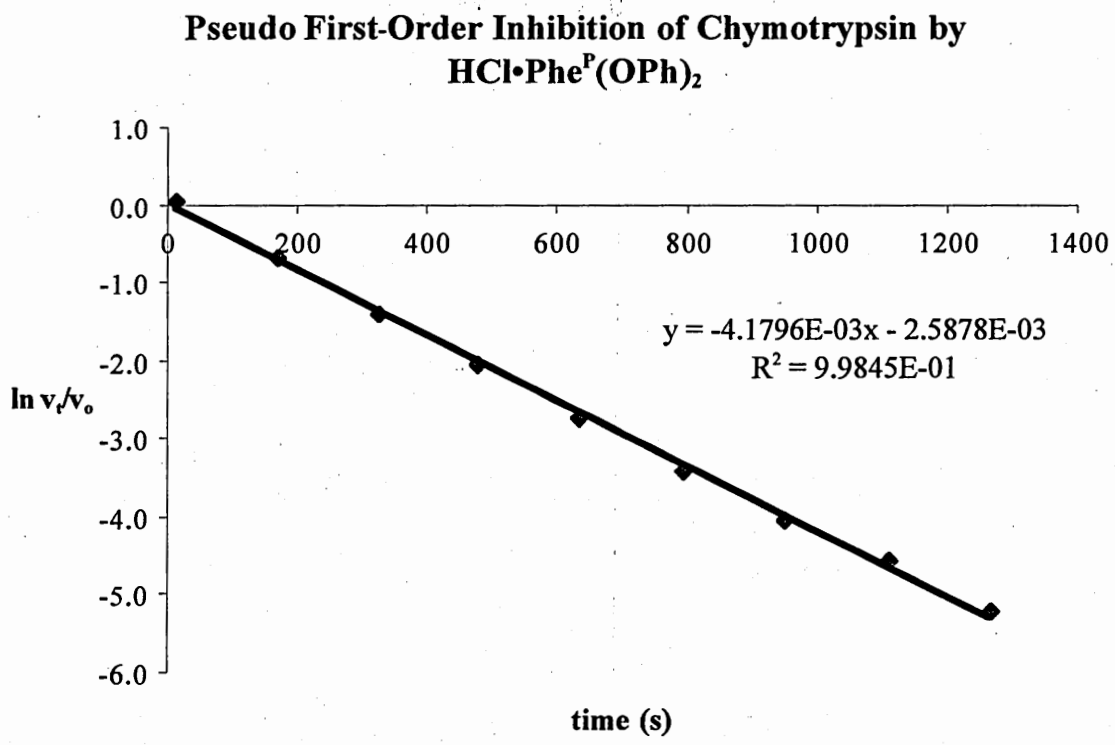

Figure 1.7 Pseudo First-Order Inhibition of Chymotrypsin by HCl•Phe^{P}(OPh)$_2$.

by active enzyme. The slope of the line for each inhibitor was then compared to the slope of the line from the control reaction to give the percent activity from the equation

$$\% \text{ Activity} = \frac{\text{slope}_{\text{inhib.}}}{\text{slope}_{\text{control}}} \times 100$$

Percent inhibition can then be calculated from the equation

$$\% \text{ Inhibition} = 100 - \% \text{ Activity}$$

The percent inhibition can then be used to compare inhibitory activity between compounds even when there is insufficient enzyme available for detailed kinetic studies.

Specificity of GrH, ChT, and Cat G. P1 specificity is partially conferred by the amino acid residue located six positions (position 189) to the N-terminal side of the active site serine (Ser^{195}). Granzyme H, cathepsin G, and chymotrypsin all contain uncharged residues at this position, which forms the bottom of the S1 binding pocket, suggesting that cathepsin G and granzyme H both exhibit chymotrypsin-like activity, which is in agreement with previously published activity studies of these enzymes.[2,4,7,11,12] In chymotrypsin, this residue is Met^{189}, while cathepsin G has Ala in this position and granzyme H has Thr. Residues 192 and 226 are also involved in determining P1 specificity, since they partially fill the S1 pocket and would restrict the size of the P1 amino acid that could fit into the subsite.[2,11] Granzyme H and cathepsin G both have Lys at position 192, while chymotrypsin has Met at this position. Position 226, however, differs slightly between the enzymes. Granzyme H, like chymotrypsin, has Gly at residue 226, suggesting that granzyme H would prefer residues such as Phe or Leu in P1, similar to chymotrypsin.[11] Cathepsin G, however, has Glu at position 226, which

accounts for the documented tolerance of Cat G for Lys at P1 of substrates as well as Phe or Trp.[11,28,33]

Although there is no published crystal structure of granzyme H, there is a crystal structure of Cat G with a phosphonate inhibitor, Suc-Val-Pro-Phe^{P}(OPh)$_2$[33], and multiple crystal structures of chymotrypsin with various inhibitors. Due to the high degree of sequence homology between GrH and Cat G (56% identity, 71% positives), it is predicted that the three dimensional structure of GrH will be very similar to that of Cat G. Sequence alignment was performed using NCBI's Blast 2 sequence program (Version BlastP 2.2.6)[34] on the sequences of human GrH (Swiss-Prot Accession number P20718), human cathepsin G (Swiss-Prot Accession number P08311), and bovine α-chymotrypsin (PDB code 4CHA). Due to the sequence homology between GrH, Cat G, and ChT, there is a good deal of similarity in both the structure and the binding specificity between these enzymes. In Cat G, the active site cleft lies along the surface of the molecule, near the intersection of two β-barrels, with the catalytic triad arranged in the center of the cleft, similar to chymotrypsin.[33] All three enzymes tend to prefer Phe or Phe analogs at P1 to varying degrees.

Peptide Phosphonates with Granzyme H. Although granzyme H has been shown to prefer Phe or Tyr at P1 by substrate analysis[4], very little is known about the specificity of granzyme H at other positions. The percent inhibition data (Table 1.2) for granzyme H with several of the (α-aminoalkyl)phosphonates helps to further elucidate the preferred specificity of this enzyme. GrH clearly prefers tripeptide sequences (Suc-Phe-Leu-Hphe^{P}(OPh)$_2$; 65% inhibition), over shorter sequences (3-phenoxybenzoyl-Hphe^{P}(OPh)$_2$; no inhibition), although it should be noted that none of the simple

Table 1.2 Inhibition of Granzyme H (GrH) by (α-Aminoalkyl)phosphonate Diphenyl Ester Inhibitors and Chloromethyl Ketones.

Inhibitors	Inhibitor Concentration (mM)[a]	% Inhibition (20-min incubation)	Ref.
Suc-Phe-Leu-Hphe^{P}(OPh)$_2$	1.0	65	
Suc-Phe-Leu-PhGly^{P}(OPh)$_2$	1.0	55	
Z-Phe-Leu-Hphe^{P}(OPh)$_2$	1.0	6	
Z-Phe-Leu-PhGly^{P}(OPh)$_2$	1.0	NI[b]	
3-Phenoxybenzoyl-Phe^{P}(OPh)$_2$	1.0	5	
3-Phenoxybenzoyl-Hphe^{P}(OPh)$_2$	1.0	NI	
3-Phenoxybenzoyl-PhGly^{P}(OPh)$_2$	1.0	NI	
FTC-Aca-Phe-Leu-Phe^{P}(OPh)$_2$	1.0	52	
FTC-Aca-Phe-Leu-Phe^{P}(OPh)$_2$	0.1	57	4
Suc-Phe-Leu-Phe-CH_2Cl	0.1	30	4
Boc-Phe-Leu-Phe-CH_2Cl	0.1	NI	4

Table 1.2 (cont'd.)

Z-Gly-Leu-Phe-CH_2Cl	0.1	NI	4
Z-Phe-Leu-$Phe^P(OPh)_2$	0.1	NI	4

[a]Inhibitor concentration in the incubation mixture; all assays were run at an inhibitor to enzyme ratio of 100:1.

[b]NI, no inhibition.

benzyloxycarbonyl amino acid phosphonates (Z-$AA_1{}^P(OPh)_2$) have been tested against GrH. GrH also has a definite preference for the N-terminal Suc group rather than the Cbz group, as shown by comparing the Suc-Phe-Leu-(Hphe/PhGly)$^P(OPh)_2$ (55-65% inhibition) sequences with the analogous Z-Phe-Leu-(Hphe/PhGly)$^P(OPh)_2$ sequences (0-6% inhibition). This preference could indicate a dislike for bulky hydrophobic groups near the P4 subsite. In the crystal structure of Cat G with Suc-Val-Pro-Phe$^P(OPh)_2$, the N-terminal succinyl group is solvent exposed.[33] Hydrophobic groups in this position, such as Cbz or Boc (*tert*-butoxycarbonyl), would react unfavorably with the solvent, and therefore the potency of inhibitors would be reduced. This is further supported by previously tested inhibitors (Z-Phe-Leu-Phe$^P(OPh)_2$, Z-Gly-Leu-Phe-CH_2Cl, and Boc-Phe-Leu-Phe-CH_2Cl)[4], also shown in Table 1.2, which showed no inhibition of GrH, despite the presence of a sequence (Phe-Leu-Phe) known to be a good substrate for this enzyme. The effectiveness of the fluorescent phosphonate derivative, FTC-Aca-Phe-Leu-Phe$^P(OPh)_2$, is in keeping with these results, as the ε-aminocaproic acid (Aca) moiety is similar in structure to the succinyl group. It has also been proposed that GrH may have a remote binding site for very hydrophobic structures such as the FTC.[4] The 3-phenoxybenzoyl derivatives showed little or no activity with GrH; the Phe derivative was the only one of the three to show any activity at 5% inhibition. As 3-phenoxybenzoyl-(4-AmPhGly)$^P(OPh)_2$ was a potent cytolysis inhibitor and was shown to inhibit GrH through localization studies, this result is rather surprising. One possible explanation for this is that the 3-phenoxybenzoyl moiety is simply too large to fit favorably along the active site cleft of GrH. ChT tends to prefer amino acids such as Lys or Pro at P2, but does not like large aromatics such as Phe (Brian J. Rukamp, unpublished results), while Cat G prefers

Pro as well. However, it is possible that the interaction of the charged side chain of the AmPhGly moiety compensated for the unfavorable effects of the 3-phenoxybenzoyl group, possibly by assuming a slightly different binding conformation. Lacking charged side chains, the 3-phenoxybenzoyl compounds synthesized in this project may have nothing to compensate for the unfavorable effects of the large 3-phenoxybenzoyl group, leading to greatly decreased potency of the compounds.

The P1 amino acid preference of GrH was also studied by comparing the members of each series. Suc-Phe-Leu-Hphe^{P}(OPh)$_2$ had a higher percent inhibition than the corresponding peptide with PhGly at P1, indicating that Hphe was slightly preferred over PhGly. This trend was also observed within the Z-Phe-Leu-AA$_1$^{P}(OPh)$_2$ series and the 3-phenoxybenzoyl-AA$_1$^{P}(OPh)$_2$ series, although the differences were slight due to the extremely low percent inhibition exhibited by these compounds. In addition, in the 3-phenoxybenzoyl-AA$_1$^{P}(OPh)$_2$ series, GrH showed a very slight preference for Phe over Hphe. One possible explanation for the preference of Hphe over PhGly is that the S1 subsite in ChT and Cat G, and presumably in GrH as well, is a relatively non-polar, substantially deep pocket.[35,36] The P1 residue should preferentially extend far enough to interact with the residues of the S1 pocket in order to maximize binding interactions for catalysis. In the case of Phe or Hphe, the P1 residue is long enough and flexible enough to fit into the bottom of the S1 pocket, making van der Waals contacts with the hydrophobic residues lining the pocket.[35] However, PhGly is one methylene group shorter and less flexible, and therefore may not fit well into the binding pocket of the enzyme, reducing the potency, but not eliminating the activity, of the inhibitor.

Peptide Phosphonates with Chymotrypsin. A number of phosphonates have been previously synthesized and tested with ChT. The results of the best phosphonates from literature, along with the data from the compounds synthesized in this project, are shown in Table 1.3. Most of the new compounds do inhibit ChT to some degree, although the best compound of the series (Suc-Phe-Leu-Hphe^{P}(OPh)$_2$) only had a k_{obs}/[I] of 873 M^{-1} s^{-1}. Clearly the most potent inhibitor for ChT is the previously synthesized Suc-Val-Pro-Phe^{P}(OPh)$_2$, which had a k_{obs}/[I] of 44,000 M^{-1} s^{-1}, and was also fairly specific for ChT over HLE and PPE.[24]

One of the clearest results is the low inhibitory activity of the phosphonate derivatives with PhGly derivatives at P1. Regardless of chain length, sequence, or N-terminal blocking group, PhGly continually exhibited the lowest rates of any of the inhibitors. For example, when comparing the simple benzyloxycarbonyl derivatives Z-Phe^{P}(OPh)$_2$, Z-Hphe^{P}(OPh)$_2$, and Z-PhGly^{P}(OPh)$_2$, the Hphe derivative exhibited a 19-fold increase in potency over the PhGly derivative, and the Phe compound was 170-fold more potent. This trend was also observed in all other series synthesized, although it was noticeably less pronounced in the 3-phenoxybenzoyl series due to the overall lack of inhibition by these compounds. As with GrH, one possible reason for the lack of inhibition by PhGly derivatives could be that the side chain is simply too short to fully make the requisite binding contacts in the S1 subsite. Since good interaction between the S1 site and the inhibitor's P1 side chain is necessary for inactivation[24], it follows that a side chain too short to interact with the hydrophobic residues deep in the S1 pocket would likely exhibit poor inhibitory potency. Previous studies have also shown that ChT prefers residues such as Phe, Leu, and Met at P1, all of which have longer side chains

Table 1.3 Inhibition of Chymotrypsin by (α-Aminoalkyl)phosphonate Diphenyl Esters.

Compound	Chymotrypsin[a] [I] (μM)[b]	Chymotrypsin[a] $k_{obs}/[I]$ (M^{-1} s^{-1})	Ref.
Z-Phe^{P}(OPh)$_2$[c]	8.2	1200	24
Z-Hphe^{P}(OPh)$_2$	13.4	139	
Z-PhGly^{P}(OPh)$_2$	13.4	7	
HCl•Phe^{P}(OPh)$_2$	8.9	441	
HCl•Hphe^{P}(OPh)$_2$	8.9	434	
HCl•PhGly^{P}(OPh)$_2$	357.1	4	
3-Phenoxybenzoyl-Phe^{P}(OPh)$_2$	17.9	8	
3-Phenoxybenzoyl-Hphe^{P}(OPh)$_2$	17.9	2	
3-Phenoxybenzoyl-PhGly^{P}(OPh)$_2$	17.9	2	
Z-Phe-Leu-Hphe^{P}(OPh)$_2$	17.9	11	
Z-Phe-Leu-PhGly^{P}(OPh)$_2$	8.9	7	
Z-Phe-Leu-Phe^{P}(OPh)$_2$[c]	10.4	110	18
Z-Phe-Pro-Phe^{P}(OPh)$_2$[c]	4.6	17,000	24
HCl•Phe-Leu-Hphe^{P}(OPh)$_2$	6.7	151	
HCl•Phe-Leu-PhGly^{P}(OPh)$_2$	44.6	4	
Suc-Phe-Leu-Hphe^{P}(OPh)$_2$	3.6	873	
Suc-Phe-Leu-PhGly^{P}(OPh)$_2$	267.9	4	
Suc-Val-Pro-Phe^{P}(OPh)$_2$[c]	5.5	44,000	24
Bi-Aca-Aca-Phe-Leu-Phe^{P}(OPh)$_2$[c]	20.8	344	18
FTC-Aca-Phe-Leu-Phe^{P}(OPh)$_2$[c]	8.3	9500	20

Table 1.3 (cont'd.)

TXR-Aca-Phe-Leu-Phe^{P}(OPh)$_2$[c]	8.3	15	[20]

[a]Enzyme concentration in the incubation mixture was 0.357 μM unless otherwise noted.

[b]Inhibitor concentration in the incubation mixture.

[c]Enzyme concentration in the incubation mixture was 1.6 μM.

than PhGly.[24] When comparing Hphe to Phe at P1, in general Phe is strongly preferred over Hphe, with a few notable exceptions. First, in the 3-phenoxybenzoyl series, Phe is only 4-fold more potent than Hphe, although this may not be significant due to the general lack of potency displayed by this series. More significant is the results from the deprotected single amino acid series (HCl•Phe^{P}(OPh)$_2$, HCl•Hphe^{P}(OPh)$_2$, and HCl•PhGly^{P}(OPh)$_2$), where the Phe and Hphe derivatives have equivalent rates. As no other rates for HCl•AA$_1$^{P}(OPh)$_2$ compounds have been published for ChT, it is difficult to rationalize this effect. However, by comparing the Z-Phe^{P}(OPh)$_2$ and Z-Hphe^{P}(OPh)$_2$ compounds to their respective HCl salts, it is possible to speculate on causes of this effect. Phe is the optimal P1 residue for ChT, and, in general, ChT prefers longer sequences such as tri or tetrapeptides over dipeptides, which in turn are favored over monopeptides.[13,18,24] In Z-Phe^{P}(OPh)$_2$, since Phe is the optimal P1 residue, it is possible that the Z group would be aligned with the S2 subsite and could exhibit favorable binding interactions at this site. Z-Hphe^{P}(OPh)$_2$, on the other hand, has a longer side chain than Z-Phe^{P}(OPh)$_2$, which could lead to crowding in the S1 subsite, potentially causing a shift in the alignment of the Z group near the S2 subsite and eliminating some of the favorable interactions seen with Z-Phe^{P}(OPh)$_2$. When the Z group is removed from the Phe derivative, the expected reduction in potency occurs, due probably to the loss of extended binding interactions. In the Hphe derivatives, however, there is an increase in potency over the blocked derivative (Z-Hphe^{P}(OPh)$_2$) when the Z group is removed. This could potentially be caused by a shift in the conformation of Hphe at the S1 subsite, reducing the crowding and assuming an alignment more similar to that exhibited by HCl•Phe^{P}(OPh)$_2$.

Regarding the N-terminal groups on the phosphonates, the tripeptides in general are favored over the amino acid phosphonates and 3-phenoxybenzoyl-blocked phosphonates. In particular, ChT clearly does not favor the 3-phenoxybenzoyl group, possibly because it is a large, relatively rigid structure that cannot interact favorably with the enzyme. ChT prefers residues such as Pro or Lys at P2, and therefore would probably not prefer extremely large hydrophobic groups in that region (Brian J. Rukamp, unpublished results).[18] This could also help explain why Z-Phe^{P}(OPh)$_2$ and Z-Hphe^{P}(OPh)$_2$ exhibit higher rates than the respective Z-Phe-Leu derivatives; Leu is not highly favored at P2, and the Z group could resemble the alignment of Pro at P2, which is highly favored. As shown in the table, although Z-Phe-Leu-Phe^{P}(OPh)$_2$ has 10-fold lower potency than Z-Phe^{P}(OPh)$_2$, the tripeptide with Pro at P2 (Z-Phe-Pro-Phe^{P}(OPh)$_2$) exhibits 14-fold higher potency than Z-Phe^{P}(OPh)$_2$.[24] This indicates that the Leu at P2 is responsible for the loss of some of the potency normally exhibited by tripeptide phosphonates. Alteration of the Z-Phe-Leu-Hphe^{P}(OPh)$_2$ derivative by changing the P2 residue from Leu to Pro would probably result in an increase in potency for this compound as well. The N-terminal group (Cbz, Suc, HCl, or extended) was also compared within the tripeptide phosphonates. In general, compounds with Z groups at the N-terminal had the lowest potency, followed by HCl derivatives. Compounds with Suc or FTC-Aca on the N-terminal exhibited the highest potency. This implies that the hydrophobic nature of the Z-group engenders unfavorable interactions near the S4 subsite of ChT, possibly because this portion of the active site is solvent exposed, as evidenced by the crystal structure of ChT with Eglin-C.[37] HCl derivatives would therefore be expected to be better tolerated, as the charged N-terminus could interact with the solvent.

The succinyl group on the N-terminal would also react favorably to the solvent exposed nature of the site, and can make binding contacts with the S4 region as well, leading to increased potency over both the HCl derivatives and the Z derivatives. For example, Suc-Phe-Leu-Hphe$^{P}(OPh)_2$ shows a 6-fold increase in potency over the corresponding HCl compound, and an 80-fold increase in potency over the Z-derivative. Also evident in the crystal structure is a large groove on the surface of ChT, just past the S4 subsite, which could potentially accommodate a large hydrophobic group such as FTC. This could possibly account for the increased activity of the FTC-Aca-Phe-Leu-Phe$^{P}(OPh)_2$ compound, as the ε-aminocaproic acid moiety is slightly longer than the succinyl group and much longer than the Z group, and the FTC could be positioned close to this groove on ChT.

CONCLUSION

While various studies have shown that GrH is a chymase, and therefore prefers Phe or Tyr at P1, analogous residues have not been studied at P1, and little is known about the enzyme's preferences at other subsites. In this project, a series of peptide (α-aminoalkyl)phosphonate diphenyl esters were synthesized and tested against GrH in order to further study the specificity of this enzyme. They were also tested against ChT for comparison, and to possibly elucidate more information about the binding site of this enzyme as well. These phosphonates are efficient irreversible inhibitors of GrH and ChT. Phosphonates are stable in physiological conditions, unreactive to most other nucleophiles, and have good cell permeability. The most potent compound of the series was Suc-Phe-Leu-Hphe^{P}(OPh)$_2$, which exhibited 65% inhibition against GrH, and had a $k_{obs}/[I]$ of 873 M^{-1} s^{-1} versus ChT. A close second in potency was Suc-Phe-Leu-PhGly^{P}(OPh)$_2$, which had 55% inhibition against GrH, although it was an extremely poor inhibitor ($k_{obs}/[I]$ = 4 M^{-1} s^{-1}) of ChT. Both of these compounds exhibit percent inhibitions with GrH equivalent to or better than the best published inhibitors for this enzyme, FTC-Aca-Phe-Leu-Phe^{P}(OPh)$_2$ (57% inhibition) and Suc-Phe-Leu-Phe-CH_2Cl (30% inhibition).[4] Although none of the phosphonates synthesized were better than currently existing compounds for ChT, they do suggest a new and interesting line of study for this enzyme, as Hphe proved to be a surprisingly efficient P1 residue.

In summary, a series of new phosphonate inhibitors has been synthesized and used to further elucidate the active site binding specificity of GrH. The results of this research should be useful in helping to define the subsite specificity requirements of GrH,

an enzyme with a significant role in lymphocyte-mediated cell death, and for designing the next generation of specific inhibitors of GrH.

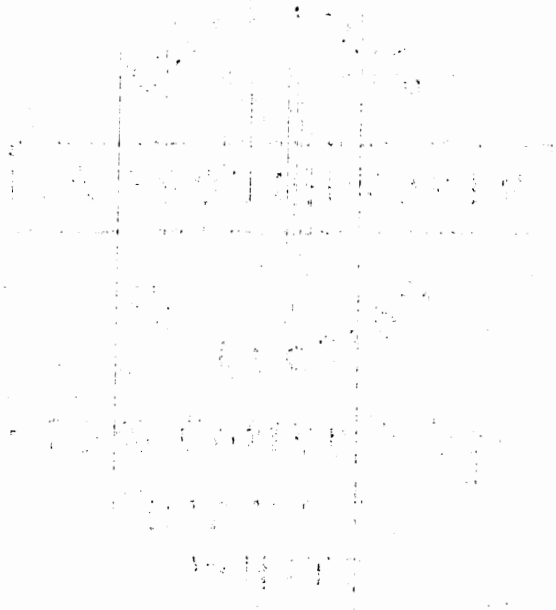

EXPERIMENTAL

Materials and Methods-Synthesis. Benzyl carbamate, triphenyl phosphite, benzaldehyde, hydrocinnamaldehyde, phenylacetaldehyde, Pd/C, 3-phenoxybenzoic acid, succinic anhydride, triethylamine, 1,3-dicyclohexylcarbodiimide, N-hydroxybenzotriazole, N-methylmorpholine, isobutylchloroformate, $CDCl_3$, DMSO-d_6, and all common reagents and solvents were purchased from Aldrich Chemical Company (Milwaukee, WI) or Fischer Scientific Chemicals (Fair Banks, NJ). The protected amino acid derivatives Z-Phe-OH and HCl•H-Leu-OMe were purchased from BACHEM Bioscience, Inc. (King of Prussia, PA). Chromatography silica gel (particle size 32-63 μm) and thin-layer chromatography plates that were pre-coated with 250 μm of silica gel (F-254) were obtained from Scientific Adsorbents, Inc. (Atlanta, GA). Kinetic data was gathered on a Molecular Devices Thermomax Microplate Reader (Molecular Devices Corporation, Menlo Park, CA). ^{1}H NMR spectra were obtained from a Varian Mercury 300 instrument. Mass spectra were collected on either a Micromass Quattro LC (ESI^+) or VG Instruments 70SE (FAB^+). High-resolution mass spectra were collected on either a VG Instruments 70SE (FAB^+) or on the Applied Biosystems QSTAR XL (ESI^+). Elemental analyses were performed by Atlantic Microlabs (Atlanta, GA). All elemental analyses were within ± 0.3% of the calculated values for the formulas shown for each compound.

N-Benzyloxycarbonylphenylalanylleucine methyl ester (Z-Phe-Leu-OMe). Z-Phe-OH (3.001 g, 0.01 mol) was dissolved in dry THF (80 mL) and cooled to -10 °C. NMM (1.014 g, 0.01 mol) was added and the mixture was stirred for 15 min at -10 °C.

IBCF (1.3658 g, 0.01 mol) was added and the mixture stirred for 20 minutes at -10 °C. The HCl•H-Leu-OMe salt (1.819 g, 0.01mol) was dissolved in dry THF (100 mL) and cooled to -10 °C, then NMM (1.014 g, 0.01 mol) was added and the solution was stirred at -10 °C for 20 min before being added to the Z-Phe-OH solution. The resulting mixture was allowed to stir at -10 °C for 30 minutes, then overnight at rt. The solvent was evaporated off, and the resulting white solid was taken up in EtOAc/H_2O. The organic layer was washed with 1M HCl (3 x 50 mL), saturated $NaHCO_3$ (3 x 50 mL), and saturated NaCl (3 x 50 mL), dried over $MgSO_4$, and evaporated to give a white solid (3.434 g, 81% yield). TLC, R_f = 0.686 (2:1 EtOAc:hexanes); ^{1}H NMR ($CDCl_3$) δ 7.4-7.0 (m, 10H), 6.2-6.0 (s, 1H), 5.4-5.2 (s, 1H), 5.1-5.0 (s, 2H), 4.6-4.3 (d, 2H), 3.7-3.6 (s, 3H), 3.2-2.9 (m, 2H), 1.7-1.3 (m, 3H), 0.9-0.7 (m, 6H).

N-Benzyloxycarbonylphenylalanylleucine (Z-Phe-Leu-OH). Z-Phe-Leu-OMe (3.434 g, 0.008 mol) was dissolved in MeOH (100 mL) with stirring. NaOH (1M, 20mL) was added and the reaction stirred at rt for 4 hours and monitored by TLC. The reaction was then cooled to 0 °C and acidified to pH 2 with 1M HCl (35 mL). EtOAc (250 mL) and water (100 mL) were added and the layers separated. The aqueous layer was extracted with EtOAc (3 x 100 mL), and the combined organic layers were washed with water (4 x 100 mL) and saturated NaCl (4 x 50 mL) and dried over $MgSO_4$. The solvent was evaporated to give a white solid (2.626 g, 79% yield). TLC, R_f = 0.230 (2:1 EtOAc:hexanes); ^{1}H NMR (DMSO-d_6) δ 8.3-8.2 (d, 1H), 7.5-7.4 (d, 1H), 7.4-7.0 (m, 10H), 5.0-4.8 (s, 2H), 4.4-4.2 (m, 2H), 3.1-2.9 (d, 1H), 2.8-2.6 (d, 1H), 1.7-1.4 (d of m, 3H), 0.9-0.7 (m, 6H).

(Benzyloxycarbonylaminophenylmethyl)phosphonic acid Diphenyl Ester (Z-PhGly^{P}(OPh)$_2$)-General Phosphonate Synthesis. Diphenyl amino acid phosphonates were synthesized by the method of Oleksyszyn et al.[26] Benzyl carbamate (3.197 g, 0.02 mol), triphenyl phosphite (6.574 g, 0.02 mol) and benzaldehyde (3.368 g, 0.03 mol) were dissolved in glacial acetic acid (25 mL), heated to 85 °C, and reacted 1 hour. The solvent was evaporated off, and the oily residue was taken up in MeOH (150 mL) and placed in the freezer to crystallize. The solid formed was filtered and recrystallized from $CHCl_3$/MeOH, filtered again and dried by vacuum to give white crystals (5.739 g, 57 % yield). Mp = 159.7-161.4 °C; TLC, R_f = 0.722 (2:1 EtOAc:hexanes); ^{1}H NMR ($CDCl_3$) δ 7.5-6.8 (m, 20H), 6.0-5.8 (s, 1H), 5.7-5.5 (q, 1H), 5.2-5.0 (q, 2H); MS (FAB$^+$) *m/z* 474 (M + 1); HRMS (FAB$^+$) *m/z* calculated for $C_{27}H_{25}NO_5P$ (M + 1) 474.14704, found 474.14713. Anal. ($C_{27}H_{24}NO_5P$) C, H, N.

(1-Benzyloxycarbonylamino-3-phenylpropyl)phosphonic acid Diphenyl Ester (Z-Hphe^{P}(OPh)$_2$). This compound was prepared in the same manner as Z-PhGly^{P}(OPh)$_2$ from benzyl carbamate (3.015 g, 0.02 mol), triphenyl phosphite (6.200 g, 0.02 mol), and hydrocinnamaldehyde (4.018 g, 0.03 mol) to give the product as white crystals (3.618 g, 36 % yield). Mp = 115.6-116.7 °C; TLC, R_f = 0.685 (2:1 EtOAc:hexanes); ^{1}H NMR ($CDCl_3$) δ 7.4-7.0 (m, 20H), 5.2-5.1 (d, 3H), 4.6-4.4 (m, 1H), 3.0-2.6 (d of m, 2H), 2.5-2.3 (s, 1H), 2.2-2.0 (s, 1H); MS (FAB$^+$) *m/z* 502 (M + 1); HRMS (FAB$^+$) *m/z* calculated for $C_{29}H_{29}NO_5P$ (M + 1) 502.17834, found 502.17730. Anal. ($C_{29}H_{28}NO_5P$ + 0.25 H_2O) C, H, N.

(1-Benzyloxycarbonylamino-2-phenylethyl)phosphonic acid Diphenyl Ester (Z-Phe^{P}(OPh)$_2$). This compound was prepared in the same manner as Z-PhGly^{P}(OPh)$_2$

from benzyl carbamate (3.115 g, 0.02 mol), triphenyl phosphite (6.375 g, 0.02 mol), and phenylacetaldehyde (3.704 g, 0.03 mol) to give the product as white crystals (2.619 g, 26 % yield). Mp = 124.0-125.1 °C; ^{1}H NMR ($CDCl_3$) δ 7.4-7.0 (m, 21H), 5.2-5.1 (d, 1H), 5.0 (s, 2H), 4.9-4.7 (m, 1H), 3.5-3.4 (m, 1H), 3.1-3.0 (m, 1H); MS (FAB^+) *m/z* 488 (M + 1); HRMS (FAB^+) *m/z* calculated for $C_{28}H_{27}NO_5P$ (M + 1) 488.16269, found 488.16197.

(1-Amino-phenylmethyl)phosphonic acid Diphenyl Ester Hydrochloride (HCl•PhGly^P(OPh)$_2$)- General N-Terminal Deprotection by Hydrogenolysis. Z-PhGly^P(OPh)$_2$ (4.034 g, 0.0085 mol) was dissolved in THF (100 mL) and excess MeOH (250 mL) with stirring. HCl (12M, 1 eq) and Pd/C (5% by wt; 10% number of mol Z-Phgly^P(OPh)$_2$) were added and the reaction mixture subjected to hydrogenolysis until no further H_2 was taken up. The reaction was filtered to remove the Pd/C, and the filtrate evaporated to give a solid, which was rinsed with cold anhydrous diethyl ether and dried by vacuum to give the product as white crystals (3.135 g, 98 % yield). Mp = 179.5-180.9 °C; TLC, R_f = 0.352 (2:1 EtOAc:hexanes); ^{1}H (DMSO-d_6) δ 9.8-9.6 (s, 2H), 7.8-6.9 (m, 15H), 5.7-5.5 (d, 1H); MS (FAB^+) *m/z* 340 ((M + 1) – HCl); HRMS (FAB^+) *m/z* calculated for $C_{19}H_{19}NO_3P$ (M + 1) 340.11026, found 340.10973. Anal. ($C_{19}H_{19}NO_3PCl$ + 0.5H_2O) C, H, N.

(1-Amino-3-phenylpropyl)phosphonic acid Diphenyl Ester Hydrochloride (HCl•Hphe^P(OPh)$_2$). This compound was prepared by hydrogenolysis from Z-Hphe^P(OPh)$_2$ (2.598 g, 0.0052 mol) to give the product as white crystals (2.101 g, quant. yield). Mp = 173.8-175.8 °C; TLC, R_f = 0.315 (2:1 EtOAc:hexanes); ^{1}H (DMSO-d_6) δ 9.4-9.2 (s, 2H), 7.5-7.1 (m, 15H), 4.2-4.0 (m, 1H), 3.0-2.8 (m, 2H), 2.4-2.2 (m, 2H); MS

(FAB$^+$) *m/z* 368 ((M + 1) – HCl); HRMS (FAB$^+$) calculated for $C_{21}H_{23}NO_3P$ (M + 1) 368.14156, found 368.14113. Anal. ($C_{21}H_{23}NO_3PCl$ + 0.5 H_2O) C, H, N.

(1-Amino-2-phenylethyl)phosphonic acid Diphenyl Ester Hydrochloride (HCl•Phe^P(OPh)$_2$). This compound was prepared by hydrogenolysis from Z-Phe^P(OPh)$_2$ (1.530 g, 0.0031 mol). The reaction was filtered to remove the Pd/C, evaporated to give a yellow oil that crystallized on cooling, and dried by vacuum to give the product as off-white crystals (1.127 g, 92% yield). Mp = 156.8-159.6 °C; ^{1}H (DMSO-d_6) δ 9.3-9.0 (s, 2H), 7.5-7.0 (m, 15H), 4.5-4.4 (m, 1H), 3.4-3.3 (d, 2H); MS (FAB$^+$) *m/z* 354 ((M + 1) – HCl); HRMS (FAB$^+$) calculated for $C_{20}H_{21}NO_3P$ (M + 1) 354.12591, found 354.12616.

[(3-Phenoxybenzoylamino)-phenylmethyl]phosphonic acid Diphenyl Ester (3-phenoxybenzoyl-PhGly^P(OPh)$_2$)- General Activated Ester Peptide Coupling Method. HCl•PhGly^P(OPh)$_2$ (1.062 g, 0.0028 mol) and 3-phenoxybenzoic acid (0.607 g, 1 eq) were dissolved in DMF (150 mL) and cooled to 0 °C. NMM (0.320 g, 1.1eq) and HOBt (0.462 g, 1.2 eq) were added and the mixture stirred at 0 °C for 15-20 min. DCC (0.702 g, 1.2 eq) was added and the reaction was stirred 1 hr at 0 °C, then overnight at 4 °C. The reaction mixture was filtered to remove DCU, and the filtrate was evaporated to give a yellow oily liquid. The oil was taken up in EtOAc (or CH_2Cl_2), washed with 1M HCL (3 x 100 mL), saturated $NaHCO_3$ (3 x 100 mL), and saturated NaCl (3 x 100 mL), dried over $MgSO_4$ and evaporated to give a yellow oil. The crude product was purified by silica gel chromatography (eluent: 5% MeOH:CH_2Cl_2) and re-crystallization (95% EtOH), then dried by vacuum to give white crystals (0.608 g, 40% yield). Mp = 113.3-116.4 °C; TLC, R_f = 0.763 (5% MeOH:CH_2Cl_2); ^{1}H NMR (DMSO-d_6) δ 9.8-9.6 (d, 1H),

7.8-6.9 (m, 24H), 6.3-6.1 (d of d, 1H); MS (FAB^+) *m/z* 536 (M + 1); HRMS (FAB^+) calculated for $C_{32}H_{27}NO_5P$ (M + 1) 536.16269, found 536.16262. Anal. ($C_{32}H_{26}NO_5P$) C, H, N.

[1-(3-Phenoxybenzoylamino)-3-phenylpropyl]phosphonic acid Diphenyl Ester (3-phenoxybenzoyl-Hphe^P(OPh)$_2$). This compound was prepared in the same manner as 3-phenoxybenzoyl-PhGly^P(OPh)$_2$ from HCl•Hphe^P(OPh)$_2$ (0.605 g, 0.0015 mol) and 3-phenoxybenzoic acid (0.325 g, 1 eq) to give the product as white crystals (0.237 g, 28% yield). Mp = 131.4-132.9 °C; TLC, R_f = 0.695 (5% MeOH:CH_2Cl_2); ^1H NMR (DMSO-d_6) δ 9.1-9.0 (d, 1H), 7.7-7.0 (m, 24H), 4.9-4.7 (m, 1H), 2.9-2.7 (m, 1H) and 2.7-2.6 (m, 1H), 2.4-2.2 (s, 2H); MS (FAB^+) *m/z* 564 (M + 1); HRMS (FAB^+) calculated for $C_{34}H_{31}NO_5P$ (M + 1) 564.19399, found 564.19526. Anal. ($C_{34}H_{30}NO_5P$) C, H, N.

[1-(3-Phenoxybenzoylamino)-2-phenylethyl]phosphonic acid Diphenyl Ester (3-phenoxybenzoyl-Phe^P(OPh)$_2$). This compound was prepared in the same manner as 3-phenoxybenzoyl-PhGly^P(OPh)$_2$ from HCl•Phe^P(OPh)$_2$ (0.975 g, 0.0025 mol) and 3-phenoxybenzoic acid (0.539 g, 1 eq) to give the product as white crystals (0.705 g, 51% yield). Mp = 118.3-121.5 °C; TLC, R_f = 0.684 (5% MeOH:CH_2Cl_2); ^1H NMR (DMSO-d_6) δ 9.1-9.0 (d, 1H), 7.5-6.9 (m, 24H), 5.1-4.9 (m, 1H), 3.4-3.1 (m, 2H); MS (FAB^+) *m/z* 550 (M + 1); HRMS (FAB^+) calculated for $C_{33}H_{29}NO_5P$ (M + 1) 550.17834, found 550.17829. Anal. ($C_{33}H_{28}NO_5P$) C, H, N.

(Benzyloxycarbonylphenylalanylleucylamino-phenylmethyl)phosphonic acid Diphenyl Ester (Z-Phe-Leu-PhGly^P(OPh)$_2$). This compound was prepared in the same manner as 3-phenoxybenzoyl-PhGly^P(OPh)$_2$ from Z-Phe-Leu-OH (1.034 g, 0.0025 mol)

and HCl•PhGly^{P}(OPh)$_2$ (0.931 g, 0.0025 mol) to give the product as white crystals (0.665 g, 37% yield). Mp = 124.8-128.3 °C; TLC, R_f = 0.509 (5% MeOH:CH_2Cl_2); ^{1}H NMR (DMSO-d_6) δ 9.7-9.3 (d of d, 1H), 8.4-8.1 (d of d, 2 H), 7.7-6.9 (m, 25H), 6.0-5.8 (m, 1H), 5.0-4.8 (d, 2H), 4.8-4.5 (m, 1H), 4.5-4.2 (m, 1H), 3.0-2.8 (m, 1H) and 2.8-2.6 (m, 1H), 1.8-1.2 (m, 3H), 0.9-0.7 (m, 6H); MS (FAB$^+$) *m/z* 734 (M + 1); HRMS (FAB$^+$) calculated for $C_{42}H_{45}N_3O_7P$ (M + 1) 734.29951, found 734.29988. Anal. ($C_{42}H_{44}N_3O_7P$) C, H, N.

(1-Benzyloxycarbonylphenylalanylleucylamino-3-phenylpropyl)phosphonic acid Diphenyl Ester (Z-Phe-Leu-Hphe^{P}(OPh)$_2$). This compound was prepared in the same manner as 3-phenoxybenzoyl-PhGly^{P}(OPh)$_2$ from Z-Phe-Leu-OH (1.226 g, 0.0029 mol) and HCl•Hphe^{P}(OPh)$_2$ (1.121 g, 0.0028 mol) except that after silica gel chromatography, the resulting oil was triturated with petroleum ether and vacuum dried to give the product as white crystals (0.781 g, 35% yield). TLC, R_f = 0.551 (5% MeOH:CH_2Cl_2); ^{1}H NMR (DMSO-d_6) δ 8.8-8.6 (m, 1H), 8.4-8.2 (m, 1H), 7.6-7.4 (m, 1H), 7.4-7.0 (m, 25H), 5.0-4.9 (s, 2H), 4.6-4.2 (m, 3H), 3.1-2.5 (m, 4H), 2.3-2.0 (s, 2H), 1.8-1.3 (m, 3H), 0.9-0.7 (m, 6H); MS (FAB$^+$) *m/z* 762 (M + 1); HRMS (FAB$^+$) calculated for $C_{44}H_{49}N_3O_7P$ (M + 1) 762.33081, found 762.32891. Anal. ($C_{44}H_{48}N_3O_7P$) C, H, N.

(Phenylalanylleucylamino-phenylmethyl)phosphonic acid Diphenyl Ester Hydrochloride (HCl•Phe-Leu-PhGly^{P}(OPh)$_2$). This compound was prepared by hydrogenolysis from Z-Phe-Leu-PhGly^{P}(OPh)$_2$ (0.611 g, 0.00083 mol), except that after filtration, the filtrate was evaporated to give a colorless oil, which was triturated in anhydrous diethyl ether for 1 hour and vacuum dried to give the product as a white solid (0.458 g, 87% yield). TLC, R_f = 0.176 (5% MeOH:CH_2Cl_2); ^{1}H NMR (DMSO-d_6) δ 9.8-

9.4 (m, 1H), 8.9-8.6 (m, 1H), 8.4-8.0 (S, 2H), 7.7-6.8 (m, 20H), 6.0-5.8 (m, 1H), 4.8-4.6 (d, 1H), 4.1-3.9 (m, 1H), 3.1-2.7 (d of m, 2H), 1.8-1.2 (m, 3H), 1.0-0.6 (m, 6H); MS (FAB^+) *m/z* 600 (M + 1); HRMS (FAB^+) calculated for $C_{34}H_{39}N_3O_5P$ (M + 1) 600.26274, found 600.26526. Anal. ($C_{34}H_{39}N_3O_5PCl$ + 1.0 H_2O) C, H, N.

(1-Phenylalanylleucylamino-3-phenylpropyl)phosphonic acid Diphenyl Ester Hydrochloride (HCl•Phe-Leu-Hphe^P(OPh)$_2$). This compound was prepared by hydrogenolysis from Z-Phe-Leu-Hphe^P(OPh)$_2$ (0.732 g, 0.00096 mol) to give the product as white crystals (0.479 g, 75% yield). TLC, R_f = 0.524 (10% MeOH:CH_2Cl_2); ^{1}H NMR (DMSO-d_6) δ 9.1-8.8 (m, 2H), 8.6-8.4 (s, 2H), 7.4-7.0 (m, 20H), 4.7-4.4 (m, 2H), 4.2-4.0 (s, 1H), 3.2-2.5 (d of m, 4 H), 2.2-2.0 (s, 2H), 1.8-1.2 (m, 3H), 1.0-0.6 (m, 6H); MS (FAB^+) *m/z* 628 (M + 1); HRMS (FAB^+) calculated for $C_{36}H_{43}N_3O_5P$ (M + 1) 628.29404, found 628.29419. Anal. ($C_{36}H_{43}N_3O_5PCl$ + 1.0 H_2O) C, H, N.

(Succinylphenylalanylleucylamino-phenylmethyl)phosphonic acid Diphenyl Ester (Suc-Phe-Leu-PhGly^P(OPh)$_2$). HCl•Phe-Leu-PhGly^P(OPh)$_2$ (0.301 g, 0.00047 mol) was dissolved in dry DMF (40 mL) with stirring. Succinic anhydride (0.049 g, 1eq) was added and the solution cooled to 0 °C for 15-20 minutes. Triethyl amine (0.050 g, 1 eq) in dry DMF (5 mL) was added and the mixture was stirred for 30 minutes at 0 °C, then overnight at rt. The reaction was evaporated to give a colorless oily liquid, which was purified by silica gel chromatography (16% MeOH:CH_2Cl_2) to give a colorless oil. Trituration with xylenes and toluene together gave a white powdery solid after solvent evaporation. The solid was further triturated with anhydrous diethyl ether to remove residual xylenes/toluene, giving the product as a yellow oil that hardened after vacuum drying to an off-white crystalline solid (0.238 g, 72% yield). TLC, R_f = 0.500 (16%

MeOH:CH_2Cl_2); ^{1}H NMR (DMSO-d_6) δ 9.6-9.2 (m, 1H), 8.4-7.9 (m, 1H), 7.8-6.8 (m, 20H), 6.0-5.8 (m, 1H), 4.7-4.4 (m, 2H), 3.0-2.8 (m, 2H), 2.7-2.5 (m, 2H), 2.4-2.1 (m, 2H), 1.7-1.2 (m, 3H), 0.9-0.6 (m, 6H); MS (FAB$^+$) *m/z* 700 (M + 1); HRMS (FAB$^+$) calculated for $C_{38}H_{43}N_3O_8P$ (M + 1) 700.27878, found 700.27684. Anal. ($C_{38}H_{42}N_3O_8P$ + 0.5 H_2O) C, H, N.

(1-Succinylphenylalanylleucylamino-3-phenylpropyl)phosphonic acid Diphenyl Ester (Suc-Phe-Leu-Hphe^P(OPh)$_2$). This compound was prepared in the same manner as Suc-Phe-Leu-PhGly^P(OPh)$_2$, from HCl•Phe-Leu-Hphe^P(OPh)$_2$ (0.357 g, 0.00054 mol) and succinic anhydride (0.056 g, 0.00054 mol), except that after initial solvent evaporation the resulting yellow oily liquid was triturated with xylenes/toluene prior to silica gel chromatography (one column in 16% MeOH:CH_2Cl_2 followed by a second column in 20% MeOH:EtOAc). The product was triturated with anhydrous diethyl ether and vacuum dried to give a flaky white solid (0.120 g, 31% yield). TLC, R_f = 0.554 (16% MeOH:CH_2Cl_2), R_f = 0.592 (20% MeOH:EtOAc); ^{1}H NMR (DMSO-d_6) δ 8.7-8.6 (m, 1H), 8.3-8.0 (m, 2H), 7.4-7.0 (m, 20H), 4.6-4.3 (m, 3H), 3.1-2.5 (m, 4H), 2.4-2.0 (m, 6H), 1.7-1.3 (m, 3H), 0.9-0.7 (m, 6H); MS (FAB$^+$) *m/z* 728 (M + 1); HRMS (FAB$^+$) calculated for $C_{40}H_{47}N_3O_8P$ (M + 1) 728.31008, found 728.31251. Anal. ($C_{40}H_{46}N_3O_8P$ + 0.5 H_2O) C, H, N.

Materials and Methods-Enzyme Kinetics. The bovine pancreatic α-chymotrypsin and the thiobenzyl ester substrate Suc-Phe-Leu-Phe-SBzl were purchased from Sigma Chemical Company (St. Louis, MO). The para-nitroanilide substrate Suc-Ala-Ala-Pro-Phe-pNA (chymotrypsin: K_m=60μM, k_{cat}/K_m=3.6 x 10^5 M^{-1} s^{-1})[38] was purchased from BACHEM Bioscience, Inc. (King of Prussia, PA). Granzyme H assays

were performed by Edward Fellows in Dr. Dieter Jenne's lab at the Max Planck-Institute fur Neurobiologie.

Enzyme Kinetics-Incubation Method. The chymotrypsin stock solution was a 20 μM solution in 1 mM HCl (pH 3) and was stored at -20 °C prior to use. Inhibition of chymotrypsin was initiated by adding 50 μL of inhibitor stock solution (0.02-4.0 mM in DMSO) to a solution of 500 μL of assay buffer (0.1 M Hepes, 0.5 M NaCl, pH 7.5) and 10 μL chymotrypsin stock solution at 25 °C. Aliquots of 50 μL were withdrawn from the incubation mixture at various time intervals and added to the assay mixture. The assay mixture contained 200 μL assay buffer and 10 μL of 2 mM Suc-Ala-Ala-Pro-Phe-pNA in DMSO. The residual enzyme activity was measured at 405 nm.

Pseudo first-order inactivation rate constants (k_{obs}) were obtained from plots of ln (v_t/v_o) vs. time. Each k_{obs} value was calculated from 5-10 activity determinations extending to 2-3 half-lives for a given reaction. Control experiments were carried out in the same manner as described above, except DMSO was added in place of the inhibitor stock solution in DMSO. A minimum of two k_{obs} values per inhibitor were determined for each enzyme.

Enzyme Kinetics-Percent Inhibition Assays. Percent inhibition assays of human granzyme H by peptide phosphonates were performed as follows. Stock granzyme H (4.5 μL; 11.11 μM in 25mM MES, 300mM NaCl, pH 6) was incubated for 20 minutes with 0.5 μL of inhibitor stock (10 mM in DMSO) at rt. After 20 minutes, the incubation mixture (5 μL) was diluted by the addition of 95 μL of assay buffer (50 mM Tris, 150 mM NaCl, pH 8). An aliquot (10 μL) of this solution was added to 40 μL of assay buffer in a well of a 96-well plate. A mixture of 2.25 μL of a substrate solution

(Suc-Phe-Leu-Phe-SBzl; 20 mM in DMSO), 2.25 μL of a DTNB solution (20 mM in DMSO) and 45.5 μL of assay buffer was added to the well. The residual enzyme activity was monitored by following the change in absorbance over 45 minutes at 405 nm. A control reaction, substituting DMSO for inhibitor, was monitored for the same length of time to ensure that substrate depletion was not a factor.

Percent inhibition for each inhibitor was calculated from triplicate assays as follows. The data obtained for each inhibitor was averaged and plotted as absorbance vs. time. The slope of the line for each compound was then compared to the slope of the line for the control reaction to give the percent inhibition of the enzyme from the equation

$$\% \text{ Inhibition} = 100 - \% \text{ Activity}$$

where

$$\% \text{ Activity} = \frac{\text{slope}_{\text{inhib}}}{\text{slope}_{\text{control}}} \times 100$$

REFERENCES

(1) Woodard, S. L.; Fraser, S. A.; Winkler, U.; Jackson, D. S.; Kam, C.-M. et al. Purification and characterization of lymphocyte Chymase I, a granzyme implicated in perforin-mediated lysis. *J. Immunol.* **1998**, *160*, 4988-4993.

(2) Kam, C.-H.; Hudig, D.; Powers, J. C. Granzymes (lymphocyte serine proteases): characterization with natural and synthetic substrates and inhibitors. *Biochim. Biophys. Acta* **2000**, *1477*, 307-323.

(3) Masson, D.; Tschopp, J. A Family of Serine Esterases in Lytic Granules of Cytolytic T Lymphocytes. *Cell* **1987**, *49*, 679-685.

(4) Edwards, K. M.; Kam, C.-M.; Powers, J. C.; Trapani, J. The human cytotoxic T cell granule serine protease granzyme H has chymotrypsin-like (chymase) activity and is taken up into cytoplasmic vesicles reminiscent of granzyme B-containing endosomes. *J. Biol. Chem.* **1999**, *274*, 30468-30473.

(5) Atkinson, E. A.; Bleakley, R. C. Mechanisms of lysis by cytotoxic T cells. *Critical Rev. Immunol.* **1995**, *15*, 359-384.

(6) Podack, E. R. Perforin: structure, function, and regulation. *Curr. Top. Microbiol. Immunol.* **1992**, *178*, 175-184.

(7) Hudig, D.; Allison, N. J.; Pickett, T. M.; Winkler, U.; Kam, C.-M. et al. The function of lymphocyte proteases. Inhibition and restoration of granule-mediated lysis with isocoumarin serine protease inhibitors. *J. Immunol.* **1991**, *147*, 1360-1368.

(8) Hudig, D.; Gregg, N. J.; Kam, C.-M.; Powers, J. C. Lymphocyte granule-mediated cytolysis requires serine protease activity. *Biochem. Biophys. Res. Commun.* **1987**, *149*, 882-888.

(9) Hudig, D.; Allison, N. J.; Kam, C.-M.; Powers, J. C. Selective isocoumarin serine protease inhibitors block RNK-16 lymphocyte granule-mediated cytolysis. *Mol. Immunol.* **1989**, *26*, 793-798.

(10) Woodard, S. L.; Jackson, D. S.; Abuelyaman, A. S.; Powers, J. C.; Winkler, U. et al. Chymase-directed serine protease inhibitor that reacts with a single 30 kDa granzyme and blocks NK-mediated cytotoxicity. *J. Immunol.* **1994**, *153*, 5016-5025.

(11) Haddad, P.; Jenne, D.; Tschopp, J.; Clement, M. V.; Mathieu-Mahul, D. et al. Structure and evolutionary origin of the human granzyme H gene. *Int. Immunol.* **1991**, *3*, 57-66.

(12) Martin, S. J.; Amarante-Mendes, G. P.; Shi, L.; Chuang, T.-H.; Casiano, C. A. et al. The cytotoxic cell protease granzyme B initiates apoptosis in a cell-free system by proteolytic processing and activation of the ICE/CED-3 family protease, CPP32, via a novel two-step mechanism. *EMBO J.* **1996**, *15*, 2407-2416.

(13) Odake, S.; Kam, C.-M.; Narasimhan, L.; Poe, M.; Blake, J. T. et al. Human and murine cytotoxic T lymphocyte serine proteases: subsite mapping with peptide thioester substrates and inhibition of enzyme activity and cytolysis by isocoumarins. *Biochemistry* **1991**, *30*, 2217-2227.

(14) Ewoldt, G. R.; Smyth, M. J.; Darcy, P. K.; Harris, J. L.; Craik, C. S. et al. RNKP-4 and RNKP-7, new granzyme serine proteases expressed in activated rat lymphocytes. *J. Immunol.* **1997**, *158*, 4574-4583.

(15) Shi, L.; Kraut, R. P.; Aebersold, R.; Greenberg, A. H. A natural killer cell granule protein that induces DNA fragmentation and apoptosis. *J. Exp. Med.* **1992**, *175*, 553-566.

(16) Shi, L.; Kam, C.-M.; Powers, J. C.; Aebersold, R.; Greenberg, A. H. Purification of three cytotoxic lymphocyte granule serine proteases that induce apoptosis through distinct substrate and target cell interactions. *J. Exp. Med.* **1992**, *176*, 1521-1529.

(17) Heusel, J. W.; Wesselschmidt, R. L.; Shresta, S.; Russel, J. H.; Ley, T. J. Cytotoxic lymphocytes require granzyme B for the rapid induction of DNA fragmentation and apoptosis in allogeneic target cells. *Cell* **1994**, *76*, 977-987.

(18) Abuelyaman, A. S.; Jackson, D. S.; Hudig, D.; Woodard, S. L.; Powers, J. C. Synthesis and kinetic studies of diphenyl 1-(*N*-peptidylamino)alkanephosphonate esters and their biotinylated derivatives as inhibitors of serine proteases and probes for lymphocyte granzymes. *Arch. Biochem. Biophys.* **1997**, *344*, 271-180.

(19) Schecter, I.; Berger, A. On the size of the active site in protease. 1. Papain. *Biochem. Biophys. Res Commun.* **1967**, *27*, 157-162.

(20) Abuelyaman, A. S.; Hudig, D.; Woodard, S. L.; Powers, J. C. Fluorescent derivatives of diphenyl[1-(*N*-peptidylamino)alkyl]phosphonate esters: synthesis and use in the inhibition and cellular localization of serine proteases. *Bioconjugate Chem.* **1994**, *5*, 400-405.

(21) Jackson, D. S.; Fraser, S. A.; Ni, L.-M.; Kam, C.-M.; Winkler, U. et al. Synthesis and evaluation of diphenyl phosphonate esters as inhibitors of the trypsin-like granzymes A and K and mast cell tryptase. *J. Med. Chem.* **1998**, *41*, 2289-2301.

(22) Hamilton, R.; Walker, B. J.; Walker, B. A convenient synthesis of N-protected diphenyl phosphonate ester analogues of ornithine, lysine, and homolysine. *Tetrahedron Letters* **1993**, *34*, 2847-2850.

(23) Oleksyszyn, J.; Powers, J. C. Amino acid and peptide phosphonate derivatives as specific inhibitors of serine peptidases. *Meth. Enzymol.* **1994**, *244*, 442-457.

(24) Oleksyszyn, J.; Powers, J. C. Irreversible inhibition of serine proteases by peptide derivatives of (α-aminoalkyl)phosphonate diphenyl esters. *Biochemistry* **1991**, *30*, 485-493.

(25) Oleksyszyn, J.; Powers, J. C. Irreversible inhibition of serine proteases by peptidyl derivatives of alpha-aminoalkylphosphonate diphenyl esters. *Biochem Biophys Res Commun* **1989**, *161*, 143-149.

(26) Oleksyszyn, J.; Subotkowsa, L.; Mastalerz, P. Diphenyl 1-aminoalkanephosphonates. *Synthesis* **1979**, 985-986.

(27) Voet, D.; Voet, J. G. Serine proteases. *Biochemistry*; John Wiley & Sons, Inc.: New York, 1995; pp 389-400.

(28) Powers, J. C.; Zimmerman, M. Inhibitors of elastases, chymases, and cathepsin G. *Design of Enzyme Inhibitors as Drugs*; Oxford University Press: Oxford, 1989.

(29) Powers, J. C.; Harper, J. W. Inhibitors of serine proteases. *Proteinase Inhibitors*; Elsevier: Amsterdam, 1985; pp 55-152.

(30) Dixon, M.; Webb, E. C. *Enzymes*; Second ed.; Academic Press, Inc.: New York, 1964; 950.

(31) Bender, M. L.; Wedler, F. C. Phosphate and carbonate ester "aging" reactions with α-chymotrypsin. Kinetics and mechanism. *J Am Chem Soc* **1972**, *94*, 2101-2109.

(32) Kitz, R.; Wilson, I. B. Esters of methanesulfonic acid as irreversible inhibitors of acetylcholinesterase. *J. Biol. Chem.* **1962**, *237*, 3245-3249.

(33) Hof, P.; Mayr, I.; Huber, R.; Korzus, E.; Potempa, J. et al. The 1.8 Å crystal structure of human cathepsin G in complex with Suc-Val-Pro-Phe^{P}-$(OPh)_2$: a Janus-faced proteinase with two opposite specificities. *Embo J* **1996**, *15*, 5481-5491.

(34) NCBI National Center for Biotechnological Information. *http://www.ncbi.nlm.nih.gov*.

(35) Steitz, T. A.; Henderson, R.; Blow, D. M. Structure of crystalline alpha-chymotrypsin. 3. Crystallographic studies of substrates and inhibitors bound to the active site of alpha-chymotrypsin. *J Mol Biol* **1969**, *46*, 337-348.

(36) Schellenberger, V.; Braune, K.; Hofmann, H. J.; Jakubke, H. D. The specificity of chymotrypsin. A statistical analysis of hydrolysis data. *Eur J Biochem* **1991**, *199*, 623-636.

(37) Frigerio, F.; Coda, A.; Pugliese, L.; Lionetti, C.; Menegatti, E. et al. Crystal and molecular structure of the bovine alpha-chymotrypsin-eglin c complex at 2.0 Å resolution. *J Mol Biol* **1992**, *225*, 107-123.

(38) Ermolieff, J.; Boudier, C.; Laine, A.; Meyer, B.; Bieth, J. G. Heparin protects cathepsin G against inhibition by protein proteinase inhibitors. *J Biol Chem* **1994**, *269*, 29502-29508.

CHAPTER 2

PEPTIDE α-KETO AMIDES AS INHIBITORS OF CASPASES

INTRODUCTION

Apoptosis, or programmed cell death, is the normal means of cell turnover in an organism, responsible for both homeostasis of the organism as well as defense against pathogens. Apoptosis is a well ordered process, characterized by DNA fragmentation, membrane blebbing, chromatin condensation, and cell shrinkage.[1] This process involves a cascade of enzymes known as caspases, which mediate many of the proteolytic events involved in apoptosis.[2] There are two major apoptotic pathways, extrinsic and intrinsic, that are employed in programmed cell death, both of which lead to activation of the downstream effector caspases (Figure 2.1a). The extrinsic pathway, which relies on a cell-surface stimulus, transmits a death signal to the cell's interior through the interaction of a death ligand, such as tumor necrosis factor, with its receptor, thereby activating the initiator caspases 8 and 10. The intrinsic pathway is mediated by cytochrome c in the mitochondria and is activated by cellular stress. This pathway relies on the activation of caspase 9 to begin the apoptotic cascade by activating the downstream caspases.[3-5] Excessive apoptosis has been linked to a variety of disease states, including ischemic injury (myocardial infarction and stroke), neurodegenerative disorders (Alzheimer's disease and Parkinson's disease), multiple sclerosis, and many others.[6-9] In models related to Parkinson's disease, stroke, and other disease states, inhibition of various caspases has blocked apoptosis in the afflicted area.[7,10,11] Caspases are therefore

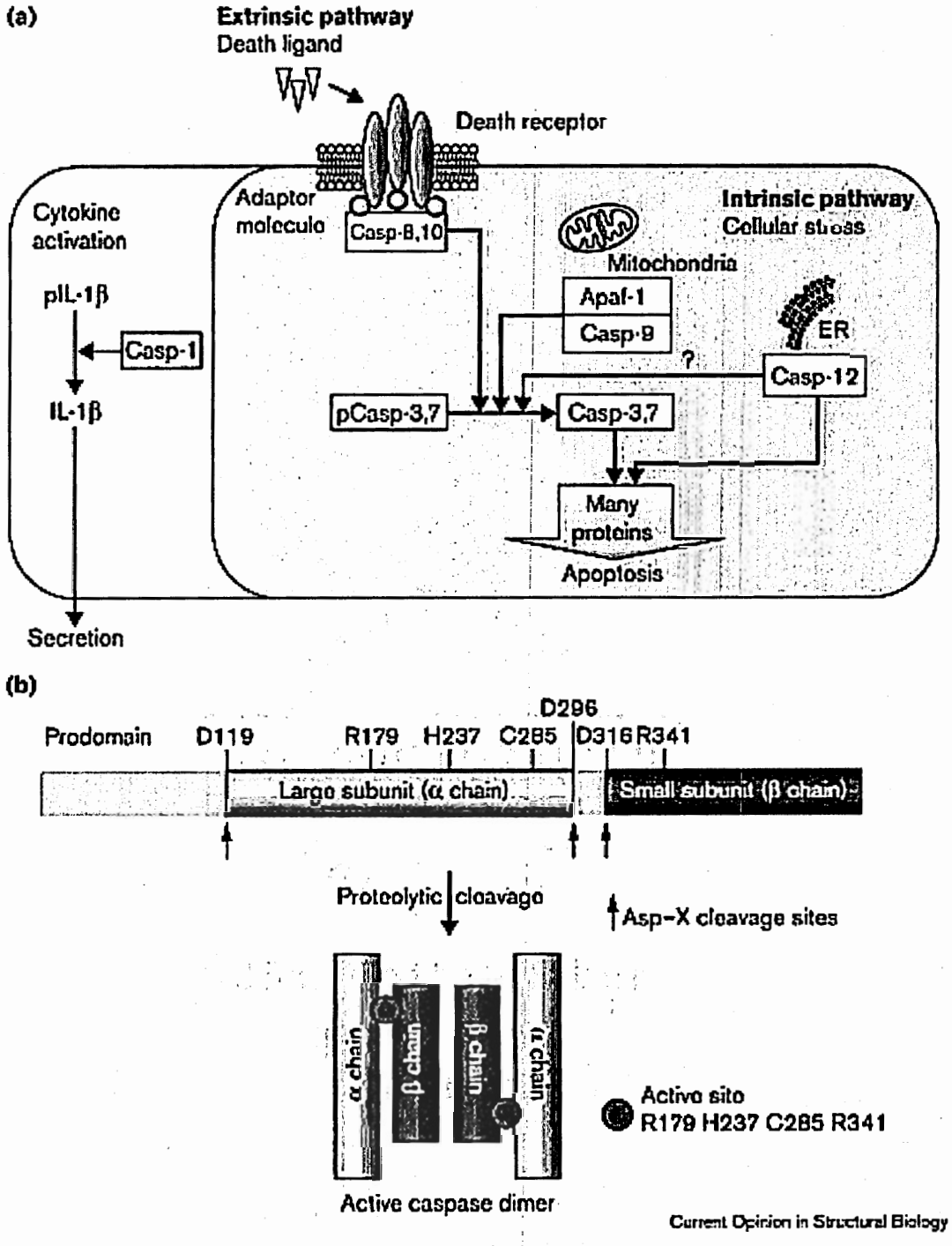

Figure 2.1 Role of Caspases in the Major Apoptotic Pathways. **a)** Schematic representation of the known pathways in which caspases are involved. **b)** Schematic representation of the proteolytic activation of caspases.[5]

therapeutically significant targets for drug design.

Caspases (*c*ysteine *asp*artate-specific prote*ases*) are a family of cysteine proteases with a very stringent and unusual specificity for Asp at the P1 subsite. The only other known mammalian protease with this specificity is the serine protease granzyme B, which is also involved in apoptosis. The fourteen members of the caspase family can be divided into three main groups, each with a different cellular function. Group I caspases (caspases 1, 4, 5, 11, 12, 13 and 14) are involved primarily in the inflammation pathways of the cell, but are not directly involved in apoptosis. The effectors of apoptosis, group II caspases (caspases 2, 3, and 7), are involved in cleavage of key homeostatic and structural proteins in the cell, which leads to cell death (Figure 2.2).[2,12] Caspase 3, especially, is considered to be a very important enzyme in the apoptotic cascade, since it activates other caspases (6 and 9) and also cleaves most of the nuclear and cytoplasmic targets.[1,13] Group III caspases (caspases 6, 8, 9, and 10) are considered to be the initiator caspases, involved in the early stages of apoptosis and often functioning to activate other caspases in the cascade.[1] Caspase 6 is particularly distinctive in that it is the only known caspase to cleave the lamins, which are the main structural proteins of the nuclear envelope.[14] Caspase 8 is also unique in that it can cleave the proenzymes of all other known caspases and is believed to be at the very top of the apoptotic cascade.[12] Caspases 3, 6, and 8 are believed to be key players in apoptosis, and specific inhibitors for each caspase would be particularly useful in elucidating their specific roles.

Caspases are activated by the removal of a variable length (2-25 kDa) N-terminal peptide from the inactive proenzyme form (Figure 2.1b).[1,5] Specific cleavage of a short linker peptide within the proteolytic domain is also required in order to generate the large

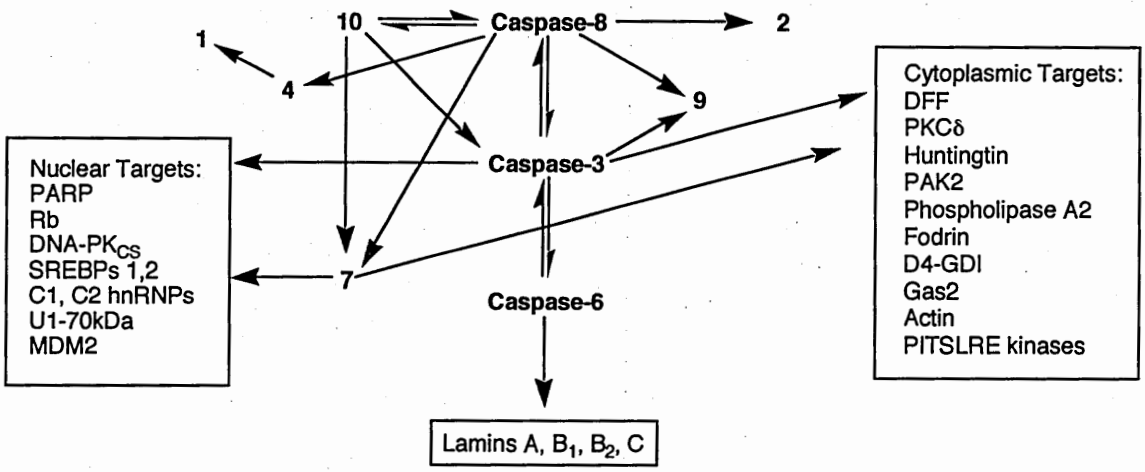

Figure 2.2 The Relationship Between Various Caspases and Some Natural Substrates.[12]

and small subunits of the active enzyme.[1,5,15] The downstream effector caspases are activated through proteolysis by the active initiator caspases. Caspase 8, as an initiator caspase, is activated by a slightly different method. The caspase 8 proenzyme has limited proteolytic activity, and at high concentrations, it can activate itself by intramolecular processing.[5,16]

The secondary, tertiary, and quaternary structures of the members of the caspase family are very similar. A representative structure is shown in Figure 2.3.[17] All active caspases are heterodimers composed of two subunits, a large (17-21 kDa) α subunit and a smaller (10-13 kDa) β subunit.[1,2,5] Each α/β heterodimer is made up of a central β-sheet core (consisting of five parallel and one anti-parallel β-strands) surrounded by five α-helices (two on one side, and three on the other).[5,17] The two subunits are very closely associated, and the catalytic domain is located at the interface between the two subunits, at the C-terminal end of the parallel β-strands.[5] Each subunit contributes important residues to the active site, which lies in a groove on the surface of the dimer.[1,2,5] In

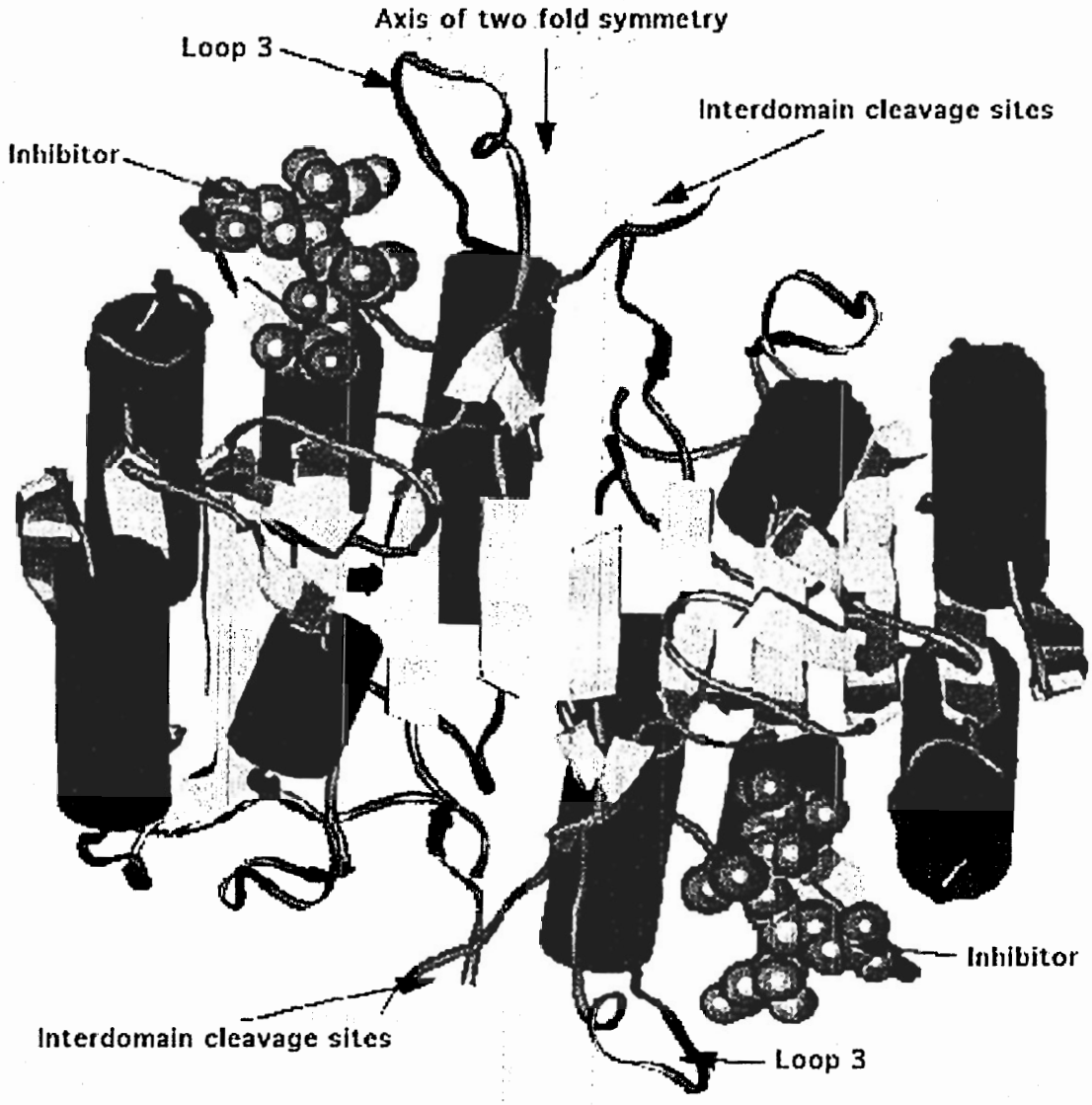

Figure 2.3 Tetrameric Structure of Caspase 3. Arrows represent β-strands, while cylinders represent α-helices.[17]

solution, two heterodimers associate into an $(\alpha/\beta)_2$ tetramer, which is believed to be the active form of the enzymes.[1,2,5] The catalytic diad of Cys^{285} and His^{237}, both of which are found on the large subunit, is conserved in all members of the caspase family. The residues Arg^{179}, Gln^{283}, and Arg^{341}, which confer the specificity for Asp at P1 and help to stabilize that Asp residue through hydrogen bonding interactions, are also conserved in all caspases.[1,2,5]

The caspases have a stringent requirement for Asp at P1. Substituting Glu for Asp results in greater than 100 fold reduction in the rate of activity.[18,19] They also require at least four amino acids on the N-terminal side of the scissile bond for specificity. In fact, the amino acid at P4 is the single most important determinant of specificity between various caspases.[1,2,5,20] The substrate specificity for each of the three groups of caspases has been determined using positional scanning substrate libraries.[20] Group I caspases have Trp-Glu-His-Asp as their optimal peptide sequence, although other large hydrophobic and aromatic amino acids are also tolerated at P4. Group II caspases prefer the sequence Asp-Glu-*Xaa*-Asp, where *Xaa* is any of a variety of hydrophobic amino acids. It is interesting to note that group II caspases have an absolute requirement for Asp at P4, due largely to a highly restricted S4 binding site.[1] Group III caspases prefer the sequence (Leu/Val)-Glu-*Xaa*-Asp, where *Xaa*, as with group II caspases, can be a variety of hydrophobic amino acids. Group III caspases can tolerate a wide variety of amino acids at P4, but they strongly prefer branched hydrophobic residues, especially Leu, Val, Ile, and Thr. All three groups of caspases strongly prefer Glu at the P3 position.[1,2,20]

In addition to data from the synthetic substrate libraries, the optimal sequences for caspases 3, 6, and 8 have been determined from their natural substrate cleavage sites.[20] The preferred substrate sequence for caspase 3 is Asp-Glu-Val-Asp. Several of the cellular targets of caspase 3, such as poly(ADP-ribose) polymerase and DNA-dependent protein kinase also contain this sequence.[21,22] The optimal sequence for caspase 6 determined from the synthetic substrate library studies is Val-Glu-His-Asp. However, the sequence Val-Glu-Val-Asp is also very good for caspase 6, and is very similar to the natural cleavage site of lamin A (Val-Glu-Ile-Asp), which is known to be cleaved almost exclusively by caspase 6.[23,24]. Based on results from the synthetic libraries, the optimal sequence for caspase 8 is Leu-Glu-Thr-Asp. This sequence is very similar to the activation cleavage sequence of caspase 3 (Ile-Glu-Thr-Asp), which is believed to be one of the natural substrates of caspase 8.[1,20,25,26]

A variety of reversible inhibitors have been synthesized for several of the caspases, such as peptide aldehydes and α-keto derivatives. Several peptide aldehydes have been designed for the caspases, especially caspase 1, and are potent inhibitors.[27] Ac-Asp-Glu-Val-Asp-H inhibited caspase 3 with a K_i of 0.23 nM, caspase 1 with a K_i of < 6 nM, and caspase 8 with a K_i of 0.92 nM.[27] Although this compound discriminated well between caspase 3 and caspases 6 and 10, it showed very poor selectivity between caspase 3 and caspases 1 and 8 (only 4-fold more potent towards caspase 3 than caspase 8). A second compound, Boc-Ile-Glu-Thr-Asp-H, inhibited caspase 8 with a K_i of 1.05 nM, but also inhibited caspase 6 with a K_i of 5.6 nM (5-fold selectivity between the two enzymes). Therefore, it is still not possible to differentiate between the caspases, since the peptide aldehydes tend to be less selective.[27] Also, peptide aldehydes cannot be

extended to the prime side (P') of the scissile bond and can only interact with the S subsites, limiting their contact with the enzyme active site.

In contrast to peptide aldehydes, peptide α-keto derivatives (Figure 2.4) are easily extended in the P' direction, allowing for greater potency and selectivity of the inhibitor.

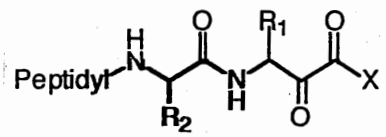

α-keto acid, X = OH
α-keto ester, X = OR'
α-keto amide, X = NHR'

Figure 2.4 General Structure of Peptide α-Keto Derivatives.

Peptide α-keto derivatives (esters, amides, and acids) were initially studied as reversible inhibitors of serine proteases,[28] based on the crystal structure of the α-keto acid 4-amidinophenylpyruvate (APPA) with trypsin.[29,30] This structure showed that trypsin's active site serine had added to the N-terminal side carbonyl of APPA, giving a tetrahedral adduct with the oxyanion stabilized by interactions with the enzyme's oxyanion hole. Peptide α-keto esters inhibit various serine proteases, such as HLE, PPE, ChT, trypsin, plasmin and thrombin.[28,31,32] Later, α-keto derivatives were studied with cysteine proteases, including papain, calpain, and cathepsin B (Cat B).[32-35] Hu and Abeles synthesized a series of α-keto esters, α-keto amides, and α-keto acids for Cat B and papain, with K_i values ranging from 0.15 μM – 23 μM. Their results showed that the second carbonyl group was necessary for inhibition. Analogues with only a single carbonyl had K_i values 65-2000 fold higher than the corresponding compounds with two

carbonyls.[35] Hu and Abeles also found that α-keto ester and α-keto amide inhibitors were more potent inhibitors than α-keto acids for papain.[35] Other studies have shown that, in general, α-keto acids are more potent than α-keto amides, which are better than α-keto esters, *in vitro*. However, due to their sensitivity to esterases, α-keto esters are highly unstable *in vivo*, and α-keto acids have poor membrane permeability due to their charge.[36,37] In contrast, α-Keto amides are stable *in vivo*, since they are not susceptible to esterases. Previous studies have shown that α-keto amides have good membrane permeability. In studies of α-keto amides designed for caspase 1, cell permeability was tested by a peripheral blood mononuclear cell assay, which measures the ability of an inhibitor to penetrate a cell and inhibit the target enzyme. Most of the potent inhibitors, such as Ac-Tyr-Glu-Val-Asp-CO-NH-$(CH_2)_2$Ph, also had good cell permeability, with an IC_{50} of < 2 μM (James C. Powers, unpublished results). α-Keto amides, which are competitive reversible transition state inhibitors that often exhibit slow binding inhibition, have demonstrated biological activity *in vivo*.[38-40] The biggest advantage over other classes of inhibitors, however, is that α-keto amides can be extended in the P' direction, allowing for additional enzyme-inhibitor interactions and generating increased potency.

α-Keto amides have an extremely electrophillic carbonyl at the scissile bond and, when inhibiting the enzyme, resemble the tetrahedral transition state of enzyme-substrate reactions.[41] In the enzyme-inhibitor complex, the active site cysteine adds to the electrophillic carbonyl (closer to the N-terminal), giving a hemithioketal adduct, but cannot complete the hydrolysis due to the lack of a good leaving group. This is similar to the previously observed adduct formation between peptide aldehydes and papain.[35] The

active site cysteine attacks at the carbonyl closer to the N-terminal of the peptide because it is located where the scissile bond of natural substrates would be. The second carbonyl, on the P' side of the scissile bond, is unfavorably positioned in the active site for the necessary reaction with cysteine to occur. Evidence for this theory is that reduction of the first carbonyl (N-terminal side) leads to complete loss of inhibitory activity.[35] Also, in previous studies of α-keto amides with serine proteases, ^{13}C NMR has shown that the active site serine adds only to the first carbonyl.[32] Finally, in previous crystal structures of caspase 1 complexed with α-keto amide inhibitors, such as 4-Cl-$PhCH_2CH_2CO$-Val-Ala-Asp-CO-NH-CH_2CH_2Ph, Cys^{285} adds to the N-terminal carbonyl, generating a tetrahedral intermediate (Figure 2.5).[42]

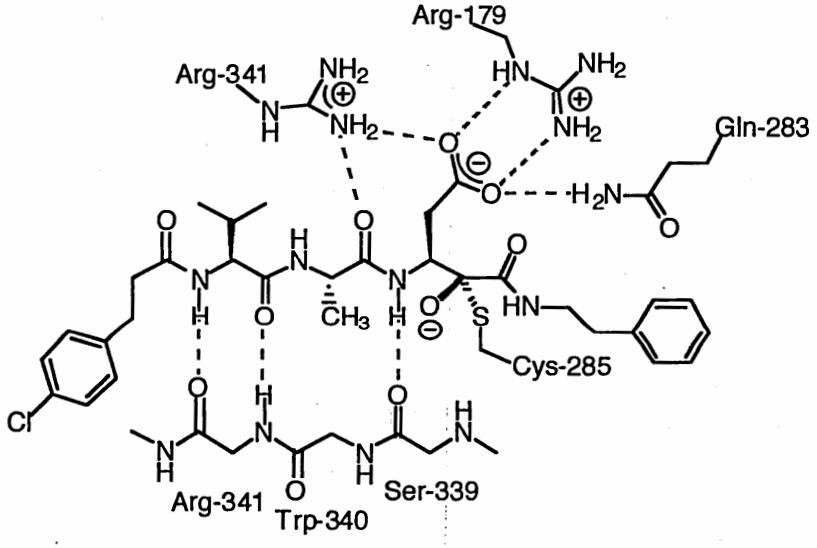

Figure 2.5 Schematic of the Binding of an α-Keto Amide Inhibitor, 4-Cl-$PhCH_2CH_2CO$-Val-Ala-Asp-CO-NH-CH_2CH_2Ph, with Caspase 1.[42]

Clearly, potent inhibitors for caspases 3, 6, and 8 would be advantageous in the study of the apoptotic cascade, as well as potential therapeutic agents. α-Keto amides, with their ability to be extended to the P' side, biological activity *in vivo*, resistance to esterases, and good membrane permeability, are ideal candidates for inhibitor design. Some α-keto amides have already proven to be good inhibitors of caspases 1 and 3. Boc-Asp-Glu-Val-Asp-CO-NH$(CH_2)_2$Ph had a K_i for caspase 1 of 12.5 nM, and a K_i for caspase 3 of 5 nM (James C. Powers, unpublished results). Since no selective and potent inhibitors have been discovered for caspases 6 and 8, it is logical to extend the α-keto amide design to these caspases. Based on the optimal tetrapeptide sequences for these caspases, a series of α-keto amide inhibitors was designed, utilizing a variety of P' residues in order to elucidate the P' preferences of the different caspases and generate greater potency (Figure 2.6).

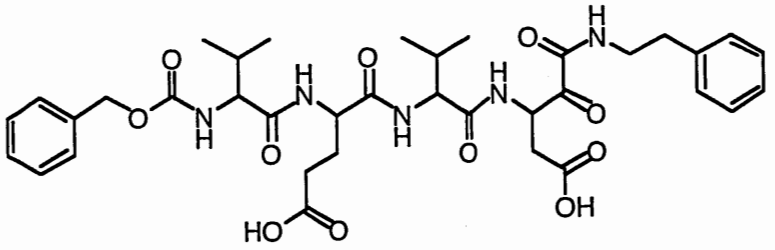

Caspase 6 Inhibitor: Z-Val-Glu-Val-Asp-CO-NH-$(CH_2)_2$Ph

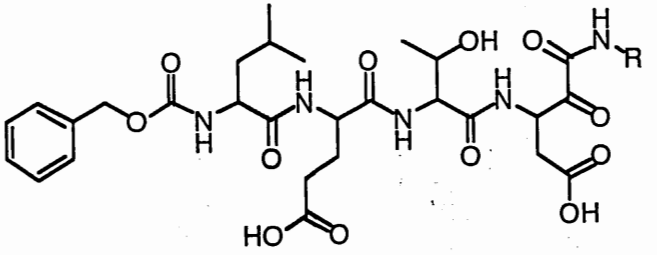

R = CH_2Ph, $(CH_2)_2$Ph, $(CH_2)_3$Ph, or $(CH_2)_3OCH_3$

Caspase 8 Inhibitors: Z-Leu-Glu-Thr-Asp-CO-NH-R

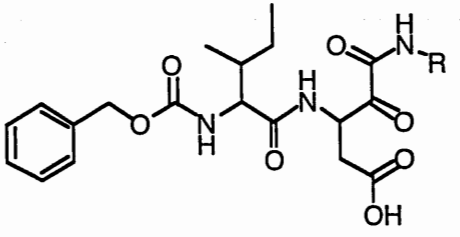

R = $(CH_2)_3$Ph or $(CH_2)_3OCH_3$

Dipeptide Inhibitors: Z-Ile-Asp-CO-NH-R

Figure 2.6 α-Keto Amide Inhibitors Synthesized for Caspases.

RESULTS AND DISCUSSION

Based on the optimal substrate sequences previously reported for caspases 6 and 8, a series of peptide α-keto amide inhibitors was synthesized. These α-keto amides were designed to study the preferences of caspase 6 and 8 on the prime side of the scissile bond, and hopefully generate more potent inhibitors. The first group of compounds synthesized was based on the optimal sequence for caspase 8, Z-Leu-Glu-Thr-Asp.[20] A compound based on the optimal sequence of caspase 6, Z-Val-Glu-Val-Asp,[20] was also synthesized, as were two dipeptides.

Synthesis. The parent compounds, N-terminal and side chain protected aspartyl α-keto amides, were synthesized by an adaptation of the method of Wasserman and Ho (Scheme 2.1).[41] Triphenyl cyanomethyl phosphonium bromide (**1**) is synthesized by refluxing bromoacetonitrile with triphenyl phosphine. The cyanophosphorane generated *in situ* from compound **1** was then added to the mixed anhydride derivative of Cbz-Asp(*t*Bu)-OH to generate an aspartyl phosphorane (**2**). Ozonolysis of the aspartyl phosphorane **2** at -78 °C gave a highly reactive dicarbonylnitrile intermediate, which was immediately treated with the appropriate amine to generate blocked aspartyl α-keto amides (**3a-3d**). The Cbz group was removed from compounds **3a-3d** by hydrogenolysis, giving the α-keto amides as salts (**4a-4d**). These salts were then coupled (Scheme 2.2) to either a peptide sequence (Z-Val-Glu(*t*Bu)-Val-OH or Z-Leu-Glu(*t*Bu)-Thr-OH) or to a single amino acid (Z-Ile-OH) by the mixed anhydride coupling method to give the peptide derivatives (**5a-b**, **6**, and **7a-d**). The side chains of these peptides were then deprotected with TFA to give the final compounds (**8a-b**, **9**, and **10a-d**). All final

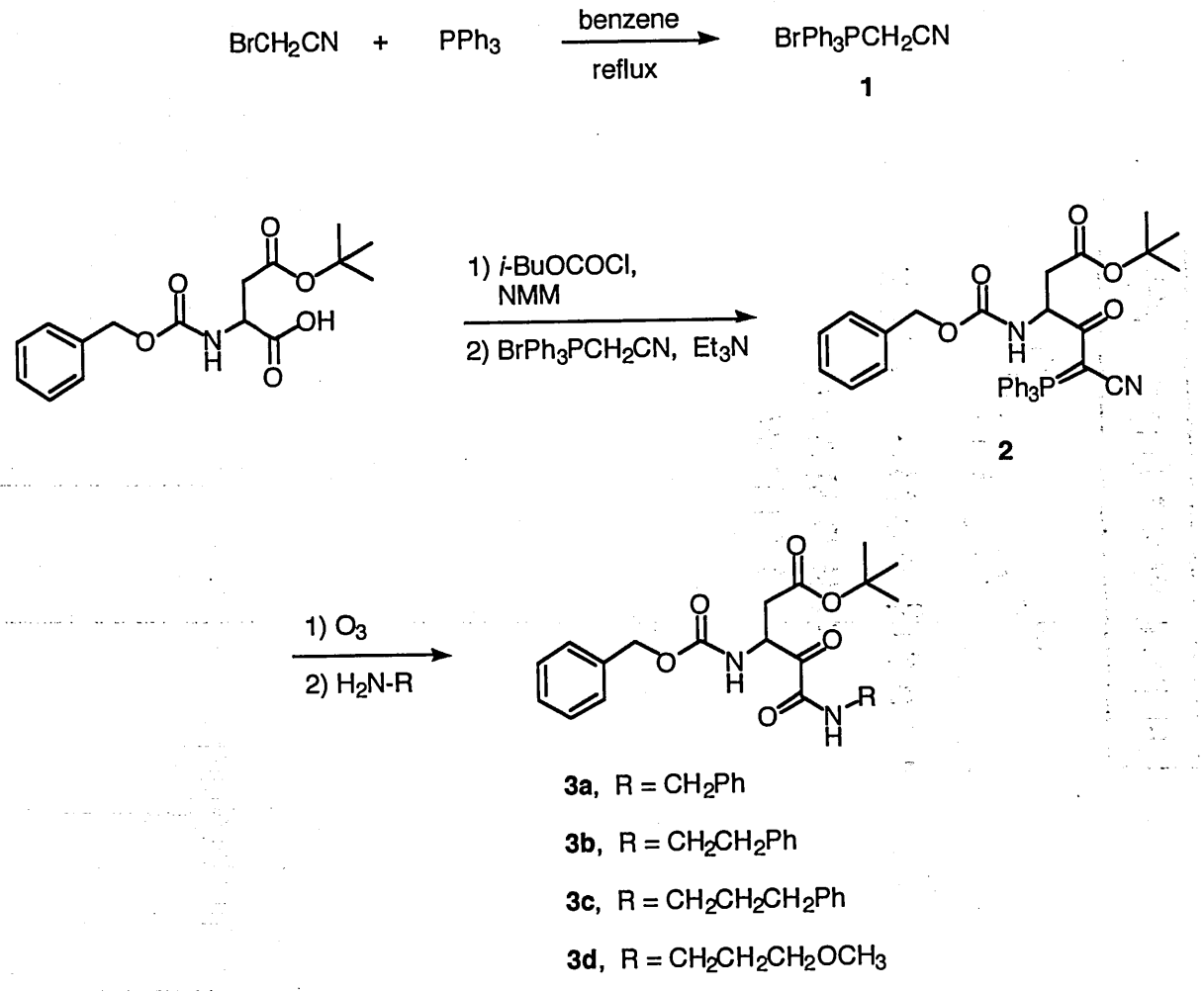

Scheme 2.1 Synthesis of α-Keto Amides.

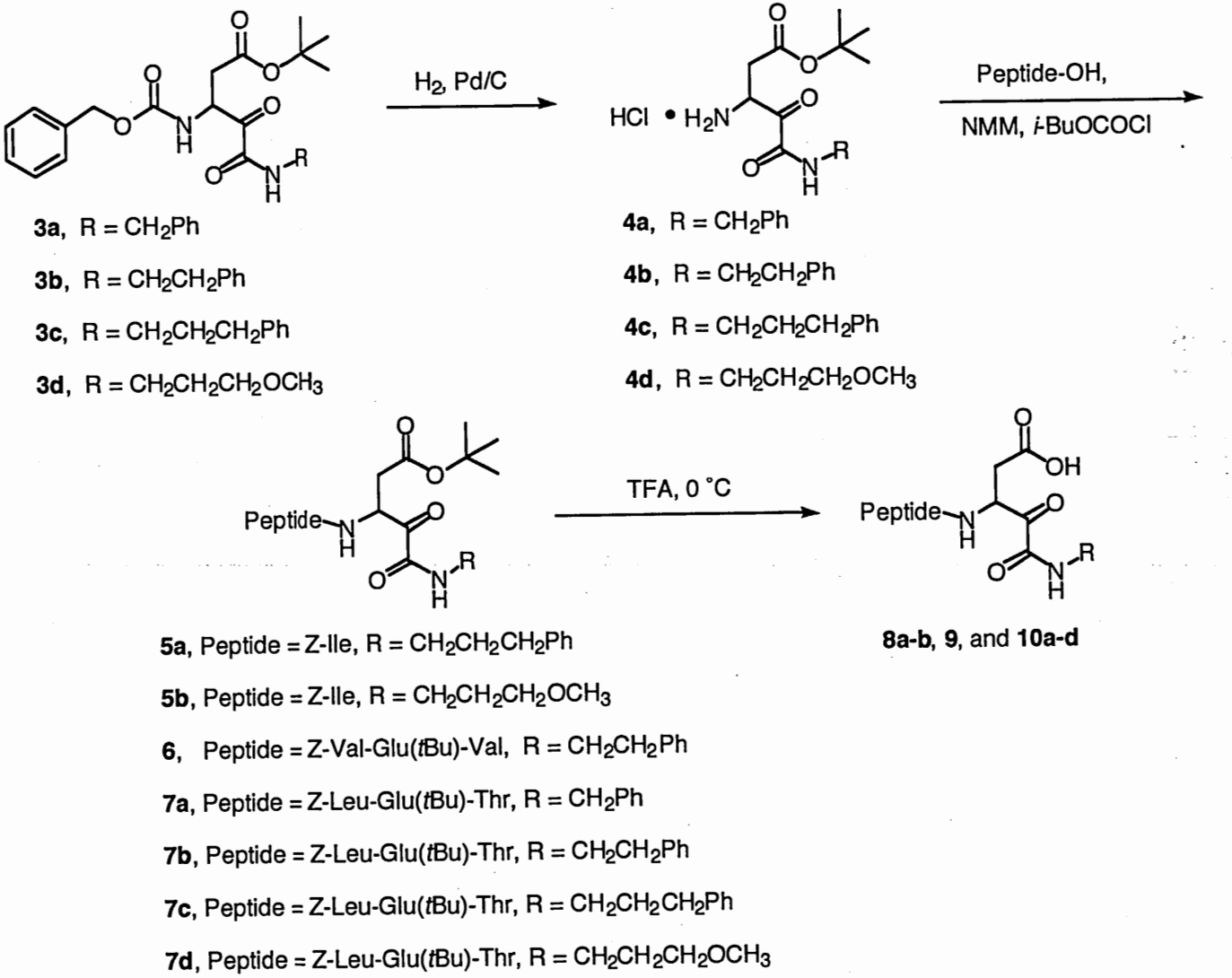

3a, R = CH_2Ph

3b, R = CH_2CH_2Ph

3c, R = $CH_2CH_2CH_2Ph$

3d, R = $CH_2CH_2CH_2OCH_3$

4a, R = CH_2Ph

4b, R = CH_2CH_2Ph

4c, R = $CH_2CH_2CH_2Ph$

4d, R = $CH_2CH_2CH_2OCH_3$

5a, Peptide = Z-Ile, R = $CH_2CH_2CH_2Ph$

5b, Peptide = Z-Ile, R = $CH_2CH_2CH_2OCH_3$

6, Peptide = Z-Val-Glu(*t*Bu)-Val, R = CH_2CH_2Ph

7a, Peptide = Z-Leu-Glu(*t*Bu)-Thr, R = CH_2Ph

7b, Peptide = Z-Leu-Glu(*t*Bu)-Thr, R = CH_2CH_2Ph

7c, Peptide = Z-Leu-Glu(*t*Bu)-Thr, R = $CH_2CH_2CH_2Ph$

7d, Peptide = Z-Leu-Glu(*t*Bu)-Thr, R = $CH_2CH_2CH_2OCH_3$

8a-b, **9**, and **10a-d**

Scheme 2.2 Synthesis of Peptide α-Keto Amide Derivatives.

compounds were characterized by ^{1}H NMR, HRMS, and elemental analysis (Table 2.1).

Cysteine Proteases. The caspases are members of a class of enzymes called cysteine proteases, or thiol proteases, based on the primary active site residue involved in catalysis.[43] Rawlings and Barrett[44,45] have further organized this class of proteases into clans and families, based on their evolutionary relationships. A family of proteases is defined as a group of enzymes whose evolutionary relationship has been determined in one of three ways: by similar tertiary structures, by common sequence motifs surrounding the catalytic residues, or by the order of catalytic residues in their sequences.[43] Clans consist of several related families, all of whom arose from a single evolutionary origin.[43] The caspases are clan CD proteases, of the C14 family. Clan CD proteases are cysteine nucleophillic proteins with the catalytic residues in their sequence arranged His, then Cys. Family C14 is one type family of clan CD, which contains all the caspases, as well as caspase homologs.[46,47]

Unlike serine proteases, the mechanism of substrate hydrolysis for cysteine proteases is not well defined. Most cysteine proteases are believed to utilize a catalytic diad of Cys and His, while the possibility of a third residue involved in catalysis is still under debate. A theoretical mechanism for hydrolysis in cysteine proteases (Figure 2.7)[48] has been developed, based on study of papain, one of the best-known cysteine proteases.[48,49] It is strikingly similar to the mechanism for serine proteases, with several notable exceptions. First, there is the lack of a definite third residue involved in the catalysis. Second, the active entity in cysteine proteases appears to be a thiolate/imidazolium ion pair, which is formed by the polarization of the SH group of the cysteine by the imidazole of the histidine. This allows for de-protonation of the active

Table 2.1 Elemental Analysis of α-Keto Amide Inhibitors for Caspases.

Compound	Formula	Calculated			Found		
		C	H	N	C	H	N
Z-Val-Glu-Val-Asp-CO-$NHCH_2CH_2Ph$	$C_{36}H_{47}N_5O_{11}$•2.5 H_2O	56.10	6.75	9.09	55.81	6.44	8.97
Z-Leu-Glu-Thr-Asp-CO-$NHCH_2CH_2Ph$	$C_{36}H_{47}N_5O_{12}$•1.75 H_2O	55.92	6.54	9.06	56.02	6.25	8.79
Z-Leu-Glu-Thr-Asp-CO-$NHCH_2Ph$	$C_{35}H_{45}N_5O_{12}$•1.0 H_2O	56.38	6.31	9.40	56.42	6.47	9.45
Z-Leu-Glu-Thr-Asp-CO-$NHCH_2CH_2CH_2Ph$	$C_{37}H_{49}N_5O_{12}$	58.78	6.54	9.27	58.57	6.65	9.04
Z-Leu-Glu-Thr-Asp-CO-$NHCH_2CH_2CH_2OCH_3$	$C_{32}H_{47}N_5O_{13}$•0.3 TFA	52.64	6.37	9.42	52.97	6.71	9.07
Z-Ile-Asp-CO-$NHCH_2CH_2CH_2Ph$	$C_{28}H_{35}N_3O_7$•0.25 H_2O	63.46	6.70	7.93	63.38	6.70	7.88
Z-Ile-Asp-CO-$NHCH_2CH_2CH_2OCH_3$	$C_{23}H_{33}N_3O_8$•0.25 H_2O	57.08	6.93	8.69	57.11	6.96	8.75
Z-Asp(tBu)-CO-$NHCH_2CH_2CH_2OCH_3$	$C_{21}H_{30}N_2O_7$•0.67 HCN	59.09	6.97	8.49	58.79	7.03	8.25

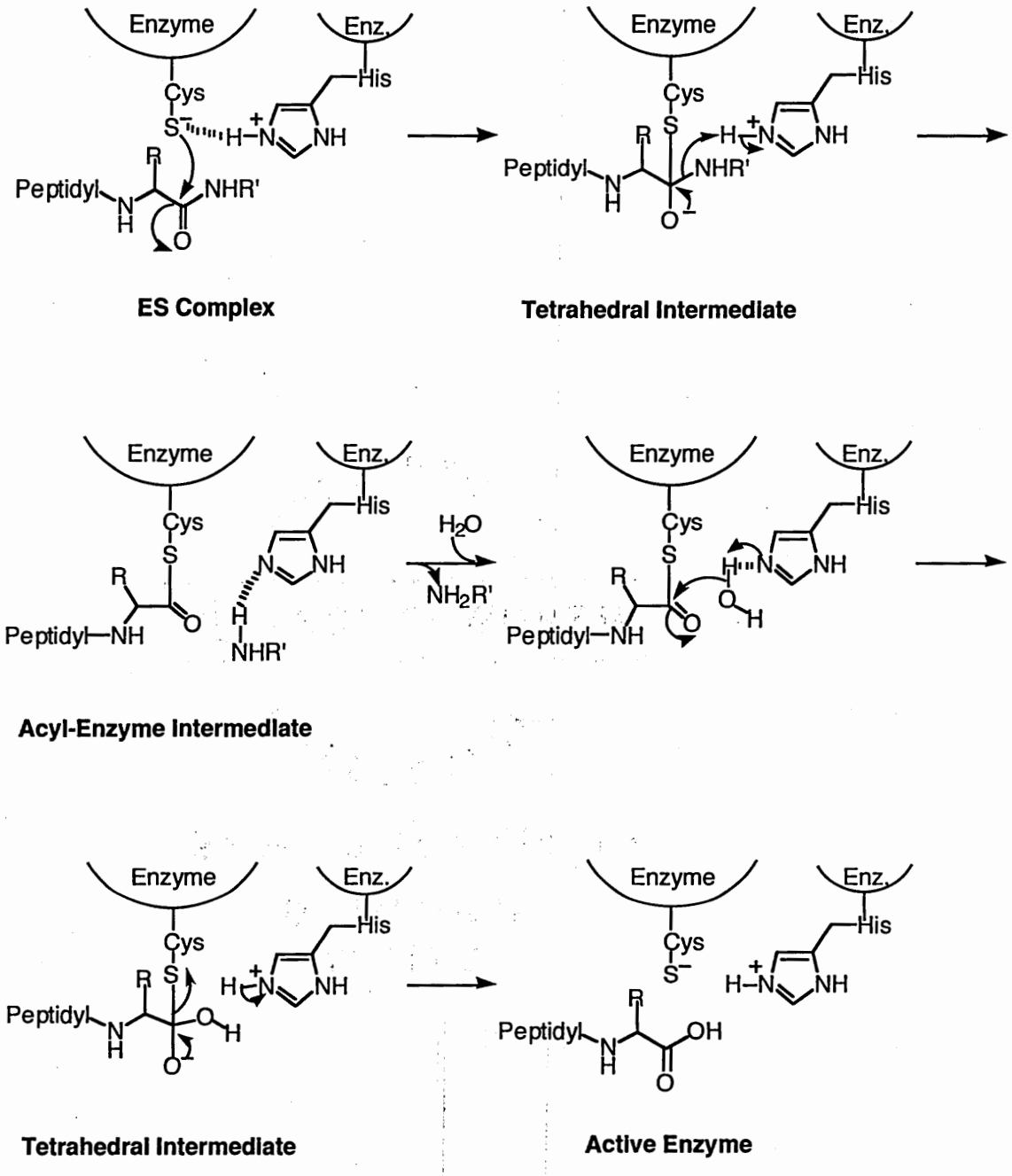

Figure 2.7 Mechanism of Substrate Hydrolysis by Cysteine Proteases.[48,49]

site Cys, even at neutral to weakly acidic pH. This thiolate anion attacks the scissile bond carbonyl of the substrate, forming a tetrahedral intermediate, which decomposes to form the acyl-enzyme intermediate. Deacylation occurs through the same mechanism as serine proteases, using water as the nucleophile to attack the acyl-enzyme. This forms a tetrahedral intermediate, which collapses to regenerate the active enzyme and releases the peptide acid. Although the mechanism is still not definitively established, the evidence shows that cysteine proteases usually have a catalytic diad of Cys and His, which makes these two residues the best targets for inhibitor design.[50]

Enzyme Inhibitors. Several types of inhibitors exist for cysteine proteases, which can be classed as either covalent or non-covalent, also known as irreversible or reversible inhibitors.[49] Examples of reversible inhibitors of cysteine proteases include α-keto carboxylic acid derivatives, and difluoro- and trifluoro methyl ketones. Examples of irreversible inhibitors include chloromethyl ketones and diazomethanes.[49] Irreversible inhibition is time-dependent, with the degree of inactivation progressively increasing over time until complete inhibition is reached, providing that the inhibitor is stable and is sufficiently in excess of the enzyme.[51] The mechanism of irreversible inhibition involves covalent bond formation after the initial enzyme-inhibitor complex is formed. The potency of irreversible inhibitors is expressed by a rate constant, $k_{obs}/[I]$, where k_{obs} is the pseudo first-order inhibition constant, and [I] is the concentration of the inhibitor.[51,52] Reversible inhibitors depend on binding interactions with the active site for potency, since the enzyme-inhibitor complex dissociates easily. Enzymatic activity can therefore be restored simply by removing the inhibitor from the system, either by degradation of the compound, or through physical means such as dialysis.[51] The equilibrium between

inhibitor and enzyme is the defining characteristic of reversible inhibition. This equilibrium is usually represented by an constant, K_i, which is the dissociation constant for the enzyme-inhibitor complex and is a measure of the effectiveness of the inhibitor.[52] Reversible inhibition exhibits a specific degree of inactivation of the enzyme, usually attained quickly, that is determined by the concentration of the inhibitor in the system. Once this degree of inactivation is reached, the reaction is independent of time as long as the inhibitor is not degraded.[51]

α-Keto Amide Inhibitors. Peptide carbonyl derivatives such as α-keto acids, α-keto esters, and α-keto amides are reversible inhibitors of a variety of serine and cysteine proteases, often exhibiting slow-binding inhibition.[35,37] α-Keto amides have several advantages over other reversible inhibitors, including α-keto esters and α-keto acids. Unlike peptide aldehydes, α-keto amides can be extended in the prime direction (P' side of the scissile bond), allowing for greater interaction with the enzyme site, and potentially increasing the potency of the inhibitor. α-Keto esters can also be extended in the P' direction; however, they are also extremely susceptible to esterase cleavage and are therefore less stable *in vivo*.[36,37] α-Keto acids, although more potent than α-keto amides *in vitro*, show very poor cell membrane permeability due to their charged nature.[36] α-Keto amides are stable to esterase activity, since they have an amide bond rather than an ester at the scissile bond. Previous studies with calpains, cathepsin B, papain, and caspase 1 have also shown that α-keto amides have good membrane permeability (by platelet membrane permeability assays) and demonstrated biological activity *in vivo* in animal models of stroke.[37-40]

α-Keto amides posses an extremely electrophillic carbonyl at the scissile bond, and, when inhibiting the enzyme, resemble the tetrahedral transition state of substrate hydrolysis.[41] The mechanism of inhibition (Figure 2.8) is believed to begin with attack of the active site Cys on the electrophillic carbonyl (CI), generating a stable but reversible hemithioketal adduct,

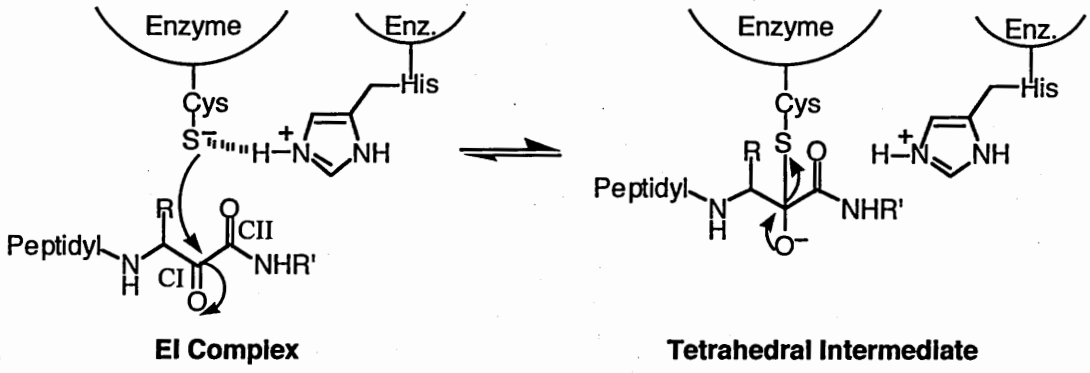

Figure 2.8 Mechanism of Inhibition of Cysteine Proteases by α-Keto Amides.

similar to the transition state of substrate hydrolysis.[35,49] As there is no good leaving group, the reaction cannot proceed to the acyl-enzyme intermediate, but instead decomposes to regenerate the active enzyme.[37] The second carbonyl (CII) is believed to enhance the electrophilicity of CI, as well as potentially interacting with enzyme residues.[35] A wide variety of evidence has demonstrated that the attack by the cysteine nucleophile occurs at CI. Reduction of CI leads to total loss of inhibitory activity, and ^{13}C NMR studies of α-keto amides with serine proteases have shown that the serine adds only to CI.[32,35] Finally, Brady et al. has published a crystal structure of caspase 1 complexed with an α-keto amide inhibitor, 4-Cl-$PhCH_2CH_2CO$-Val-Ala-Asp-CO-NH-

CH_2CH_2Ph, which shows the active site Cys^{285}(caspase 1 proenzyme numbering) bound to the CI carbonyl (see Figure 2.5).[42]

α-Keto amides often exhibit slow-binding inhibition of the target enzyme. This effect generally occurs in the longer peptide sequences, especially if the sequence is optimal for the target enzyme. In this study, the five tetrapeptides synthesized showed slow-binding activity against all three caspases, but the two dipeptides did not. The dipeptides are simple competitive reversible inhibitors of all three caspases.

Inhibition Kinetics. Reversible inhibition of caspases 3, 6, and 8 was measured by a progress curve method. Buffer, inhibitor, and a fluorogenic substrate were placed together in a well, and an aliquot of the enzyme solution was added to initiate the reaction. Enzyme activity was measured over a period of time (15 – 40 minutes, depending on the enzyme) by monitoring the increase in fluorescence caused by substrate hydrolysis. For simple competitive inhibitors, such as the dipeptide α-keto amides, a plot of product formation (from substrate hydrolysis) versus time was linear over the entire assay period (Figure 2.9). For compounds displaying slow-binding inhibition, however, a plot of product formation versus time (Figure 2.10) is curved, with a linear initial velocity and a linear steady-state velocity, joined by a transitional curve. This is believed to be the result of transitioning from an initial reversible enzyme inhibitor (EI) complex, to a second, more tightly associated complex (EI*). Since the control assay was linear over the entire assay time, substrate depletion is not a factor in the kinetics, and there is no evidence in the literature to suggest that the α-keto amides are being degraded, so product inhibition is not likely a problem. Although the increase in fluorescence in the steady-state region is linear, it is not a flat line as would be seen with irreversible inhibitors,

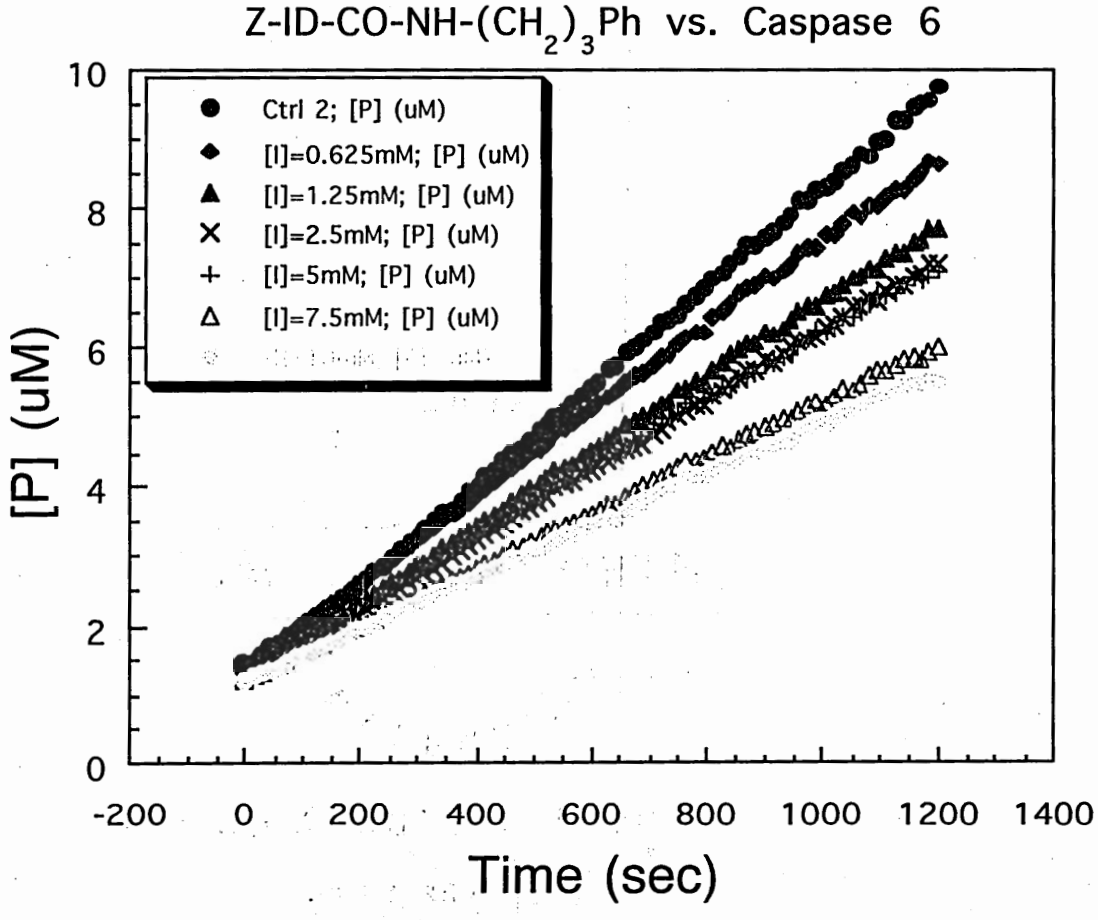

Figure 2.9 Simple Competitive Inhibition of Caspases by Dipeptide α-Keto Amides.

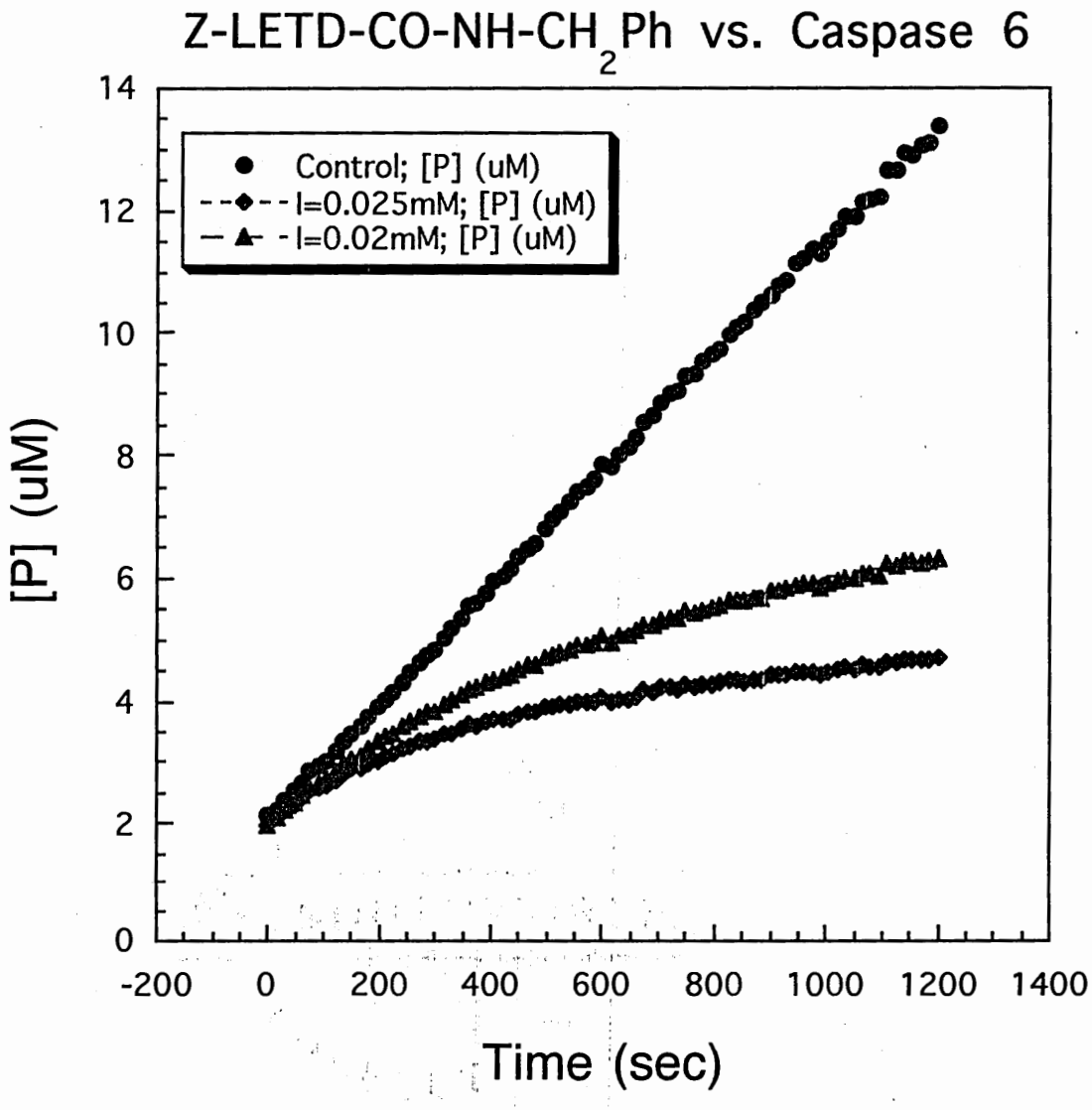

Figure 2.10 Slow-binding Inhibition of Caspases by Tetrapeptide α-Keto Amides.

indicating that substrate hydrolysis by active enzyme is ongoing, albeit at a slower rate. The mathematics for analyzing the transitional phase are extremely complex, requiring multiple experiments at a variety of substrate and inhibitor concentrations, as well as both enzyme initiated and substrate initiated (pre-incubation) assays. Because of the complexity involved in these mathematics, most studies of α-keto amide inhibitors have described only the initial K_i values ($K_{i(initial)}$), based on the initial rates, and occasionally the final K_i values ($K_{i(final)}$), generated by analysis of the linear steady-state region, are also reported. Inhibition in each region (initial and steady-state) is treated as simple competitive inhibition, and can be analyzed by standard kinetic methods. In this study, we have chosen to report both $K_{i(initial)}$ and $K_{i(final)}$ values for all compounds displaying slow-binding inhibition, using a range of inhibitor concentrations at a fixed substrate concentration. To calculate $K_{i(initial)}$, data from the first 300 seconds of each assay were used, and to determine $K_{i(final)}$, data from the last 300 seconds of each assay were used. For simple competitive inhibition, such as the dipeptides, a K_i value was determined in the same manner as for $K_{i(initial)}$ of the slow-binding compounds, using data from the first 300 seconds of the assay.

The equations for competitive reversible inhibition are defined by the following model

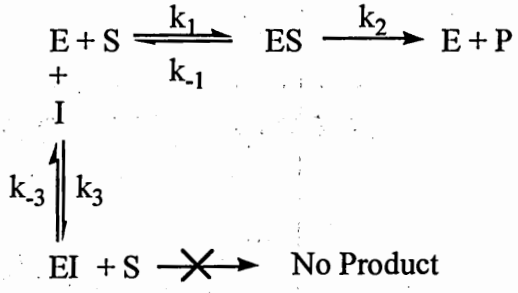

where E is the enzyme, S is the substrate, I is the inhibitor, P is the product of substrate hydrolysis, ES is the enzyme-substrate complex, and EI is the enzyme-inhibitor complex. The rate of formation of the ES complex is given by k_1, k_{-1} is the rate of dissociation of the ES complex back to free enzyme and substrate, and k_2 is the rate of formation of product from the ES complex. The rate of formation of the EI complex is denoted by k_3, and the dissociation of the EI complex back to free enzyme and inhibitor is given by k_{-3}. The inhibition constant, K_i, is a measure of the equilibrium between free enzyme and inhibitor and the EI complex, or

$$K_i = \frac{[E][I]}{[EI]} = \frac{k_{-3}}{k_3}$$

where [E] is the free enzyme concentration in the solution, [I] is the free inhibitor concentration in the solution, and [EI] is the concentration of the enzyme-inhibitor complex in the solution. The K_i can be determined from the Michaelis-Menten equation for a competitive inhibition system

$$v_i = \frac{V[S]}{K_m\left(1 + \frac{[I]}{K_i}\right) + [S]}$$

Hunter and Downs[53] developed a method of determining both K_i and K_m from a single equation by using fractional activity to describe the data. This method allows for the calculation of K_i even if data includes measurements in which both substrate and inhibitor concentration vary, by recalculating the data so that they are comparable. If K_m is already known, this method provides a simple means for determining K_i from a plot of

percent inhibition versus inhibitor concentration. In the Hunter and Downs method, fractional activity (α) is defined as

$$\alpha = \frac{v_i}{v}$$

where v_i is the velocity in the presence of the inhibitor, and v is the velocity in the absence of inhibitor (control) for a given set of data. The velocities are the slopes of the lines found by graphing [P] versus time, in the presence or absence of inhibitor (Figure 2.11). The fractional inhibition of the enzyme can then be defined as $1-\alpha$, and the percent inhibition would be $100 * (1-\alpha)$. In the absence of inhibitor (the control reaction), the velocity is described by the Michaelis-Menten equation

$$v = \frac{V[S]}{K_m + [S]}$$

By combining this equation with the Michaelis-Menten equation for competitive inhibition systems

$$v_i = \frac{V[S]}{K_m\left(1 + \frac{[I]}{K_i}\right) + [S]}$$

Hunter and Downs obtained the equation

$$\frac{v}{v_i} = \frac{K_m\left(1 + \frac{[I]}{K_i}\right) + [S]}{K_m + [S]}$$

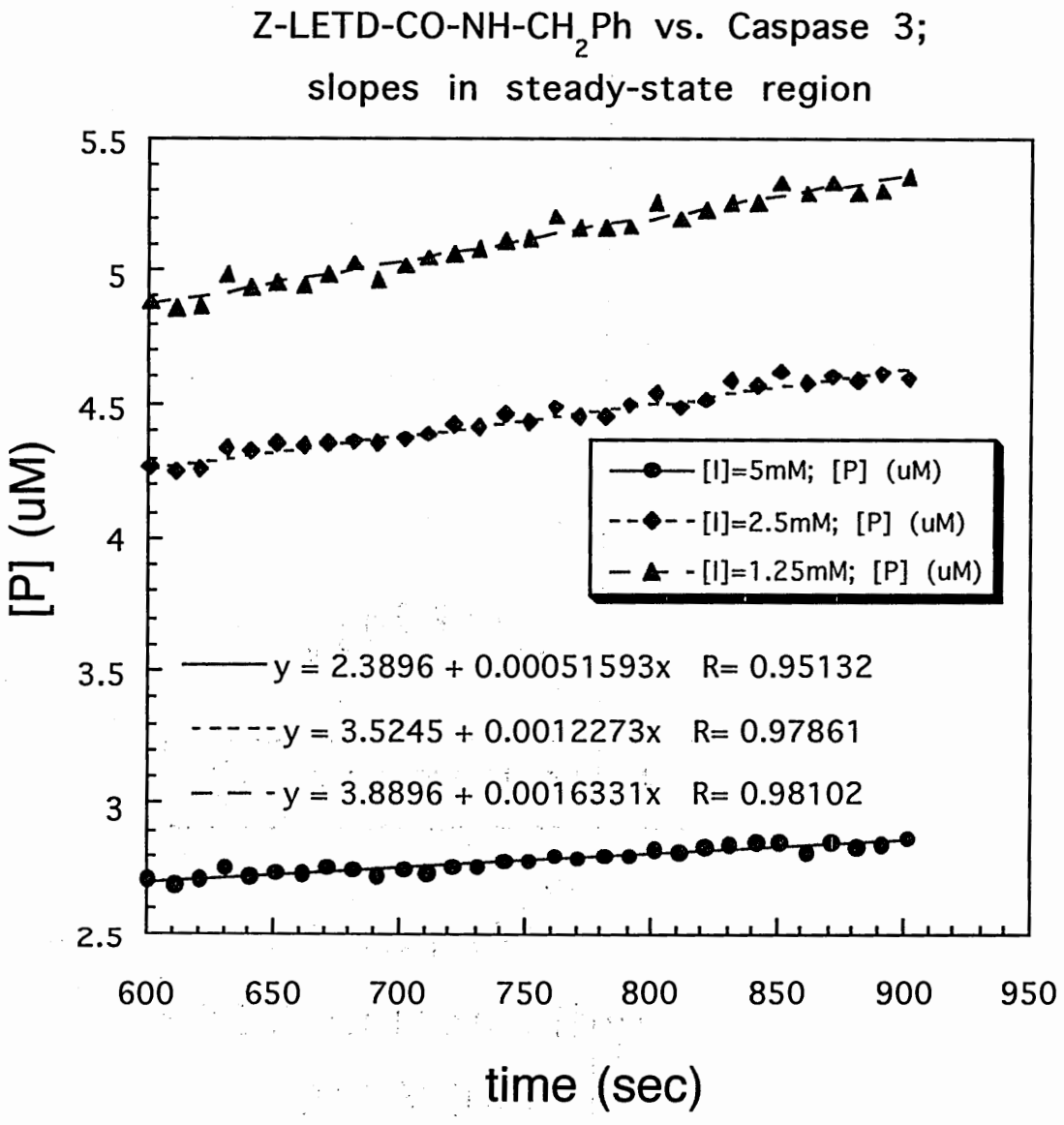

Figure 2.11 Determination of Velocities for Hunter and Downs Method.[53]

This equation can be simplified by using the definition of fractional activation ($\alpha = v_i/v$) to give

$$\frac{1}{\alpha} = 1 + \frac{K_m[I]}{K_i(K_m + [S])}$$

Rearranging this equation to solve for K_i gives

$$K_i = \frac{K_m[I]}{\left(K_m + [S]\right)\left(\frac{1}{\alpha} - 1\right)}$$

or, alternatively,

$$\frac{[I]\alpha}{(1 - \alpha)} = K_i + \frac{K_i}{K_m}[S]$$

By defining the left side of the equation as $K_{i,app}$ and rearranging to solve for K_i, the equation can be transformed to

$$K_i = \frac{K_{i,app}}{\left(1 + \frac{[S]}{K_m}\right)}$$

where $K_{i,app}$ is defined as

$$K_{i,app} = \frac{[I]\alpha}{(1 - \alpha)}$$

By solving for α, plugging the value of α found back into the equation, and rearranging to isolate the fractional inhibition term $(1- \alpha)$, the equation becomes

$$(1 - \alpha) = \frac{[I]}{[I] + K_{i,app}}$$

Converting fractional inhibition to percent inhibition gives the final equation

$$\% \text{ Inhibition} = 100 * \frac{[I]}{[I] + K_{i,app}}$$

When % inhibition versus inhibitor concentration is plotted, the curve generated can be fitted to this equation in order to generate $K_{i,app}$ (Figure 2.12). This value can then be used, along with the K_m and substrate concentration, to generate K_i for a set of data. For slow-binding inhibitors, using data from the initial rate region to arrive at a value of $K_{i,app}$ gives the values of $K_{i(initial)}$ and the $K_{i,app}$ determined from data in the steady-state region generates $K_{i(final)}$. For simple competitive inhibitors such as the dipeptide α-keto amides, only data from the initial 300 seconds (initial rate region) is used to generate a K_i value.

Caspase Specificity. Members of the caspase family exhibit similarity in secondary, tertiary, and quaternary structures, leading to many similarities in substrate specificity.[17] For this section, all protein numbering will be based on the caspase 1 proenzyme, which is the best studied member of the caspase family. The catalytic unit of the caspases is composed of a dyad of Cys^{285} and His^{237}, rather than the catalytic triad (Cys/His/Asn) found in members of the papain family of cysteine proteases.[54] The amino acid at position 177 is also involved in the catalytic unit, with the backbone carbonyl of this residue interacting with the active site His^{237}.[55-57] In a crystal structure of caspase 8 with the aldehyde inhibitor Ac-Ile-Glu-Thr-Asp-CHO, Watt et al. showed that there was a clear interaction between the Nε of His^{237} and the carbonyl oxygen of Arg^{177} (caspase 1

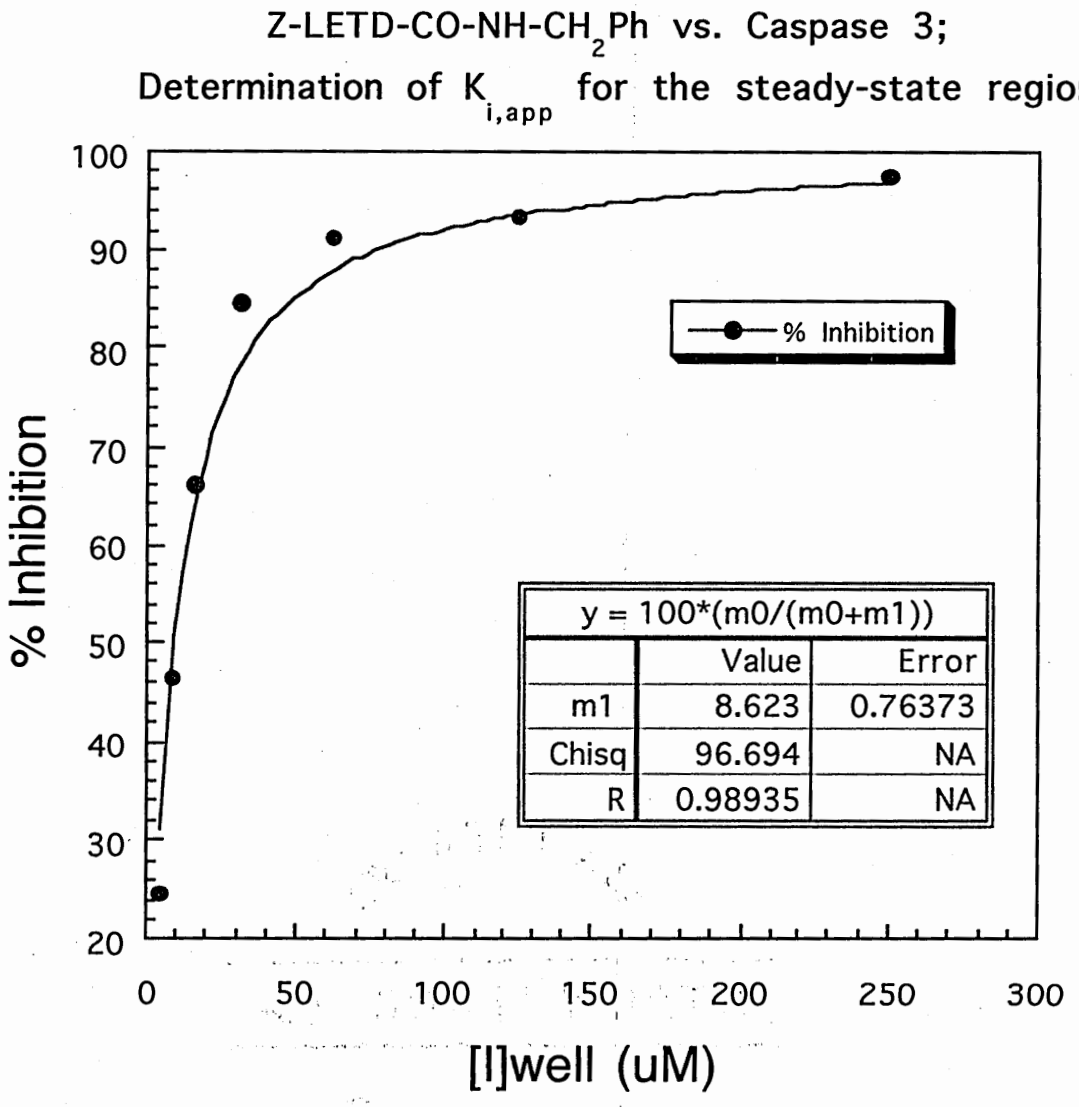

Figure 2.12 Determination of $K_{i,app}$ from a graph of % Inhibition versus [I] for a set of steady-state data. Variable m1 is $K_{i,app}$, which can be used to solve for $K_{i(final)}$, in this case.

proenzyme numbering; the equivalent residues based on caspase 8 proenzyme numbering are His^{317} and Arg^{258}).[57]

Crystal structures have been determined for caspases 1[42,55,58], 3[54,56], and 8[57,59]. From these structures, it is evident that the active site of the caspases lies in a shallow groove on the surface of the enzyme.[17] The P1-P4 requirements for the caspases have been well documented, but the prime side has remained unstudied. The P1 site is the primary specificity determinant, with all members of the caspase family requiring Asp at P1. This unusual specificity requirement is caused by the amino acids lining the S1 pocket, a particular triad of Arg^{341}, Arg^{179}, and Gln^{283}, which are conserved in all members of the caspase family and interact with Asp at P1.[17,57] The carboxyl oxygen of the Asp side chain forms hydrogen bonds with Gln^{283}, and salt bridges with the two Arg residues.[57]

The P2 binding site is not well defined in the caspases, thereby causing the lack of significant preferences for P2. From the crystal structures, the S2 pocket is mostly hydrophobic, with the amino acids at positions 338 and 340 being the main residues forming the site. These residues are generally Tyr, Trp, or Val, although caspase 6 has His at position 340 (caspase 1: Val^{338} and Trp^{340}; caspase 8: Val^{338} and Tyr^{340}; caspase 3: Tyr^{338} and Trp^{340}; caspase 6: Tyr^{338} and His^{240}).[17,57] The area around the S2 pocket is generally open and flat, with a few non-specific interactions, as shown in the crystal structure of caspase 3 with Ac-Asp-Glu-Val-Asp-CHO.[56]

All caspases prefer Glu at P3, due to the presence of several Arg residues at the P3 binding site. The S3 pocket in caspase 8 is a cleft defined by Arg^{341}, Arg^{177}, Pro^{343}, and Asn^{180}.[57] The Arg^{341} is the same residue involved in P1 Asp binding, and also forms

a salt bridge to the Glu side chain, while the other three residues interact with the P3 Glu through solvent mediated interactions.[57] The S3 pocket is similar for the other caspases, although the effect is enhanced in caspase 8 due to the Arg^{177} and Asn^{180},[57] which are Pro^{177}/Thr^{180}, Thr^{177}/Ser^{180}, and Pro^{177}/Arg^{180} in caspases 1, 3, and 6 respectively, as determined by sequence alignments of the caspase 1 (Swiss-Prot Accession number P29466), 3 (Swiss-Prot Accession number P42574), 6 (Swiss-Prot Accession number P55212), and 8 (Swiss-Prot Accession number Q14790) proenzymes. Sequence alignment was performed using NCBI's Blast 2 sequence program.[60]

The amino acid at P4 is the single most important residue in determining specificity between the members of the caspase family.[2,5,20,61] The wide variations in P4 preference between caspase members is mainly influenced by differences in one of the loops in the structure. Loop 3 (Figure 2.13)[5] forms one side of the S4 binding pocket, and varies in length from one enzyme to the next.[57,59] This causes the size of the binding pocket to vary as well, due to the loop folding over the top of the binding pocket.[17] Caspase 1, which has the shortest loop 3 of caspases 1, 3, and 8, also has the widest S4 pocket, and is known to prefer large hydrophobic groups such as Trp, Tyr, or Phe at P4.[5,20] Caspase 3, which has the longest loop 3 sequence, has a restricted S4 binding pocket and strongly prefers Asp at P4. This is due not only to the interactions with loop 3, but also to the presence of a large number of potential hydrogen bonding interactions (e.g. Asn^{342}). Trp^{348} also helps to form the S4 binding pocket, further restricting the size of the pocket.[2,5,17] The size of loop 3 in caspase 8 is midway between those in caspase 1 and caspase 3, giving a slightly less restrictive S4 subsite than that found in caspase 3.[5] Caspase 8 is known to prefer hydrophobic residues in P4, especially Leu, Ile, and Val.

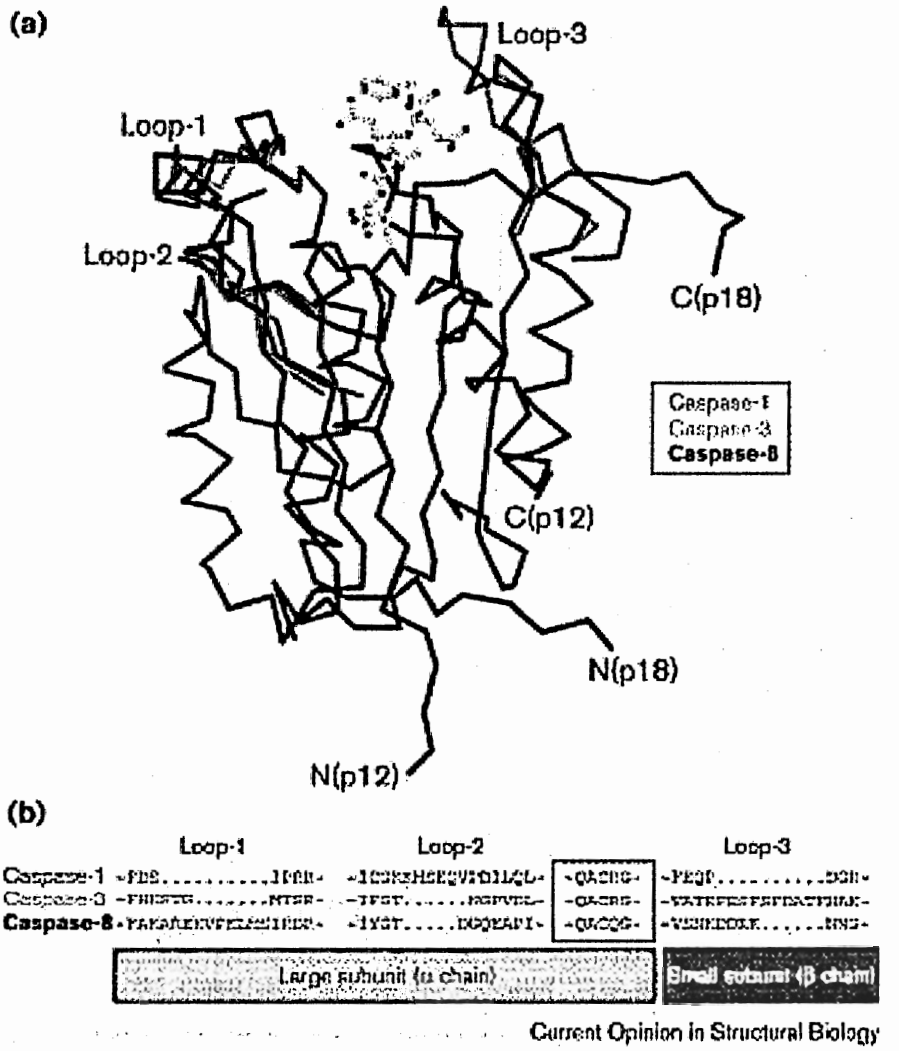

Figure 2.13 A Comparison of the Loop Regions in Caspases 1, 3, and 8.[5]

Some of the hydrogen bond interactions found in caspase 3 are replaced in caspase 8 by non-polar interactions between the P4 residue and the amino acids lining the S4 pocket. The aromatic groups Trp^{348} and Tyr^{340} can sandwich the side chain of a hydrophobic amino acid between them, forming favorable non-polar interactions.[57]

Although there is currently no crystal structure of caspase 6, previous substrate studies give a general idea of the binding sites in this caspase. Caspase 6, like other caspases, shows no strong preference for any amino acid at P2, and shares the strict requirement for Asp at P1 and Glu at P3 with other caspases, implying that the S1-S3 binding sites are very similar between caspase 6 and caspases 1, 3, and 8.[20] The substrate profile of caspase 6 indicates that it prefers hydrophobics at P4, similar to caspase 8. However, it exhibits a stronger preference for Val or Thr at P4 than caspase 8 does, and a weaker preference for Leu or Ile at this position.[20] This could help to confer some degree of selectivity between the two enzymes, although studies of caspase 6 and 8 with an aza-peptide epoxide inhibitor, Z-Leu-Glu-Thr-AAsp-EP-COOEt, showed equivalent potency for both enzymes.[62]

As the crystal structures of caspases available to date do not use inhibitors extending into the prime side, there is little known about what structures are preferred in this region. The current work, involving α-keto amides that can be extended in the P' direction, should help to elucidate the P' preferences of some of the caspases, thereby generating more potent and selective inhibitors.

α-Keto Amides with Caspase 8. Four of the seven compounds synthesized utilized the predicted optimal sequence for caspase 8, Cbz-Leu-Glu-Thr-Asp. These four compounds, along with the tetrapeptide utilizing the caspase 6 optimal sequence, Cbz-

Val-Glu-Val-Asp, demonstrated slow-binding inhibition of all three caspases, while the two dipeptides showed simple competitive reversible inhibition. The K_i values for the initial equilibrium ($K_{i(initial)}$) and for the final steady-state equilibrium ($K_{i(final)}$) were determined for all five tetrapeptides (Table 2.2). All four of the Cbz-Leu-Glu-Thr-Asp α-keto amides were potent inhibitors of caspase 8, with $K_{i(final)}$ values ranging from 3 nM to 13 nM. The most potent compound of the series was Cbz-Leu-Glu-Thr-Asp-CO-NH-$(CH_2)_2$Ph, which had a $K_{i(final)}$ of 3 nM, and was twice as potent as the next best inhibitor, Z-Leu-Glu-Thr-Asp-CO-NH-$(CH_2)_3OCH_3$ ($K_{i(final)}$ = 6 nM). The benzyl keto amide (Z-Leu-Glu-Thr-Asp-CO-NH-CH_2Ph) and the phenylpropyl derivative (Z-Leu-Glu-Thr-Asp-CO-NH-$(CH_2)_3$Ph) were approximately equipotent, with $K_{i(final)}$ values of 11 nM and 13 nM respectively, but were four-fold less potent than the best compound of the series. These results seem to indicate the presence of a hydrophobic area on the S' side of the active site groove, potentially at the S2' subsite. The C-terminal chain of the phenethyl derivative is long enough to position the phenyl ring in this hydrophobic area, while the benzyl derivative is slightly shorter and the phenylpropyl derivative is too long to make the same interactions. The fact that all four compounds are potent inhibitors of caspase 8 indicates that, despite the potential lack of optimal interactions with the S2' subsite, large hydrophobic groups are still well tolerated in the active site groove. The methoxypropyl derivative (Z-Leu-Glu-Thr-Asp-CO-NH-$(CH_2)_3OCH_3$) is twice as potent as the analogous phenylpropyl derivative. This could be caused by favorable hydrogen bonding interactions of the C-terminal ether of the compound with residues of the active site, or by interactions with solvent. The methoxypropyl chain is flexible enough to assume that the ether portion may be solvent exposed, rather than interacting with the active site at the

Table 2.2 α-Keto Amides as Slow-Binding Inhibitors of Caspases 3, 6, and 8.

Compound	Caspase 3		Caspase 6		Caspase 8	
	$K_{i(initial)}$ (μM)	$K_{i(final)}$ (μM)	$K_{i(initial)}$ (μM)	$K_{i(final)}$ (μM)	$K_{i(initial)}$ (μM)	$K_{i(final)}$ (μM)
Z-Val-Glu-Val-Asp-CO-NH-$(CH_2)_2$Ph	0.317	0.243	0.126	0.080	0.042	0.029
Z-Leu-Glu-Thr-Asp-CO-NH-CH_2Ph	3.638	0.762	0.968	0.156	0.125	0.011
Z-Leu-Glu-Thr-Asp-CO-NH-$(CH_2)_2$Ph	2.588	0.564	1.191	0.153	0.187	0.003
Z-Leu-Glu-Thr-Asp-CO-NH-$(CH_2)_3$Ph	3.249	0.733	1.972	0.461	0.120	0.013
Z-Leu-Glu-Thr-Asp-CO-NH-$(CH_2)_3OCH_3$	2.905	0.679	1.619	0.363	0.094	0.006

S2' subsite.

Interestingly, the compound designed based on the caspase 6 optimal sequence, Z-Val-Glu-Val-Asp-CO-NH-$(CH_2)_2$Ph, was also an extremely potent inhibitor of caspase 8, with a $K_{i(final)}$ value of 29 nM. The almost ten-fold loss in potency compared to the analogous compound Z-Leu-Glu-Thr-Asp-CO-NH-$(CH_2)_2$Ph is probably attributable to the fact that Val is less preferred by caspase 8 at P4 and P2. However, Val is the second best tolerated amino acid at these positions[20], which would account for the high potency of the compound with caspase 8. The lack of significant differences in the P4 and P2 specificities of caspases 6 and 8 indicates difficulty in designing selective inhibitors for these two caspases.

The two dipeptides exhibited simple competitive reversible inhibition of the caspases, and are extremely poor inhibitors, as shown in Table 2.3. The K_i values for Cbz-Ile-Asp-CO-NH-$(CH_2)_3$Ph and Cbz-Ile-Asp-CO-NH-$(CH_2)_3OCH_3$ were 13.017 μM and 15.425 μM, respectively. This is an approximately 5000-fold decrease in potency compared to the best tetrapeptide sequence, Cbz-Leu-Glu-Thr-Asp-CO-NH-$(CH_2)_2$Ph. The main reason for the lack of potency of these compounds is probably that caspase 8,

Table 2.3 α-Keto Amides as Competitive Reversible Inhibitors of Caspases 3, 6, and 8.

Compound	Caspase 3 K_i (μM)	Caspase 6 K_i (μM)	Caspase 8 K_i (μM)
Z-ID-CO-NH-$(CH_2)_3$Ph	19.9	462	13.0
Z-ID-CO-NH-$(CH_2)_3OCH_3$	57.1	1070	15.4

like the other caspases, strongly prefers tetrapeptide sequences for recognition, due to a greater number of favorable binding interactions, with the P3 and P4 amino acids being critical residues for determining specificity.[2,5,20,61] There is virtually no difference in potency between the two dipeptides, indicating that any potential favorable reactions caused by the P' groups are negated by the poor interactions of the dipeptides with the S side of the enzyme.

α-Keto Amides with Caspase 6. As with caspase 8, all five tetrapeptides exhibited slow-binding inhibition with caspase 6 (see Table 2.2). The most potent inhibitor was the one based on the caspase 6 optimal sequence, Cbz-Val-Glu-Val-Asp-CO-NH-$(CH_2)_2$Ph, which had a $K_{i(final)}$ of 80 nM. It is interesting that this compound, supposedly an optimal sequence for caspase 6, is actually more potent against caspase 8. One explanation for this could be that the best sequence for caspase 6 from substrate libraries has His at P2, and Val is actually the second best amino acid for that position.[20] However, His is a very challenging amino acid for synthetic purposes, and as Val was only slightly less preferred, it was substituted for His in this study. The lack of the best P2 residue could account for some of the lowered potency of this compound. Also, as can be seen from the Cbz-Leu-Glu-Thr-Asp series of keto amides, caspase 6 strongly prefers smaller groups in the P1'-P2' region. The benzyl (CH_2Ph) and phenethyl (CH_2CH_2Ph) derivatives of the Leu-Glu-Thr series are approximately equipotent, with $K_{i(final)}$ values of 0.156 μM and 0.153 μM respectively, but are two-fold less potent than the Val-Glu-Val derivative. This is due to the sequence preferences of caspase 6, which does not prefer Thr at P2, and does not tolerate Leu at P4 very well.[20] However, the benzyl and phenethyl derivatives of the Leu-Glu-Thr series are three-fold more potent than the

phenylpropyl derivative ($CH_2CH_2CH_2Ph$), which had a $K_{i(final)}$ of 0.461 μM, and are two-fold more potent than the methoxypropyl derivative ($CH_2CH_2CH_2OCH_3$), which had a $K_{i(final)}$ of 0.363 μM. These results indicate that the prime side subsites of caspase 6 are potentially smaller or narrower than that of caspase 8, and therefore cannot tolerate the longer groups in the S1'-S2' subsites.

The two dipeptides tested were particularly poor inhibitors for caspase 6 (see Table 2.3). Cbz-Ile-Asp-CO-NH-$(CH_2)_3Ph$ had a K_i of 462.272 μM, and Cbz-Ile-Asp-CO-NH-$(CH_2)_3OCH_3$ had a K_i of 1068.722 μM. These results are probably due to a combination of lack of tolerance for longer groups on the prime side, as seen in the tetrapeptide studies, and the previously mentioned preference of the caspases for tetrapeptides over dipeptides. Caspase 6 appears to have a particularly stringent requirement for a tetrapeptide sequence, as the two dipeptides were 36-70 fold more potent against caspase 8 than caspase 6.

α-Keto Amides with Caspase 3. As with caspases 6 and 8, all five tetrapeptides exhibited slow-binding inhibition against caspase 3. Although all five compounds inhibited caspase 3, they were noticeably poorer inhibitors against this enzyme than against caspases 6 and 8 (Table 2.2). The best inhibitor for caspase 3 was the tetrapeptide Cbz-Val-Glu-Val-Asp-CO-NH-$(CH_2)_2Ph$, which had a $K_{i(final)}$ of 0.243 μM. This is somewhat interesting, as caspase 3 is believed to have a very stringent requirement for Asp at P4. This compound is also not a particularly good inhibitor for caspase 3, however, since a previously synthesized keto amide, Boc-Asp-Glu-Val-Asp-CO-$NH(CH_2)_2Ph$, had a K_i for caspase 3 of 5 nM (James C. Powers, unpublished results). Within the Cbz-Leu-Glu-Thr series of tetrapeptides, the best inhibitors for caspase 3 were

the phenethyl derivative, which had a $K_{i(final)}$ of 0.564 μM, and the methoxypropyl derivative, which had a $K_{i(final)}$ of 0.679 μM. The benzyl and phenylpropyl derivatives were approximately equipotent ($K_{i(final)}$ values of 0.762 μM and 0.733 μM, respectively), but were poorer inhibitors of caspase 3. These results indicate that the phenethyl group is apparently positioned correctly to interact with the S1'-S2' subsite regions of the enzyme, while the benzyl and phenylpropyl derivatives are of an inappropriate length to make favorable interactions with the enzyme. The methoxypropyl derivative, which is only a slightly less potent inhibitor than the phenethyl compound, is likely to be either solvent exposed, or less bulky and flexible enough to take advantage of binding interactions with the prime side subsites of the enzyme.

The two dipeptides are very poor inhibitors for caspase 3, as can be seen in Table 2.3, but they are not nearly as poorly tolerated by caspase 3 as by caspase 6. Cbz-Ile-Asp-CO-NH-$(CH_2)_3$Ph has a K_i of 19.904 μM, while Cbz-Ile-Asp-CO-NH-$(CH_2)_3OCH_3$ has a K_i of 57.131 μM. These results indicate a preference for smaller, less bulky groups on the prime side of the inhibitor, just as was indicated by the tetrapeptides. Also, although caspase 3 shares the family preference for tetrapeptides over dipeptides, the requirement is not nearly as stringent as that shown by caspase 6.

Selectivity Between Caspases 3, 6, and 8. Several of the inhibitors demonstrated selectivity between the three caspases studied. Cbz-Leu-Glu-Thr-Asp-CO-NH-$(CH_2)_2$Ph was 51 times more potent against caspase 8 than caspase 6, and 188 times more potent than against caspase 3. The methoxypropyl tetrapeptide derivative showed similar selectivity, with 61-fold greater potency against caspase 8 than caspase 6, and 113-fold greater potency than shown against caspase 3. Similarly, the phenylpropyl

derivative showed 36-fold greater potency against caspase 8 than caspase 6, and 56-fold greater potency against caspase 8 than against caspase 3. Of the Leu-Glu-Thr series, the benzyl derivative showed the lowest selectivity, with 14-fold greater potency against caspase 8 than caspase 6, and 69-fold greater potency than that shown against caspase 3. Interestingly, the compound that displayed the least selectivity of the tetrapeptides was Cbz-Val-Glu-Val-Asp-CO-NH-$(CH_2)_2$Ph, which had only 3-fold greater activity against caspase 8 than caspase 6, and 8-fold greater activity against caspase 8 than against caspase 3. The dipeptides were also fairly non-selective between caspases 3 and 8, although there was a marked decrease in activity against caspase 6 (18-fold less active for the methoxypropyl derivative, and 23-fold less active for the phenylpropyl derivative, compared to activity with caspase 3).

Perspectives. Of the seven compounds synthesized, the best inhibitors were the tetrapeptides Z-Leu-Glu-Thr-Asp-CO-NH-$(CH_2)_2$Ph ($K_{i,(final)}$ = 3 nM), and Z-Leu-Glu-Thr-Asp-CO-NH-$(CH_2)_3OCH_3$, ($K_{i,(final)}$ = 6 nM), which were based on the optimal sequence for caspase 8. Both of these compounds are very selective between the caspases tested, being 50 and 60 fold, respectively, more potent towards caspase 8 than towards caspase 6, and 113 and 188 fold, respectively, more potent against caspase 8 than against caspase 3. Although these inhibitors show 3-fold lower potency than the best previously published aldehyde inhibitors, Boc-Ile-Glu-Thr-Asp-H (K_i = 1.05 nM for caspase 8) and Ac-Asp-Glu-Val-Asp-H (K_i = 0.92 nM for caspase 8), they are much more selective than the literature compounds.[27] Boc-Ile-Glu-Thr-Asp-H differentiates well between caspase 8 and caspase 3, but only has 5-fold greater potency against caspase 8 than against caspases 1 and 6. Ac-Asp-Glu-Val-Asp-H had a 34-fold

difference in potency between caspases 6 (K_i = 31 nM) and 8, but only a 4-fold difference in activity between caspase 8 and caspase 3 (K_i = 0.23 nM). Therefore the inhibitors synthesized in this study, while slightly lower in potency than literature compounds, exhibit much greater selectivity between the caspases. Combined with the cell permeability and stability of α-keto amides in general, these results indicate that the compounds synthesized could be valuable tools for cell-based assays to help clarify the roles of individual caspases.

CONCLUSION

In this project, a series of α-keto amide inhibitors was designed for testing with caspases 3, 6, and 8, based on the previously studied optimal tetrapeptide sequences for each enzyme. α-Keto amides are competitive reversible transition state inhibitors that often exhibit slow binding inhibition. They have the advantage of being fairly stable and having decent cell permeability, as well as demonstrated biological activity *in vivo*. The biggest advantage, however, is that α-keto amides can be extended in the P' direction, allowing for additional enzyme-inhibitor interactions and generating increased potency and specificity.

The inhibitors synthesized in this project incorporated a variety of groups on the P' side of the scissile bond, as well as optimal sequences for caspases 8 and 6. Of the seven inhibitors, the five tetrapeptides exhibited slow-binding inhibition against all three caspases, while the two dipeptides showed simple competitive inhibition. The tetrapeptides designed for caspase 8, which utilized the sequence Cbz-Leu-Glu-Thr-Asp, were potent inhibitors of caspase 8, with $K_{i(final)}$ values ranging from 3 nM to 13 nM. With 14 - 60 fold greater potency against caspase 8 than against caspase 6, these compounds demonstrated some degree of selectivity over caspase 6. These compounds also showed a degree of selectivity between caspase 8 and caspase 3, with 56 - 188 fold greater potency exhibited against caspase 8 over caspase 3. The compound designed as a caspase 6 inhibitor, Cbz-Val-Glu-Val-Asp-CO-NH-$(CH_2)_2$Ph, was a potent inhibitor of caspase 6 ($K_{i(final)}$ = 80 nM), but was 3-fold more potent against caspase 8 ($K_{i(final)}$ = 29 nM). This compound, although potent, does not differentiate as well between the

caspases as the compounds based on the Leu-Glu-Thr sequence. The dipeptides were poor inhibitors of the caspases, and were also poorly selective, as predicted by previous studies showing that caspases prefer tetrapeptides for binding and specificity.[2,5,20,61]

In summary, a series of potent, selective α-keto amide inhibitors has been designed and synthesized. Two of these compounds, Z-Leu-Glu-Thr-Asp-CO-NH-$(CH_2)_2$Ph and Z-Leu-Glu-Thr-Asp-CO-NH-$(CH_2)_3OCH_3$, showed slightly lower potency than the best inhibitors for caspase 8 in the literature.[27] However, they are also much more selective than the previously published compounds, making them ideal for further studies and optimization. The results of this work should help to further clarify the S' specificities of the various caspases, which in turn could lead to the development of even more potent inhibitors, capable of differentiation between the various caspases. Lastly, because α-keto amides are known to exhibit good cell permeability and biological activity *in vivo*, cell-based studies using these inhibitors could help define the roles of the various caspases in apoptosis.

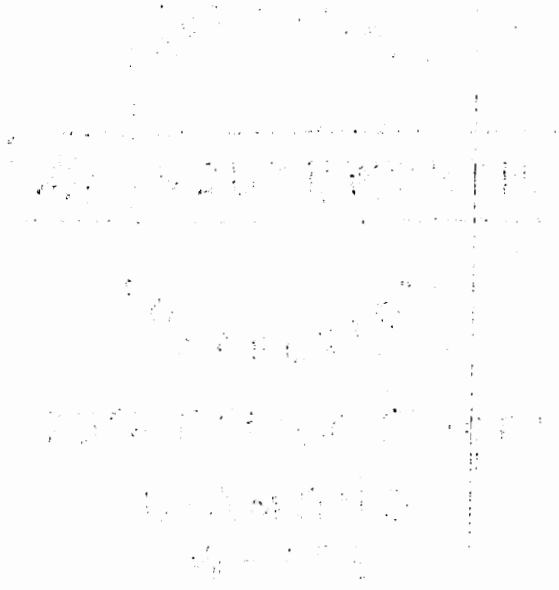

Materials and Methods-Synthesis. Unless otherwise stated, all chemicals, common reagents, and solvents were purchased from Aldrich Chemical Company (Milwaukee, WI) or Fischer Scientific Chemicals (Fair Banks, NJ). The protected amino acid derivatives Z-Glu(*t*Bu)-OH, Z-Asp(*t*Bu)-OH, Z-Leu-OH, Z-Val-OH, Z-Ile-OH, HCl•H-Val-OMe and HCl•H-Thr-OMe were purchased from BACHEM Bioscience, Inc. (King of Prussia, PA). Chromatography silica gel (particle size 32-63 μm) and thin-layer chromatography plates that were pre-coated with 250 μm of silica gel (F-254) were obtained from Scientific Adsorbents, Inc. (Atlanta, GA). ^{1}H NMR spectra were obtained from a Varian Mercury 400 instrument. Mass spectra were collected on either a Micromass Quattro LC (ESI^+) or VG Instruments 70SE (FAB^+). High resolution mass spectra were collected on either a VG Instruments 70SE (FAB^+) or on the Applied Biosystems QSTAR XL (ESI^+). Elemental analyses were performed by Atlantic Microlabs (Atlanta, GA). All elemental analyses were within ± 0.3% of the calculated values for the formulas shown for each compound.

Benzyloxycarbonyl(δ-*tert*-butylglutamyl)threonine Methyl Ester (Z-Glu(*t*Bu)-Thr-OMe)-General Coupling Procedure. Z-Glu(*t*Bu)-OH (5.598 g, 0.017 mol) was dissolved in CH_2Cl_2 (100 mL) with stirring and cooled to -10 °C. NMM (1.684 g, 1 eq.) was added and the reaction stirred at -10 °C for 10 minutes, then IBCF (2.269 g, 1 eq) was added and the mixture stirred for an additional 20 minutes at -10 °C. HCl•Thr-OMe (2.814 g, 0.017 mol) was dissolved in CH_2Cl_2 (100 mL) and cooled to -10 °C. NMM (1.680 g, 1 eq) was added and the mixture was stirred at -10 °C for 30 minutes,

then was added to the mixture containing Z-Glu(*t*Bu)-OH. The resulting solution was stirred at -10 °C for 1 hour, then warmed to rt and stirred overnight. The reaction was washed with 1M HCl (3 x 100 mL), saturated $NaHCO_3$ (3 x 100 mL), and saturated NaCl (3 x 100 mL), dried over $MgSO_4$, filtered and the solvent evaporated to give the product as a sticky white foam (6.631 g, 88% yield), which was used with no further purification. ^{1}H NMR ($CDCl_3$) δ 7.4-7.1 (m, 5H), 7.1-6.9 (d, 1H), 5.7-5.6 (d, 1H), 5.1-5.0 (s, 2H), 4.6-4.5 (d, 1H), 4.4-4.2 (m, 2H), 3.8-3.6 (s, 3H), 2.5-2.3 (m, 2H), 2.2-1.9 (d of m, 2 H), 1.5-1.3 (m, 9H), 1.3-1.1 (m, 3H); MS (ESI^+) *m/z* 453 (M + 1).

Benzyloxycarbonyl(δ-*tert*-butylglutamyl))valine Methyl Ester (Z-Glu(*t*Bu)-Val-OMe). This compound was synthesized by the general peptide coupling procedure, from Z-Glu(*t*Bu)-OH (8.081 g, 0.024 mol) and HCl•Val-OMe (4.007 g, 0.024 mol) except that the crude product was further purified by silica gel chromatography using 2%MeOH:CH_2Cl_2 to give the final product as a pale yellow oil (8.570 g, 80% yield). ^{1}H NMR ($CDCl_3$) δ 7.4-7.2 (m, 5H), 7.0-6.8 (d, 1H), 5.8-5.6 (d, 1H), 5.2-5.0 (s, 2H), 4.6-4.4 (m, 1H), 4.4-4.2 (m, 1H), 3.8-3.6 (s, 3H), 2.5-2.3 (m, 2H), 2.2-1.9 (m, 3H), 1.6-1.3 (m, 9H), 1.0-0.8 (m, 6H); MS (ESI^+) *m/z* 451 (M + 1).

(δ-*tert*-Butylglutamyl)threonine Methyl Ester Hydrochloride (HCl•Glu(*t*Bu)-Thr-OMe)-General Hydrogenolysis Procedure. Z-Glu(*t*Bu)-Thr-OMe (6.441 g, 0.014 mol) was dissolved in excess MeOH (200 mL) with stirring. HCl (12M, 1 eq., 1.2 mL) and Pd/C (5% w/w, 10% mol peptide, 3.030 g) were added and the reaction mixture subjected to hydrogenolysis until no further H_2 was taken up. The reaction was filtered to remove the Pd/C, and the filtrate evaporated to give the product as a sticky white foam (5.369 g, quant. yield). ^{1}H NMR (DMSO-d_6) δ 8.9-8.8 (d, 1H), 8.4-8.0 (s, 2H), 4.3-4.2

(m, 1H), 4.2-4.0 (m, 2H), 3.8-3.6 (s, 3H), 2.5-2.3 (m, 2H), 2.1-1.8 (m, 2H), 1.5-1.3 (m, 9H), 1.2-1.0 (m, 3H); MS (ESI^+) *m/z* 319 ((M + 1) - HCl).

(δ-*tert*-Butylglutamyl)valine Methyl Ester Hydrochloride (HCl•Glu(*t*Bu)-Val-OMe). This compound was synthesized by hydrogenolysis from Z-Glu(*t*Bu)-Val-OMe (8.421 g, 0.019 mol) to give the product as an off-white sticky foam (6.815 g, quant. yield). ^1H NMR (DMSO-d_6) δ 8.9-8.8 (d, 1H), 8.5-8.0 (s, 2H), 4.3-4.1 (m, 1H), 4.1-3.9 (m, 1H), 3.7-3.5 (s, 3H), 2.4-2.2 (m, 2H), 2.2-1.8 (m, 3H), 1.6-1.2 (m, 9H), 1.0-0.8 (m, 6H); MS (ESI^+) *m/z* 317 ((M + 1) - HCl).

Benzyloxycarbonylleucyl(δ-*tert*-butylglutamyl)threonine Methyl Ester (Z-Leu-Glu(*t*Bu)-Thr-OMe). This compound was synthesized by the general coupling procedure, from Z-Leu-OH (3.962 g, 0.015 mol) and HCl•Glu(*t*Bu)-Thr-OMe (5.289 g, 0.015 mol) to give the product as a white sticky foam (6.768 g, 80% yield), which was used with no further purification. ^1H NMR (DMSO-d_6) δ 8.1-7.8 (d of d, 2H), 7.5-7.4 (d, 1H), 7.4-7.2 (m, 5H), 5.1-4.9 (s, 2H), 4.5-4.3 (m, 1H), 4.3-4.2 (m, 1H), 4.2-4.0 (m, 2H), 3.6-3.5 (s, 3H), 2.3-2.1 (m, 2H), 2.0-1.8 (m, 1H) and 1.8-1.7 (m, 1H), 1.7-1.5 (m, 1H), 1.5-1.2 (m, 11H), 1.1-1.0 (m, 3H), 0.9-0.7 (m, 6H); MS (ESI^+) *m/z* 566 (M + 1).

Benzyloxycarbonylvalyl(δ-*tert*-butylglutamyl)valine Methyl Ester (Z-Val-Glu(*t*Bu)-Val-OMe). This compound was synthesized by the general coupling procedure, from Z-Val-OH (1.808 g, 0.0072 mol) and HCl•Glu(*t*Bu)-Val-OMe (2.530 g, 0.0072 mol), except that the crude product was further purified by silica gel chromatography using 5% MeOH:CH_2Cl_2 to give the final product as a white solid (3.019 g, 77% yield). ^1H NMR ($CDCl_3$) δ 7.4-7.2 (m, 5H), 7.2-7.1 (d, 1H), 7.1-6.9 (d, 1H), 5.5-

5.3 (d, 1H), 5.2-5.0 (s, 2H), 4.6-4.4 (m, 2H), 4.1-4.0 (m, 1H), 3.8-3.6 (s, 3H), 2.6-2.3 (m, 2H), 2.3-1.8 (m, 4H), 1.6-1.4 (m, 9H), 1.1-0.8 (m, 12H); MS (ESI^+) *m/z* 550 (M + 1).

Benzyloxycarbonylleucyl(δ-*tert*-butylglutamyl)threonine (Z-Leu-Glu(*t*Bu)-Thr-OH). Z-Leu-Glu(*t*Bu)-Thr-OMe (0.535 g, 0.00095 mol) was dissolved in a minimum amount of MeOH. NaOH (1N, 2mL) was added and the reaction stirred and monitored by TLC until all starting material was used up. The solvent was evaporated, and the residue was re-dissolved in H_2O, cooled to 0 °C, and acidified to pH 4.5 with 1M HCl, giving a white ppt. EtOAc was added to re-dissolve the solid, the layers separated, and the aqueous layer was extracted with EtOAc (3 x 100 mL). The combined organic layers were washed with cold saturated NaCl solution (3 x 30 mL), dried over $MgSO_4$, filtered, and the solvent evaporated to give a yellow oil. The oil was triturated with diethyl ether and filtered to give the product as white crystals (0.181 g, 35% yield). TLC, R_f = 0.085 (5% MeOH:CH_2Cl_2); ^1H NMR (DMSO-d_6) δ 8.1-7.9 (d, 1H), 7.8-7.6 (d, 1H), 7.5-7.4 (d, 1H), 7.4-7.2 (m, 5H), 5.1-4.9 (s, 2H), 4.5-4.3 (m, 1H), 4.2-3.9 (m, 3H), 2.3-2.1 (m, 2H), 2.0-1.8 (m, 1H) and 1.8-1.7 (m, 1H), 1.7-1.5 (m, 1H), 1.5-1.3 (m, 11H), 1.1-0.9 (m, 3H), 0.9-0.7 (m, 6H); MS (ESI^+) *m/z* 552 (M + 1).

Benzyloxycarbonylvalyl(δ-*tert*-butylglutamyl)valine (Z-Val-Glu(*t*Bu)-Val-OH). This compound was synthesized in the same manner as Z-Leu-Glu(*t*Bu)-Thr-OH, from Z-Val-Glu(*t*Bu)-Val-OMe (1.990 g, 0.0036 mol) except that the residual oil was rinsed with both diethyl ether and CH_2Cl_2 and vacuum dried to give the product as an off-white solid (1.455 g, 75% yield). TLC, R_f = 0.224 (5% MeOH:CH_2Cl_2); ^1H NMR (DMSO-d_6) δ 8.1-7.8 (m, 2H), 7.4-7.2 (m, 6H), 5.1-4.9 (s, 2H), 4.4-4.3 (d, 1H), 4.2-4.0 (t,

1H), 3.9-3.8 (t, 1H), 2.3-2.1 (m, 2H), 2.1-1.6 (m, 4H), 1.5-1.3 (m, 9H), 1.0-0.7 (m, 12H); MS (ESI^+) *m/z* 536 (M + 1).

Triphenyl Cyanomethyl Phosphonium Bromide ($BrPh_3PCH_2CN$). Bromoacetonitrile (6.120 g, 0.051 mol) and triphenyl phosphine (16.018 g, 2 eq) were refluxed in benzene for 30-40 minutes, then allowed to cool overnight. The mixture was filtered and the solid collected was washed with diethyl ether and vacuum dried to give the product as a white solid (18.048 g, 93% yield). ^1H NMR (DMSO-d_6) δ 8.1-7.8 (m, 15H), 5.9-5.7 (d, 2H); MS (ESI^+) *m/z* 302 ((M + 1)-Br).

5-Cyano-5-triphenylphosphoranylidene-4-keto-3-benzyloxycarbonylamino pentanoic acid *tert*-Butyl Ester (Z-Asp(*t*Bu)-C(CN)=PPh_3). Z-Asp(*t*Bu)-OH (6.593 g, 0.02 mol) was dissolved with stirring in CH_2Cl_2 (100 mL) and cooled to -10 °C. NMM (2.064 g, 1 eq.) was added, the solution stirred for 10 minutes, then IBCF (2.783 g, 1 eq.) was added and the solution stirred for an additional 15-20 minutes. $BrPh_3PCH_2CN$ (7.787 g, 0.02 mol) was suspended in CH_2Cl_2 (125 mL) with stirring and cooled to 0 °C. Triethyl amine (2.064 g, 1 eq.) was added and the reaction stirred at 0 °C for 10 minutes, then it was warmed to rt and stirred for 20 minutes before being added to the mixture containing Z-Asp(*t*Bu)-OH. The resulting solution was stirred 30 minutes at -10 °C, then 4 hours at rt. The solvent was evaporated, and the resulting orange semi-solid was purified by silica gel chromatography (2:1 EtOAc:hexanes) and vacuum dried to give the product as a yellow oil (6.912 g, 56% yield). TLC, R_f = 0.453 (2:1 EtOAc:hexanes); ^1H NMR (DMSO-d_6) δ 7.8-7.2 (m, 21H), 5.1-5.0 (s, 2H), 4.9-4.8 (m, 1H), 2.8-2.6 (m, 1H) and 2.5-2.3 (m, 1H), 1.4-1.2 (m, 9H); MS (ESI^+) *m/z* 607 (M + 1).

3-Benzyloxycarbonylamino-4-oxo-4-phenethylcarbamoylbutanoic acid *tert*-Butyl Ester (Z-Asp(*t*Bu)-CO-NH(CH_2)$_2$Ph)-General Synthesis of α-Keto amides by Ozonolysis. Z-Asp(*t*Bu)-C(CN)=PPh_3 (6.912 g, 0.012 mol)was dissolved in a minimum of CH_2Cl_2 (60 ml; <10mL/mmol) and cooled to -78 °C. Ozone was bubbled through the solution until a blue/green color persisted, at which time the reaction was purged with O_2 for 15 minutes. After the purge, phenethylamine (1.388 g, 1 eq) was added, and the solution was stirred at -78 °C for 1 hour, then at rt for 3-4 hours. The solvent was evaporated to give a red oil, which was purified by silica gel chromatography (2:1 EtOAc:hexanes) and recrystallization from hot EtOAc/rt hexanes (3 x) to give the product as white crystals (0.531 g, 10% yield). TLC, R_f = 0.735 (2:1 EtOAc:hexanes); ^{1}H NMR (DMSO-d_6) δ 7.5-7.0 (m, 10H), 5.1-4.9 (d, 2H), 4.6-4.4 (m, 1H), 3.4-3.2 (m, 2H), 2.8-2.6 (m, 2H), 2.6-2.5 (m, 1H) and 2.4-2.2 (m, 1H), 1.5-1.2 (m, 9H); MS (ESI$^+$) *m/z* 455 (M + 1).

3-Benzyloxycarbonylamino-4-oxo-4-(3-phenylpropylcarbamoyl)butanoic acid *tert*-Butyl Ester (Z-Asp(*t*Bu)-CO-NH(CH_2)$_3$Ph). This compound was synthesized by the general ozonolysis procedure from Z-Asp(*t*Bu)-C(CN)=PPh_3 (9.307 g, 0.015 mol) and phenylpropylamine (2.084 g, 1 eq.) to give the product as off-white crystals (0.597 g, 8% yield). TLC, R_f = 0.569 (2:1 EtOAc:hexanes); ^{1}H NMR (DMSO-d_6) δ 7.4-7.0 (m, 10H), 5.1-4.9 (m, 2H), 4.6-4.4 (m, 1H), 3.2-3.0 (m, 2H), 2.6-2.5 (m, 2H), 2.5-2.2 (m, 2H), 1.8-1.6 (m, 2H), 1.4-1.1 (m, 9H); MS (ESI$^+$) *m/z* 469 (M + 1) and 496 ((M + 1) + HCN).

4-Benzylcarbamoyl-3-benzyloxycarbonylamino-4-oxo-butanoic acid *tert*-Butyl Ester (Z-Asp(*t*Bu)-CO-NHCH$_2$Ph). This compound was synthesized by the

general ozonolysis procedure from Z-Asp(*t*Bu)-C(CN)=PPh_3 (5.516 g, 0.0091 mol) and benzylamine (0.975 g, 1 eq.) to give the product as needle-like white crystals (0.410 g, 10% yield). TLC, R_f = 0.644 (2:1 EtOAc:hexanes); ^{1}H NMR ($CDCl_3$) δ 7.5-7.0 (m, 11H), 6.0-5.8 (d, 1H), 5.2-5.0 (s, 2H), 4.6-4.3 (m, 3H), 3.0-2.7 (m, 1H) and 2.5-2.3 (m, 1H), 1.5-1.3 (m, 9H); MS (ESI^+) *m/z* 441 (M + 1) and 469 ((M + 1) + HCN).

3-Benzyloxycarbonylamino-4-(3-methoxypropylcarbamoyl)-4-oxo-butanoic acid *tert*-Butyl Ester (Z-Asp(*t*Bu)-CO-NH$(CH_2)_3OCH_3$). This compound was synthesized by the general ozonolysis procedure, from Z-Asp(*t*Bu)-C(CN)=PPh_3 (9.350 g, 0.0154 mol) and methoxypropylamine (1.397 g, 1 eq.), except that there was no recrystallization, to give the product as a yellow oil (4.124 g, 63% yield). TLC, R_f = 0.770 (2:1 EtOAc:hexanes); ^{1}H NMR ($CDCl_3$) δ 7.6-7.2 (m, 5H), 5.2-5.0 (m, 2H), 4.7-4.3 (d of m, 1H), 3.6-3.2 (m, 7H), 3.1-2.7 (m, 1H) and 2.5-2.4 (m, 1H), 1.9-1.7 (m, 2H), 1.5-1.3 (m, 9H); MS (FAB^+) *m/z* 423 (M + 1) and 450 ((M + 1) + HCN); HRMS (FAB^+) calculated for $C_{21}H_{31}N_2O_7$ (M + 1) 423.21313, found 423.21579. Anal. ($C_{21}H_{30}N_2O_7$ + 0.67 HCN) C, H, N.

3-Amino-4-oxo-4-phenethylcarbamoylbutanoic acid *tert*-Butyl Ester Hydrochloride (HCl•Asp(*t*Bu)-CO-NH$(CH_2)_2$Ph). This compound was synthesized by hydrogenolysis from Z-Asp(*t*Bu)-CO-NH$(CH_2)_2$Ph (1.482 g, 0.003 mol), except that the product was rinsed with diethyl ether and vacuum dried to give the final product as a yellow solid (1.291 g, quant. yield). ^{1}H NMR (DMSO-d_6) δ 7.4-7.0 (m, 5H), 4.1-3.8 (m, 3H), 3.1-2.9 (m, 2H), 2.9-2.6 (m, 2H), 1.6-1.2 (m, 9H); MS (ESI^+) *m/z* 322 ((M + 1) - HCl).

3-Amino-4-oxo-4-(3-phenylpropylcarbamoyl)butanoic acid *tert*-Butyl Ester Hydrochloride (HCl•Asp(*t*Bu)-CO-NH(CH_2)$_3$Ph). This compound was synthesized by hydrogenolysis from Z-Asp(*t*Bu)-CO-NH(CH_2)$_3$Ph (0.483 g, 0.001 mol), except that the product was rinsed with diethyl ether and hexanes and vacuum dried to give the final product as a pale yellow solid (0.440 g, quant. yield). ^{1}H NMR (DMSO-d_6) δ 7.4-7.0 (m, 5H), 3.9-3.4 (m, 3H), 3.4-2.9 (m, 2H), 2.7-2.5 (m, 2H), 1.8-1.6 (m, 2H), 1.5-1.1 (m, 9H); MS (FAB$^+$) *m/z* 336 ((M + 1) - HCl).

3-Amino-4-benzylcarbamoyl-4-oxo-butanoic acid *tert*-Butyl Ester Hydrochloride (HCl•Asp(*t*Bu)-CO-NHCH_2Ph). This compound was synthesized by hydrogenolysis from Z-Asp(*t*Bu)-CO-NHCH_2Ph (1.573 g, 0.0036 mol) to give the final product as a yellow solid (1.377 g, quant. yield). ^{1}H NMR (DMSO-d_6) δ 7.4-7.0 (m, 5H), 4.4-4.1 (m, 2H), 3.9-3.6 (m, 1H), 2.8-2.6 (m, 1H) and 2.5-2.2 (m, 1H), 1.5-1.1 (m, 9H); MS (FAB$^+$) *m/z* 308 ((M + 1) - HCl).

3-Amino-4-(3-methoxypropylcarbamoyl)-4-oxo-butanoic acid *tert*-Butyl Ester Hydrochloride (HCl•Asp(*t*Bu)-CO-NH(CH_2)$_3$$OCH_3$). This compound was synthesized by hydrogenolysis from Z-Asp(*t*Bu)-CO-NH(CH_2)$_3$$OCH_3$ (3.386 g, 0.008 mol), except that the product was re-dissolved in diethyl ether and CH_2Cl_2 then re-concentrated (3 x), and vacuum dried to give the final product as a sticky yellow solid (2.611 g, quant. yield). ^{1}H NMR (DMSO-d_6) δ 3.9-3.6 (m, 1H), 3.4-3.2 (m, 2H), 3.2-2.8 (m, 7H), 1.7-1.5 (m, 2H), 1.5-1.2 (m, 9H); MS (FAB$^+$) *m/z* 290 ((M + 1) - HCl).

3-Benzyloxycarbonylisoleucylamino-4-oxo-4-(3-phenylpropylcarbamoyl)butanoic acid *tert*-Butyl Ester (Z-Ile-Asp(*t*Bu)-CO-NH(CH_2)$_3$Ph). This compound was synthesized by the general peptide coupling

procedure, from Z-Ile-OH (0.609 g, 0.0023 mol) and HCl•Asp(*t*Bu)-CO-NH$(CH_2)_3$Ph (0.839 g, 0.0023 mol) except that the crude product was purified by silica gel chromatography (1:4 EtOAc:CH_2Cl_2), followed by a very short (~3 inch long, ~1 inch diameter) silica gel column using 2 % MeOH:CH_2Cl_2 as the eluent. The resulting oil was recrystallized from hot EtOAc/ rt hexanes to give the product as a flaky white solid (0.047 g, 4% yield). ^{1}H NMR ($CDCl_3$) δ 7.4-7.1 (m, 10H), 7.0-6.8 (m, 3H), 5.4-5.2 (m, 1H), 5.2-5.0 (s, 2H), 4.2-4.1 (m, 1H), 3.4-3.3 (m, 2H), 3.1-2.9 (t, 1H), 2.7-2.6 (m, 2H), 2.0-1.8 (m, 4H), 1.5-1.3 (m, 9H), 1.2-1.0 (m, 2H), 1.0-0.8 (m, 6H); MS (ESI^+) *m/z* 582 (M + 1).

3-Benzyloxycarbonylisoleucylamino-4-(3-methoxypropylcarbamoyl)-4-oxo-butanoic acid *tert*-Butyl Ester (Z-Ile-Asp(*t*Bu)-CO-NH$(CH_2)_3OCH_3$). This compound was synthesized by the general peptide coupling procedure, from Z-Ile-OH (0.980 g, 0.0037 mol) and HCl•Asp(*t*Bu)-CO-NH$(CH_2)_3OCH_3$ (1.082 g, 0.0037 mol) except that the crude product was purified by silica gel chromatography (eluent: 1:4 EtOAc:CH_2Cl_2 followed by 5% MeOH:CH_2Cl_2 ramping up to 10% MeOH:CH_2Cl_2), then recrystallized from hot EtOAc/ rt hexanes to give the product as an off-white solid (0.062 g, 4% yield). ^{1}H NMR ($CDCl_3$) δ 7.6-7.2 (m, 5H), 7.0-6.8 (d, 1H), 5.4-5.3 (m, 1H), 5.3-5.2 (m, 1H), 5.2-5.0 (m, 2H), 4.2-4.0 (m, 1H), 3.6-3.3 (m, 7H), 3.1-2.9 (t, 1H), 2.0-1.8 (m, 4H), 1.6-1.3 (m, 9H), 1.3-1.0 (m, 2H), 1.0-0.8 (m, 6H); MS (ESI^+) *m/z* 536 (M + 1).

3-Benzyloxycarbonylvalyl(δ-*tert*-butylglutamyl)valylamino-4-oxo-4-phenethylcarbamoylbutanoic acid *tert*-Butyl Ester (Z-Val-Glu(*t*Bu)-Val-Asp(*t*Bu)-CO-NH$(CH_2)_2$Ph). This compound was synthesized by the general peptide coupling procedure, from Z-Val-Glu(*t*Bu)-Val-OH (0.645 g, 0.0012 mol) and HCl•Asp(*t*Bu)-CO-

$NH(CH_2)_2Ph$ (0.420 g, 0.0012 mol) except that the crude product was purified twice by silica gel chromatography (first column eluent: 5% MeOH:CH_2Cl_2; second column eluent 1:2:17 MeOH:EtOAc:CH_2Cl_2), then triturated in diethyl ether to give a yellow oil (0.099 g, 10% yield). ^1H NMR ($CDCl_3$) δ 7.6-7.2 (m, 12H), 7.1-6.9 (m, 1H), 5.4-5.2 (m, 1H), 5.2-5.0 (s, 2H), 4.7-4.6 (s, 1H), 4.6-4.2 (m, 2H), 4.1-3.9 (m, 1H), 3.6-3.4 (m, 2H), 3.0-2.7 (m, 2H), 2.6-1.9 (m, 8H), 1.6-1.2 (m, 18H), 1.1-0.7 (m, 12H); MS (FAB^+) *m/z* 838 (M + 1).

3-Benzyloxycarbonylleucyl(δ-*tert*-butylglutamyl)threonylamino-4-oxo-4-phenethylcarbamoylbutanoic acid *tert*-Butyl Ester (Z-Leu-Glu(*t*Bu)-Thr-Asp(*t*Bu)-CO-NH(CH₂)₂Ph). This compound was synthesized by the general peptide coupling procedure, from Z-Leu-Glu(*t*Bu)-Thr-OH (0.687 g, 0.0012 mol) and HCl•Asp(*t*Bu)-CO-$NH(CH_2)_2Ph$ (0.449 g, 0.0012 mol) except that no further purification was done following the initial washings, giving the product as a yellow sticky foam (0.380 g, 36% yield). ^1H NMR ($CDCl_3$) δ 7.4-7.1 (m, 10H), 7.0-6.8 (m, 1H), 5.4-5.2 (m, 1H), 5.2-5.0 (s, 2H), 4.6-4.0 (m, 4H), 4.0-3.8 (m, 1H), 3.7-3.3 (m, 2H), 3.0-2.7 (m, 2H), 2.6-1.8 (m, 6H), 1.8-1.6 (m, 3H0, 1.6-1.2 (m, 18H), 1.2-1.0 (m, 3H), 1.0-0.8 (m, 6H).

4-benzylcarbamoyl-3-benzyloxycarbonylleucyl(δ-*tert*-butylglutamyl)threonylamino-4-oxo-butanoic acid *tert*-Butyl Ester (Z-Leu-Glu(*t*Bu)-Thr-Asp(*t*Bu)-CO-NHCH₂Ph). This compound was synthesized by the general peptide coupling procedure, from Z-Leu-Glu(*t*Bu)-Thr-OH (1.051 g, 0.0019 mol) and HCl•Asp(*t*Bu)-CO-$NHCH_2Ph$ (0.657 g, 0.0019 mol) except that the crude oil was purified by silica gel chromatography (7% MeOH:CH_2Cl_2) to give the product as a yellow foam (0.386 g, 24% yield). TLC, R_f = 0.388 (7% MeOH:CH_2Cl_2); ^1H NMR

($CDCl_3$) δ 7.5-7.2 (m, 10H), 5.2-5.0 (s, 2H), 4.7-4.0 (m, 7H), 3.0-2.8 (m, 2H), 2.6-2.0 (m, 6H), 1.9-1.8 (s, 1H), 1.8-1.3 (m, 18H), 1.2-1.0 (m, 3H), 1.0-0.8 (m, 6H); MS (ESI^+) *m/z* 840 (M + 1).

3-Benzyloxycarbonylleucyl(δ-*tert*-butylglutamyl)threonylamino-4-oxo-4-(3-phenylpropylcarbamoyl)butanoic acid *tert*-Butyl Ester (Z-Leu-Glu(*t*Bu)-Thr-Asp(*t*Bu)-CO-NH(CH_2)$_3$Ph). This compound was synthesized by the general peptide coupling procedure, from Z-Leu-Glu(*t*Bu)-Thr-OH (0.970 g, 0.0018 mol) and HCl•Asp(*t*Bu)-CO-NH(CH_2)$_3$Ph (0.636 g, 0.0018 mol) except that the crude product was purified by silica gel chromatography (7% MeOH:CH_2Cl_2) followed by repeated rinsing with diethyl ether/hexanes and vacuum dried to give the final product as a sticky yellow solid (0.320 g, 22% yield). TLC, R_f = 0.333 (7% MeOH:CH_2Cl_2); MS (ESI^+) *m/z* 868 (M + 1).

3-Benzyloxycarbonylleucyl(δ-*tert*-butylglutamyl)threonylamino-4-(3-methoxypropylcarbamoyl)-4-oxo-butanoic acid *tert*-Butyl Ester (Z-Leu-Glu(*t*Bu)-Thr-Asp(*t*Bu)-CO-NH(CH_2)$_3$$OCH_3$). This compound was synthesized by the general peptide coupling procedure, from Z-Leu-Glu(*t*Bu)-Thr-OH (0.937 g, 0.0017 mol) and HCl•Asp(*t*Bu)-CO-NH(CH_2)$_3$$OCH_3$ (0.556 g, 0.0017 mol) except that it was purified by silica gel chromatography (7% MeOH:CH_2Cl_2) to give the product as a yellow oil (1.075 g, 78% yield). ^{1}H NMR ($CDCl_3$) δ 7.4-7.2 (m, 5H), 5.2-5.0 (m, 2H), 4.7-4.0 (m, 5H), 3.6-3.2 (m, 7H), 3.0-2.8 (m, 2H), 2.6-2.2 (m, 3H), 2.2-1.6 (m, 6H), 1.6-1.3 (m, 18H), 1.2-1.0 (m, 3H), 1.0-0.8 (m, 6H); MS (ESI^+) *m/z* 822 (M + 1).

3-Benzyloxycarbonylvalylglutamylvalylamino-4-oxo-4-phenethylcarbamoylbutanoic acid (Z-Val-Glu-Val-Asp-CO-NH(CH_2)$_2$Ph)-General

Deblocking with TFA. Z-Val-Glu(*t*Bu)-Val-Asp(*t*Bu)-CO-NH$(CH_2)_2$Ph (0.087 g, 0.0001 mol) was cooled to 0 °C and dissolved in TFA (4 mL) with stirring. The reaction was stirred at 0 °C for ~3 hours, then the solvent was removed to give a brown oil. Diethyl ether and hexanes were added, then evaporated away (repeat 10-15 times) until all TFA was removed, to give the product as a tan solid (0.067 g, 89% yield). ^{1}H NMR (DMSO-d_6) δ 12.3-12.0 (s, 2H), 8.8-7.6 (m, 5H), 7.6-7.0 (m, 10H), 5.2-5.0 (s, 2H), 4.5-4.3 (s, 1H), 4.3-4.0 (m, 2H), 4.0-3.8 (m, 1H), 2.9-2.6 (d, 2H), 2.6-2.4 (d, 2H), 2.3-2.1 (m, 4H), 2.1-1.6 (m, 4H), 1.0-0.6 (m, 12H); MS (ESI$^+$) *m/z* 726 (M + 1); HRMS (FAB$^+$) calculated for $C_{36}H_{48}N_5O_{11}$ (M + 1) 726.33503, found 726.33999. Anal. ($C_{36}H_{47}N_5O_{11}$ + 2.5 H_2O) C, H, N.

3-Benzyloxycarbonylisoleucylamino-4-oxo-4-(3-phenylpropylcarbamoyl)-butanoic acid (Z-Ile-Asp-CO-NH$(CH_2)_3$Ph). This compound was synthesized by the general TFA deblocking procedure, from Z-Ile-Asp(*t*Bu)-CO-NH$(CH_2)_3$Ph (0.037 g, 0.00006 mol) to give the product as an off-white solid (0.032 g, 96% yield). ^{1}H NMR (DMSO-d_6) δ 8.8-8.6 (d, 1H), 8.5-8.4 (d, 1H), 8.2-7.9 (m, 1H), 7.4-7.0 (m, 10H), 5.2-5.1 (m, 1H), 5.1-5.0 (s, 2H), 4.0-3.8 (s, 1H), 3.2-3.0 (d, 2H), 2.8-2.6 (m, 2H), 2.6-2.4 (m, 2H), 1.8-1.6 (m, 3H), 1.5-1.3 (m, 1H) and 1.2-1.0 (m, 1H), 0.9-0.7 (m, 6H); MS (ESI$^+$) *m/z* 526 (M + 1); HRMS (ESI$^+$) calculated for $C_{28}H_{36}N_3O_7$ (M + 1) 526.255326, found 526.2558. Anal. ($C_{28}H_{35}N_3O_7$ + 0.25 H_2O) C, H, N.

3-Benzyloxycarbonylisoleucylamino-4-(3-methoxypropylcarbamoyl)-4-oxo-butanoic acid (Z-Ile-Asp-CO-NH$(CH_2)_3OCH_3$). This compound was synthesized by the general TFA deblocking procedure, from Z-Ile-Asp(*t*Bu)-CO-NH$(CH_2)_3OCH_3$ (0.094 g, 0.0002 mol) to give the product as an off-white solid (0.081 g, 96% yield). ^{1}H NMR

(DMSO-d_6) δ 8.7-8.6 (m, 1H), 8.5-8.4 (m, 1H), 8.2-8.0 (m, 1H), 7.4-7.2 (m, 5H), 5.2-5.1 (m, 1H), 5.1-5.0 (m, 2H), 4.0-3.8 (m, 1H), 3.3-3.2 (s, 3H), 3.2-3.1 (m, 2H), 2.8-2.6 (m, 2H), 1.8-1.6 (s, 3H), 1.5-1.3 (m, 2H), 1.2-1.0 (m, 2H), 0.9-0.7 (m, 6H); MS (ESI^+) *m/z* 480 (M + 1); HRMS (ESI^+) calculated for $C_{23}H_{34}N_3O_8$ (M + 1) 480.234591, found 480.2354. Anal. ($C_{23}H_{33}N_3O_8$ + 0.25 H_2O) C, H, N.

3-Benzyloxycarbonylleucylglutamylthreonylamino-4-oxo-4-phenethylcarbamoylbutanoic acid (Z-Leu-Glu-Thr-Asp-CO-NH$(CH_2)_2$Ph). This compound was synthesized by the general TFA deblocking procedure, from Z-Leu-Glu(*t*Bu)-Thr-Asp(*t*Bu)-CO-NH$(CH_2)_2$Ph (0.751 g, 0.0009 mol) to give the product as a tan powder (0.504 g, 77% yield). ^1H NMR (DMSO-d_6) δ 7.6-7.0 (m, 10H), 5.1-5.0 (s, 2H), 4.2-3.2 (m, 7H), 2.9-2.7 (s, 2H), 2.4-2.1 (s, 2H), 2.0-1.7 (d of d, 2H), 1.7-1.6 (d, 2H), 1.5-1.3 (t, 2H), 1.3-1.2 (s, 1H), 1.2-1.0 (m, 3H), 0.9-0.7 (m, 6H); MS (ESI^+) *m/z* 742 (M + 1). Anal. ($C_{36}H_{47}N_5O_{12}$ + 1.75 H_2O) C, H, N.

4-Benzylcarbamoyl-3-benzyloxycarbonylleucylglutamylthreonylamino-4-oxo-butanoic acid (Z-Leu-Glu-Thr-Asp-CO-NHCH$_2$Ph). This compound was synthesized by the general TFA deblocking procedure, from Z-Leu-Glu(*t*Bu)-Thr-Asp(*t*Bu)-CO-NHCH$_2$Ph (0.294 g, 0.0004 mol), except that the product was further triturated twice in diethyl ether, for several hours each time, then filtered to give the product as a tan powder (0.138 g, 54% yield). ^1H NMR (DMSO-d_6) δ 7.5-7.0 (m, 10H), 5.1-5.0 (s, 2H), 4.5-3.8 (m, 7H), 2.4-2.1 (s, 2H), 2.0-1.7 (d, 2H), 1.7-1.6 (s, 2H), 1.5-1.2 (m, 3H), 1.2-1.0 (m, 3H), 1.0-0.8 (m, 6H); MS (ESI^+) *m/z* 728 (M + 1). Anal. ($C_{35}H_{45}N_5O_{12}$ + 1.0 H_2O) C, H, N.

3-Benzyloxycarbonylleucylglutamylthreonylamino-4-oxo-4-(3-phenylpropylcarbamoyl)butanoic acid (Z-Leu-Glu-Thr-Asp-CO-NH(CH_2)$_3$Ph). This compound was synthesized by the general TFA deblocking procedure, from Z-Leu-Glu(*t*Bu)-Thr-Asp(*t*Bu)-CO-NH(CH_2)$_3$Ph (0.320 g, 0.0004 mol), except that the product was further triturated three times in diethyl ether, for several hours each time, then filtered to give the product as a pale tan solid (0.140 g, 50% yield). ^{1}H NMR (DMSO-d_6) δ 7.5-7.0 (m, 10H), 5.1-5.0 (s, 2H), 4.9-3.8 (m, 7H), 3.3-3.0 (s, 2H), 2.4-2.0 (s, 2H), 2.0-1.5 (m, 6H), 1.5-1.2 (m, 3H), 1.2-1.0 (m, 3H), 1.0-0.7 (m, 6H); MS (ESI$^+$) *m/z* 756 (M + 1). Anal. ($C_{37}H_{49}N_5O_{12}$) C, H, N.

3-Benzyloxycarbonylleucylglutamylthreonylamino-4-(3-methoxy-propylcarbamoyl)-4-oxo-butanoic acid (Z-Leu-Glu-Thr-Asp-CO-NH(CH_2)$_3$OCH$_3$). This compound was synthesized by the general TFA deblocking procedure, from Z-Leu-Glu(*t*Bu)-Thr-Asp(*t*Bu)-CO-NH(CH_2)$_3$OCH$_3$ (0.434 g, 0.0005 mol), to give the product as a pale tan powder (0.318 g, 85% yield). ^{1}H NMR (DMSO-d_6) δ 7.5-7.0 (m, 5H), 5.1-5.0 (s, 2H), 4.4-3.4 (m, 7H), 3.4-3.2 (m, 3H), 2.8-2.6 (d of d, 2H), 2.4-2.1 (s, 2H), 2.0-1.8 (s, 1H), 1.8-1.5 (m, 4H), 1.5-1.3 (t, 2H), 1.3-1.2 (s, 2H), 1.2-1.0 (m, 3H), 1.0-0.7 (m, 6H); MS (ESI$^+$) *m/z* 710 (M + 1). Anal. ($C_{32}H_{47}N_5O_{13}$ + 0.3 TFA) C, H, N.

Materials and Methods-Enzyme Kinetics. Caspases 3, 6, and 8 were a gift from Dr. Guy Salvesen's lab at The Burnham Institute (La Jolla, CA). The AMC substrate Ac-Asp-Glu-Val-Asp-AMC was purchased from BIOMOL Research Laboratories (Plymouth Meeting, PA). Kinetic data was gathered on a Tecan Spectrafluor Microplate Reader (Tecan US, Research Triangle Park, NC).

Enzyme Kinetics-Progress Curve Method. Caspases 3, 6, and 8 were assayed using a progress curve method as follows. Assay buffer (40 μL; 20 mM Pipes, 0.1% CHAPS, 10% Sucrose, 100 mM NaCl, 1 mM EDTA, 10 mM DTT, pH 7.2) was placed in a well of a black 96 well plate. Substrate (Ac-Asp-Glu-Val-Asp-AMC; 5 μL of 2 mM stock in assay buffer) and inhibitor (5 μL of 0.002 – 10 mM stock in DMSO) were added, and the plate was incubated at 37 °C for 1 min. An aliquot (50 μL) of enzyme stock solution in assay buffer (stock concentration: 2 nM caspase 3; 20 nM caspase 6; 100 nM caspase 8) was added. Fluorescence of the substrate cleavage product, AMC (λ_{ex} = 360 nm, λ_{em} = 465 nm), was monitored over 15-40 minutes, depending on the enzyme (caspase 3, 15 min; caspase 6, 20 min; caspase 8, 40 min). For each inhibitor assay at a fixed substrate concentration, at least 5 inhibitor concentrations were tested.

Data Processing. For each compound tested that exhibited slow-binding inhibition, data collected during the first 300 s and the last 300 s of each assay was used to determine an initial K_i and a final K_i. Compounds exhibiting simple competitive inhibition were processed in the same manner, except that only data from the first 300 s was used to give a K_i value. Data for the first 300 s, plotted as concentration of product (in micromolar) vs. time, was examined for linearity, and the slopes of each line found by linear regression using Kaleidagraph 3.6. The slopes were expressed as a fraction of the control slope (v_i/v_o, where v_i is the slope of the inhibited mixture and v_o is the slope of the control line), which was then converted to percent inhibition. Plotting percent inhibition vs. inhibitor concentration gave a curve that was fitted to the equation

$$\% \text{ Inhibition} = 100 * \frac{[I]}{[I] + K_{i,app}}$$

where

$$K_i = \frac{K_{i,app}}{1 + \frac{[S]}{K_m}}$$

to give $K_{i(initial)}$ if the first 300 s data was used, or $K_{i(final)}$ if the last 300 s data was used. The K_m values for Ac-Asp-Glu-Val-Asp-AMC with the caspases were determined by Jowita Mikolajczyk in Dr. Guy Salvesen's Lab, and are as follows: caspase 3, 9.7 μM; caspase 6, 236.35 μM; and caspase 8, 6.79 μM.

REFERENCES

(1) Thornberry, N. A. Caspases: key mediators of apoptosis. *Chemistry & Biology* **1998**, *5*, R97-R103.

(2) Nicholson, D. W.; Thornberry, N. A. Caspases: killer proteases. *Trends in Biochem. Science* **1997**, *22*, 299-306.

(3) Ashkenazi, A.; Dixit, V. M. Death receptors: signaling and modulation. *Science* **1998**, *281*, 1305-1308.

(4) Green, D. R.; Reed, J. C. Mitochondria and apoptosis. *Science* **1998**, *281*, 1309-1312.

(5) Grütter, M. G. Caspases: key players in programmed cell death. *Curr. Opin. Struct. Biol.* **2000**, *10*, 649-655.

(6) Thompson, C. B. Apoptosis in the pathogenesis and treatment of disease. *Science* **1995**, *267*, 1456-1462.

(7) Cotman, C. W.; Anderson, A. J. A potential role for apoptosis in neurodegeneration and Alzheimer's disease. *Molecular Neurobiology* **1995**, *10*, 19-45.

(8) Mochizuki, H.; Goto, K.; Mori, H.; Mizuno, Y. Historical detection of apoptosis in Parkinson's disease. *Neurological Sci.* **1996**, *137*, 120-123.

(9) Raff, M. C.; Barres, B. A.; Burne, J. F.; Jacobson, M. D. Programmed cell death and the control of cell survival: Lessons from the nervous system. *Science* **1993**, *262*, 695-700.

(10) Schulz, J. B.; Weller, M.; Moskovitz, M. Caspases as treatment targets in stroke and neurodegenerative diseases. *Ann. Neurology* **1999**, 421-429.

(11) Hara, H.; Friedlander, R. M.; Gagliardini, V.; Ayata, C.; Fink, K. et al. Inhibition of interleukin 1β converting enzyme family proteases reduces ischemic and excitotoxic neuronal damage. *Proc. Natl. Acad. Sci. USA* **1997**, *94*, 2007-2012.

(12) Villa, P.; Kaufmann, S. C.; Earnshaw, W. C. Caspases and caspase inhibitors. *Trends in Biochem. Science* **1997**, *22*, 388-393.

(13) Thornberry, N. A. The caspase family of cysteine proteases. *Brit. Med. Bull.* **1997**, *53*, 478-490.

(14) Cohen, G. M. Caspases: The executioners of apoptosis. *Biochem. J.* **1997**, *326*, 1-16.

(15) Stennicke, H. R.; Salvesen, G. S. Catalytic properties of the caspases. *Cell Death Differ.* **1999**, *6*, 1054-1059.

(16) Muzio, M.; Stockwell, B. R.; Stennicke, H. R.; Salvesen, G. S.; Dixit, V. M. An induced proximity model for caspase-8 activation. *J. Biol. Chem.* **1998**, *273*, 2926-2930.

(17) Stennicke, H. R.; Salvesen, G. S. Properties of the caspases. *Biochem. Biophys. Acta* **1998**, *1387*, 17-31.

(18) Howard, A. D.; Kostura, M. J.; Thornberry, N.; Ding, G. J. F.; Limjuco, G. et al. IL-1-converting enzyme requires aspartic acid residues for processing of the IL-1β precursor at two distinct sites and does not cleave 31 kDa IL-1α. *J. Immunol.* **1991**, *147*, 2964-2969.

(19) Sleath, P. R.; Hendrickson, R. C.; Kronheim, S. R.; March, C. J.; Black, R. A. Substrate specificity of the protease that processes human interleukin-1β. *J. Biol. Chem.* **1990**, *265*, 14526-14528.

(20) Thornberry, N. A.; Rano, T. A.; Peterson, E. P.; Rasper, D. M.; Timkey, T. et al. A combinatorial approach defines specificities of members of the caspase family and granzyme B. Functional relationships established for key mediators of apoptosis. *J. Biol. Chem.* **1997**, *272*, 17907-17911.

(21) Casciola-Rosen, L.; Nicholson, D. W.; Chong, T.; Rowan, K. R.; Thornberry, N. A. et al. Apopain/CPP32 cleaves proteins that are essential for cellular repair: a fundamental principle of apoptotic death. *J Exp Med* **1996**, *183*, 1957-1964.

(22) Lazebnik, Y. A.; Kaufmann, S. H.; Desnoyers, S.; Poirier, G. G.; Earnshaw, W. C. Cleavage of poly(ADP-ribose) polymerase by a proteinase with properties like ICE. *Nature* **1994**, *371*, 346-347.

(23) Orth, K.; Chinnaiyan, A. M.; Garg, M.; Froelich, C. J.; Dixit, V. M. The CED-3/ICE-like protease Mch2 Is activated during apoptosis and cleaves the death substrate lamin A. *J. Biol. Chem.* **1996**, *271*, 16443-16446.

(24) Takahashi, A.; Alnemri, E.; Lazebik, Y. A.; Fernandes-Alnemri, T.; Litwack, G. et al. Cleavage of lamin A by Mch2α but not CPP32: multiple interleukin 1β-converting enzyme-related proteases with distinct substrate recognition properties are active in apoptosis. *Proc. Natl. Acad. Sci. USA* **1996**, *93*, 8395-8400.

(25) Fernandes-Alnemri, T.; Armstrong, R.; Krebs, J.; Srinivasula, S. M.; Wang, L. et al. In-Vitro Activation of CPP32 and Mch3 by Mch4, a Novel Human Apoptotic Cysteine Protease Containing 2 FADD-like Domains. *Proc. Natl. Sci. USA* **1996**, *93*, 7464-7469.

(26) Srinivasula, S. M.; Fernandes-Alnemri, T.; Zangrilli, J.; Robertson, N.; Armstrong, R. C. et al. The Ced-3/interleukin 1beta converting enzyme-like homolog Mch6 and the lamin-cleaving enzyme Mch2alpha are substrates for the apoptotic mediator CPP32. *J. Biol. Chem.* **1996**, *271*, 27099-27106.

(27) Garcia-Calvo, M.; Peterson, E. P.; Leiting, B.; Ruel, R.; Nicholson, D. W. et al. Inhibition of human caspases by peptide-based and macromolecular inhibitors. *J. Biol. Chem.* **1998**, *273*, 32608-32613.

(28) Hori, H.; Yasutake, A.; Minematsu, Y.; Powers, J. C. Inhibition of human leukocyte elastase, pancreatic elastase and cathepsin G by peptide ketones. *Peptides: Structure and Function. Proceedings of the Ninth American Peptide Symposium*; Pierce Chem. Co.: Rockford, IL, 1985; pp 819-822.

(29) Geratz, J. D. *p*-Amidinophenylpyruvic acid: a new highly effective inhibitor of enterkinase and trypsin. *Arch. Biochem. Biophysics* **1967**, *118*, 90-96.

(30) Walter, J.; Bode, W. The X-ray crystal structure analysis of the refined complex formed by bovine trypsin and *p*-amidinophenylpyruvate at 1.4 Å resolution. *Hoppe Seylers Z Physiol Chem* **1983**, *364*, 949-959.

(31) Peet, N. P.; Burkhart, J. P.; Angelastro, M. R.; Giroux, E. L.; Mehdi, S. et al. Synthesis of peptidyl fluoromethyl ketones and peptidyl α-keto esters as inhibitors of porcine pancreatic elastase, human neutrophil elastase, and rat and human neutrophil cathepsin G. *J. Med. Chem.* **1990**, *33*, 394.

(32) Angelastro, M. R.; Mehdi, S.; Burkhart, J. P.; Peet, N. P.; Bey, P. α-Diketone and α-keto ester derivatives of N-protected amino acids and peptides as novel inhibitors of cysteine and serine proteinases. *J. Med. Chem.* **1990**, *33*, 11-13.

(33) Parisi, M. F.; Abeles, R. H. Inhibition of chymotrypsin by fluorinated α-keto acid derivatives. *Biochemistry* **1992**, *31*, 9429-9435.

(34) Mehdi, S.; Angelastro, M. R.; Burkhart, J. P.; Koehl, J. R.; Peet, N. P. et al. The inhibition of human neutrophil elastase and cathepsin G by peptidyl 1,2-dicarbonyl derivatives. *Biochem. Biophys. Res. Commun.* **1990**, *166*, 595-600.

(35) Hu, L.-Y.; Abeles, R. H. Inhibition of cathepsin B and papain by peptidyl α-keto esters, α-keto amides, α-diketones, and α-keto acids. *Arch. Biochem. Biophys.* **1990**, *281*, 271-274.

(36) Li, Z.; Patil, G. S.; Golubski, Z. E.; Hori, H.; Tehrani, K. et al. Peptide α-ketoester, α-ketoamide and α-ketoacid inhibitors of calpains and other cysteine proteases. *J. Med. Chem.* **1993**, *36*, 3472-3480.

(37) Li, Z.; Ortega-Vilain, A.-C.; Patil, G. S.; Chu, D.-L.; Foreman, J. E. et al. Novel peptidyl α-keto amide inhibitors of calpains and other cysteine proteases. *J. Med. Chem.* **1996**, *39*, 4089-4098.

(38) Harriman, J. F.; Waters-Williams, S.; Chu, D. L.; Powers, J. C.; Schnellmann, R. G. Efficacy of novel calpain inhibitors in preventing renal cell death. *J. Pharmacol. Exp. Ther.* **2000**, *294*, 1083-1087.

(39) Bartus, R. T.; Baker, K. L.; Heiser, A. D.; Sawyer, S. D.; Dean, R. L. et al. Postischemic administration of AK275, a calpain inhibitor, provides substantial protection against focal ischemic brain damage. *J. Cereb. Blood Flow Metab.* **1994**, *14*, 537-544.

(40) Saatman, K. E.; Murai, H.; Bartus, R. T.; Smith, D. H.; Hayward, N. J. et al. Calpain inhibitor AK295 attenuates motor and cognitive deficits following

experimental brain injury in the rat. *Proc. Natl. Acad. Sci. USA* **1996**, *93*, 3428-3433.

(41) Wasserman, H. H.; Ho, W.-B. (Cyanomethylene)phosphoranes as novel carbonyl 1,1-dipole synthons: an efficient synthesis of α-keto acids, esters and amides. *J. Org. Chem.* **1994**, *59*, 4364-4366.

(42) Brady, K. D.; Giegel, D. A.; Grinnell, C.; Lunney, E.; Talanian, R. V. et al. A catalytic mechanism for caspase-1 and for bimodal inhibition of caspase-1 by activated aspartic ketones. *Bioorganic Med. Chem.* **1999**, *7*, 621-631.

(43) Powers, J. C.; Asgian, J. L.; Dogan Ekici, O.; James, K. E. Irreversible inhibitors of serine, cysteine, and threonine proteases. *Chemical Reviews* **2002**, *102*, 4693-4750.

(44) Rawlings, N. D.; Barrett, A. J. Evolutionary families of peptidases. *Biochem. J.* **1993**, *290*, 205-218.

(45) Rawlings, N. D.; Barrett, A. J. Families of cysteine peptidases. *Meth. Enzymol.* **1994**, *244*, 461-486.

(46) MEROPS The Peptidase Database. http://merops.sanger.ac.uk/.

(47) Rawlings, N. D.; O'Brien, E.; Barrett, A. J. MEROPS: the protease database. *Nucleic Acids Res.* **2002**, *30*, 343-346.

(48) Storer, A. C.; Menard, R. Catalytic mechanism in papain family of cysteine peptidases. *Meth. Enzymol.* **1994**, *244*, 486-500.

(49) Otto, H.-H.; Schirmeister, T. Cysteine proteases and their inhibitors. *Chem. Rev.* **1997**, *97*, 133-171.

(50) Gerhartz, B.; Niestroj, A. J.; Demuth, H.-U. Enzyme classes and mechanisms. *Proteinase and Peptidase Inhibition: Recent Potential Targets for Drug Development*; Taylor and Francis: London, 2002; pp 1-20.

(51) Dixon, M.; Webb, E. C. *Enzymes*; Second ed.; Academic Press, Inc.: New York, 1964; 950.

(52) Kam, C.-H.; Hudig, D.; Powers, J. C. Granzymes (lymphocyte serine proteases): characterization with natural and synthetic substrates and inhibitors. *Biochim. Biophys. Acta* **2000**, *1477*, 307-323.

(53) Hunter, A.; Downs, C. E. The inhibition of arginase by amino acids. *J. Biol. Chem.* **1945**, *157*, 427-446.

(54) Mittl, P. R.; Marco, S. D.; Krebs, J. F.; Bai, X.; Karanewsky, D. S. et al. Structure of recombinant human CPP32 in complex with the tetrapeptide Acetyl-Asp-Val-Ala-Asp fluoromethyl ketone. *J. Biol. Chem.* **1997**, *272*, 6539-3547.

(55) Wilson, K. P.; Black, J. F.; Thomson, J. A.; Kim, E. E.; Griffith, J. P. et al. Structure and mechanism of interleukin-1β converting enzyme. *Nature* **1994**, *370*, 270-275.

(56) Rotonda, J.; Nicholson, D. W.; Fazil, K. M.; Gallant, M.; Gareau, Y. et al. The three-dimensional structure of apopain/CPP32, a key mediator of apoptosis. *Nature Struct. Biol.* **1996**, *3*, 619-625.

(57) Watt, W.; Koeplinger, K. A.; Mildner, A. M.; Heinrikson, R. L.; Tomasselli, A. G. et al. The atomic-resolution structure of human caspase-8, a key activator of apoptosis. *Structure Fold Des.* **1999**, *7*, 1135-1143.

(58) Walker, N. P. C.; Talanian, R. V.; Brady, K. D.; Dang, L. C.; Bump, N. J. et al. Crystal structure of the cysteine protease interleukin-1β-converting enzyme: a $(p20/p10)_2$ homodimer. *Cell* **1994**, *78*, 343-352.

(59) Blanchard, H.; Kodandapani, L.; Mittl, P. R.; Marco, S. D.; Krebs, J. F. et al. The three-dimensional structure of caspase-8: an initiator enzyme in apoptosis. *Structure Fold Des.* **1999**, *7*, 1125-1133.

(60) NCBI National Center for Biotechnological Information. http://www.ncbi.nlm.nih.gov.

(61) Thornberry, N. A.; Lazebnik, Y. Caspases: enemies within. *Science* **1998**, *281*, 1312-1316.

(62) Asgian, J. L.; James, K. E.; Li, Z. Z.; Carter, W.; Barrett, A. J. et al. Aza-peptide epoxides: a new class of inhibitors selective for clan CD cysteine proteases. *J. Med. Chem.* **2002**, *45*, 4958-4960.

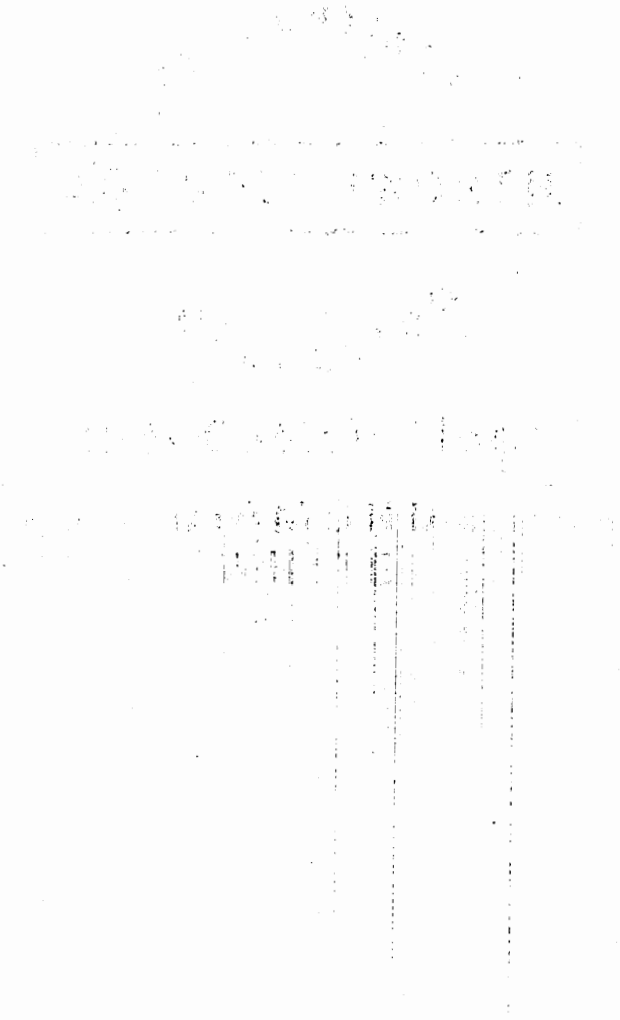

VITA

Karrie E. A. Rukamp

2550 Akers Mill Road, Apt. J-10
Atlanta, GA 30339
(770) 956-0197
(404) 385-1174
karrie.adlington@chemistry.gatech.edu

Education

Georgia Institute of Technology
Atlanta, Georgia
Ph.D. in Chemistry, December 2003
Major: Biochemistry; Minor: Bioorganic Chemistry
G.P.A. 3.65/4.00
Thesis: Design and Synthesis of Inhibitors for Serine and Cysteine Proteases.
Advisor: James C. Powers, Ph.D.

Northwestern University
Evanston, Illinois
B.A. in Chemistry, June 1997

Employment

2002 to Present	Research Assistant and Senior Teaching Assistant of Organic Chemistry laboratory, Georgia Institute of Technology
2000 to 2002	Research Assistant, Georgia Institute of Technology
1998 to 2000	Research Assistant and Teaching Assistant of Organic Chemistry laboratory, Georgia Institute of Technology
1997 to 1998	Teaching Assistant of General Chemistry laboratory, Georgia Institute of Technology
Summer 1997	Co-Op student: Process development research on new procedures for purification of off spec. products, Ciba Specialty Chemicals, McIntosh, Alabama
1996 to 1997	Laboratory Teaching Assistant for Organic Chemistry, and Organic Lab Preparatory Assistant, Northwestern University, Evanston, Illinois
Summer 1996	Co-Op student: Product development research in a unit laboratory, Ciba Specialty Chemicals, McIntosh, Alabama
Summer 1995	Co-Op Student: Maintenance and minor repair of analyzers, Stock Room Assistant for Ciba Additives Analyzer Group, Ciba Specialty Chemicals, McIntosh, Alabama

Skills

- Proficient in experimental biochemical and organic syntheses, and techniques for performing and interpreting enzymatic assays
- Spectroscopy: NMR, UV/Vis, FTIR, and interpretation of Mass Spectrometry and Combustion Elemental Analysis
- Chromatography: Gas, Thin Layer, and Column Chromatography
- Computer: Familiar with Microsoft Word, Excel and PowerPoint, Endnote, Rasmol, KaleidaGraph, and ChemDraw. Familiar with both Macintosh and Windows environments

Professional Memberships

- Alpha Chi Sigma (Professional Fraternity in Chemistry)
  Treasurer, Atlanta Professional Chapter, 1999 to 2002.
- American Chemical Society
- American Association for the Advancement of Science
- Sigma Alpha Iota International Music Fraternity for Women
  Communications Assistant: 1996 to1997
  Co-Chair of Philanthropy Committee: 1995

Honors

- CETL/BP Amoco Outstanding Graduate Teaching Assistant, Georgia Institute of Technology, 2000
- Outstanding Graduate Teaching Assistant, School of Chemistry and Biochemistry, Georgia Institute of Technology, 1999-2000
- Federal Work/Study Student Employee of the Year, Northwestern University, 1997

Activities

- Alpha Chi Sigma Teacher Workshop
  Chair, 1999 and 2000
- Personal Items Drive, St. James UMC
  Chair, 2000 and 2001
- Dress for Success Drive, St. James UMC
  Co-chair, 2000
- Habitat for Humanity
- Hands on Atlanta Day, 1997 and 1998
- St. James UMC Handbell Choir
- St. James UMC Chancel Choir

Publications

Adlington, K. E.; and Powers, J. C. Peptide Halomethyl Ketones (Excluding Fluoromethyl Ketones). In *Houben-Weyl Synthesis of Peptidomimetics;* Goodman, M., Felix, A., and Toniolo, C. (Eds.); Thieme: Stuttgart, (2003); Vol. E22d; pp. 221-225.

Adlington, K. E.; and Powers, J. C. Peptide Fluoromethyl, Difluoromethyl, and Perfluoroalkyl Ketones. In *Houben-Weyl Synthesis of Peptidomimetics;* Goodman, M., Felix, A., and Toniolo, C. (Eds.); Thieme: Stuttgart, (2003); Vol. E22d; pp. 226-243.